SMIP 1990 SEMINAR ON
SEISMOLOGICAL AND ENGINEERING IMPLICATIONS
OF RECENT STRONG-MOTION DATA

Sacramento, California
June 8, 1990

PREPRINTS

Sponsored by

Strong Motion Instrumentation Program
Division of Mines and Geology
California Department of Conservation

Supported in Part by

California Seismic Safety Commission
National Science Foundation
Applied Technology Council

CALIFORNIA
DEPARTMENT
OF CONSERVATION

Division of Mines and Geology

The Strong Motion Instrumentation Program (SMIP) is administered by the Division of Mines and Geology, California Department of Conservation. It is advised by the Strong Motion Instrumentation Advisory Committee (SMIAC), a committee of the California Seismic Safety Commission. SMIP is funded by an assessment on building permits issued in cities and counties in California.

DISCLAIMER

TABLE OF CONTENTS

THE STRONG MOTION INSTRUMENTATION PROGRAM AND DATA RECORDED DURING THE LOMA PRIETA EARTHQUAKE

A.F. Shakal and M.J. Huang
California Department of Conservation
Division of Mines and Geology

ABSTRACT

The purpose of the Strong Motion Instrumentation Program (SMIP) is to improve methods to protect California citizens and property from earthquake-induced structural hazards. Toward this end, the program records strong earthquake shaking in structures and at ground response sites to obtain the data necessary for the improvement of seismic design codes. SMIP also promotes and facilitates the improvement of seismic codes through data utilization projects. The SMIP 1990 Research Review Seminar is a component of that effort. Several sets of data recorded during the Loma Prieta earthquake are the first measurements of the performance of several standard construction types during moderate and strong earthquake shaking, and these records will be the subject of data utilization studies in 1990.

INTRODUCTION

SMIP was established after the 1971 San Fernando earthquake caused unexpectedly severe damage to structures that had been designed according to contemporary code standards. To acquire the data necessary to improve the prediction of strong motion and the detection of structural problems, many more strong-motion stations were needed than were provided by the existing federal program. SMIP was created to fill that need.

The program installs and maintains strong-motion instruments in representative structures and geological environments throughout California. Since the program's inception, over 480 installations of various types have been completed. Sites are selected for instrumentation on the basis of the recommendations of a committee of the California Seismic Safety Commission, called the Strong Motion Instrumentation Advisory Committee (SMIAC), comprised of leading engineers and seismologists from California universities, government and private industry.

Strong-motion data recovered from the instruments in the SMIP network are processed and made available to engineers and seismologists engaged in predicting or designing for earthquake shaking. A large number of earthquake records have been recorded and analyzed, including many from the 7.1 M_L 1989 Loma Prieta earthquake [1], the 5.9 M_L 1987 Whittier Narrows earthquake [2], and the very important records from the Imperial County Services Building, damaged during the 6.6 M_L 1979 Imperial Valley earthquake.

NETWORK STATUS AND INSTRUMENTATION OBJECTIVES

SMIP currently has a total of 480 stations installed at selected locations throughout the state of California. Table 1 summarizes the current and target numbers of ground-response, building, and lifeline installations.

Table 1. SMIP Network Status and Goals

Installation Type	Total Network Plan	Installed To Date	Remaining High Priority	Remaining To Complete Network
Ground-Response				
Isolated Sites	500	344	104	156
Dense Arrays	20	2	8	18
Buildings				
All Types	400	103	160	297
Lifelines				
Dams	30	21	9	9
Transportation	40	8	15	32
Water & Power	25	2	13	23
Total	1015	480	309	535

Ground-Response Instrumentation An objective of ground-response instrumentation is to measure earthquake shaking in a range of geologic conditions including rock, deep and shallow alluvium, and liquefiable deposits. Recording the motion at specific locations with respect to the earthquake fault is also important to allow study of the rupture process and the attenuation of seismic waves radiated from the source region. A total of 344 ground-response stations have been installed. The instrumentation objectives for the next 15 years include adding an additional 104 isolated sites and 8 specialized dense arrays.

Building Instrumentation A primary objective in the instrumentation of a building is to effectively record selected modes of the building's motion during strong shaking. For each building type, specific modes of response or deformation are most important, and these determine where the sensors are located. As a result, building instrumentation systems have sensors located at key points throughout a structure, all connected to a centrally-located recorder. Typically, 12 to 15 sensors are located in a building. Since the motion at the base of the building may not accurately represent the input motion, an additional 3-sensor set may be located some distance from the building. As shown in Table 1, 103 buildings have been instrumented by SMIP. Objectives for the next 15 years include the instrumentation of an additional 160 high-priority buildings.

Lifeline Instrumentation Lifeline structures instrumented by SMIP include bridges, dams, and power plants. Table 1 lists the number instrumented in several categories and the number remaining in the highest priority categories. One of the most important records obtained to date is from the Vincent Thomas suspension bridge during the 1987 Whittier earthquake, which is discussed below.

Network Maintenance Thorough training of personnel and regular, careful servicing are key elements of an effective maintenance program. For a program like SMIP, continually installing new instruments as well as maintaining previously installed instruments, the budget balance between installation and maintenance is important. An instrument installed one year increases maintenance costs for subsequent years. In addition, about 1-2% of SMIP stations have to be abandoned and re-installed each year due to change of property ownership or changing physical conditions at the site.

Accelerogram Processing SMIP's in-house digitizing facility is patterned after that developed by Trifunac and Lee [3]. In this system, the film accelerogram is scanned, while mounted on a rotating drum, by a laterally-moving photodensitometer. Studies of the system noise are used to develop signal-to-noise ratios to guide filtering during processing. SMIP is currently investigating the accuracy and feasibility of a PC-based scanning system for replacing the existing system.

Data Utilization through Directed Research An effort to increase the application of the data collected to the improvement of building codes was recently initiated. Studies are funded for analysis of strong-motion data by researchers, working when possible with graduate students and with the engineers who designed the structure being studied. These projects are aimed at answering specific questions about the response of the structures or the ground through utilization of strong-motion data. The results of these studies are presented in annual seminars and published in technical journals.

IMPORTANT DATA FROM THE 1989 LOMA PRIETA EARTHQUAKE

The Loma Prieta of October 17, 1989 produced a large set of strong-motion data from a magnitude 7.1 earthquake. These data are very important because most previous strong motion data are from earthquakes of magnitude 6 or less. SMIP obtained records from a total of 94 stations, including 53 ground-response stations and 41 extensively-instrumented structures [1]. The structures include 34 buildings, 2 dams, 2 freeway overpasses, a wharf, a tunnel, and a rapid-transit bridge.

Recorded peak horizontal acceleration values from SMIP stations are plotted on the map in Fig. 1. Stations in the epicentral area had accelerations as high as 0.64 g. Peak acceleration data from ground-response stations (or buildings with less than three stories) from the SMIP network [1] and the USGS [4] are plotted against distance in Fig. 2. The peak accelerations are higher than would be predicted by a standard model [5], and the values from many stations are more than 2 standard deviations above the median. The geologic conditions at a site can be important in causing local amplification, but Fig. 2 indicates that surficial geology is not the only factor causing the variation. The ability to more accurately predict peak ground motion for a given earthquake is a focus of data utilization studies.

The stations at Yerba Buena Island and Treasure Island were installed over 15 years ago specifically as a rock - soil station pair, respectively. Treasure Island is a man-made island, built of fill on a shallow sand spit north of Yerba Buena Island. Amplification of the motion recorded at the soft soil site compared to the rock site is clearly shown in the acceleration records and the response spectra (Fig. 3).

A particularly interesting record was obtained at a 47-story office building in San Francisco. The building, instrumented with 18 sensors, has a moment-resisting steel frame in the longitudinal direction, and a braced steel frame in the transverse direction. The peak acceleration was 0.48 g on the 44th floor and 0.16 g at the base level. The acceleration records were dominated by motions of higher modes, but the computed displacements clearly show the response in the fundamental mode. Fig. 4 shows the displacements in the longitudinal direction at the 44th floor, 16th floor, and the "B" level.

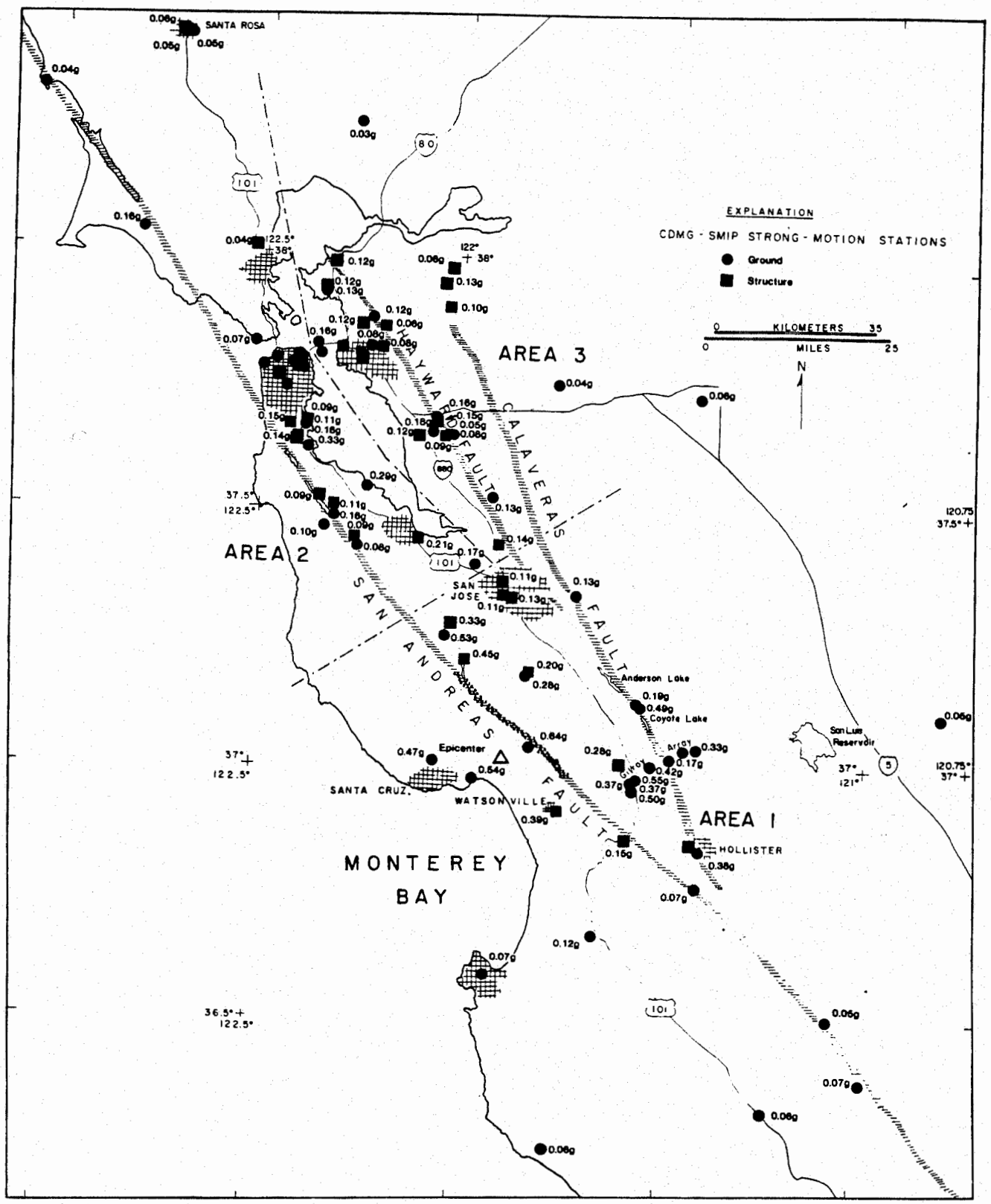

Fig. 1. Map of central coastal California showing the San Andreas fault, the epicenter and aftershock zone of the Loma Prieta earthquake, and the locations of SMIP stations that recorded the strong shaking. The peak horizontal acceleration recorded at each station is shown next to the station.

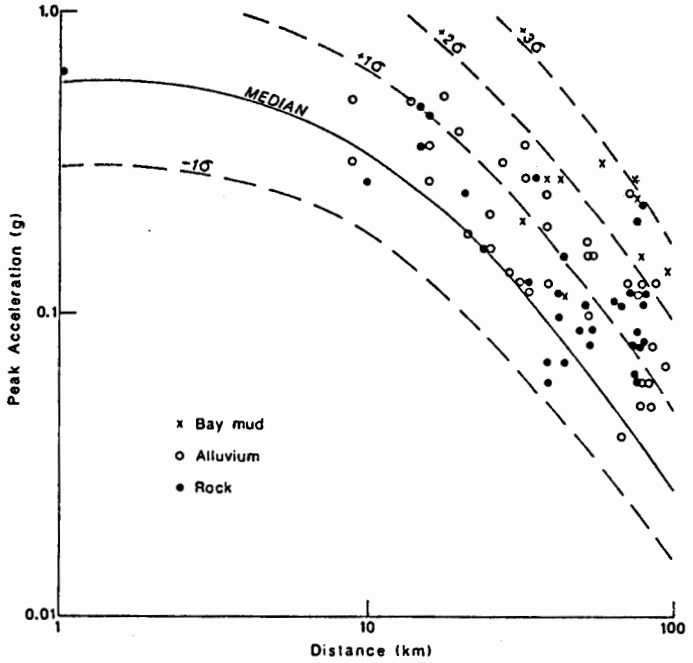

Fig. 2. Peak horizontal acceleration versus distance to the nearest point on the fault inferred from the aftershock distribution. Largest of the two horizontal components is plotted. Solid line is the median curve of Joyner and Boore, 1981, for a moment magnitude 6.9 earthquake. Dashed lines indicate -1, +1, +2, and +3 standard deviations. Site geology is shown in the key.

These records show that after about 30 seconds the building oscillated in free vibration with an amplitude of about 30 cm (one foot) and a period of about 6 seconds. The damping ratio, as estimated from the record, is about 3%. Similarly, the record shows that the fundamental mode in the transverse direction has a period of about 5 seconds. Detailed analysis of the record will allow determination of important building response parameters and allow the evaluation of seismic design provisions for tall buildings.

The record obtained at a 4-story concrete shear wall building in Watsonville is also interesting. The building was designed in 1948 and 1955. A peak acceleration of nearly 1.25 g was recorded on the roof, and about 0.4 g was recorded at the ground floor. It is clear from the record in Fig. 5 that the building vibrated at a period of about 0.35 second and this period was not changed dramatically during the shaking. The record also shows that the building experienced some torsional motion. The computed displacements [6] at three different levels in the east-west direction are also shown in Fig. 5. Note that these displacements are very similar because the building is very stiff. The relative displacement between the roof and the ground floor is less than 4 cm. Comparison to Fig. 4 illustrates the expected flexibility of a steel frame structure.

DATA FROM OTHER RECENT EARTHQUAKES

Important records have also been obtained during other recent earthquakes. One example is the record obtained at the Vincent Thomas suspension bridge near Los Angeles during the 1987 Whittier earthquake. The acceleration records from 26 sensors are shown in the SMIP Whittier report [2]. The processed data revealed that the periods of first lateral and vertical modes of the bridge deck were about 7 and 4.5 seconds, respectively. Fig. 6 shows

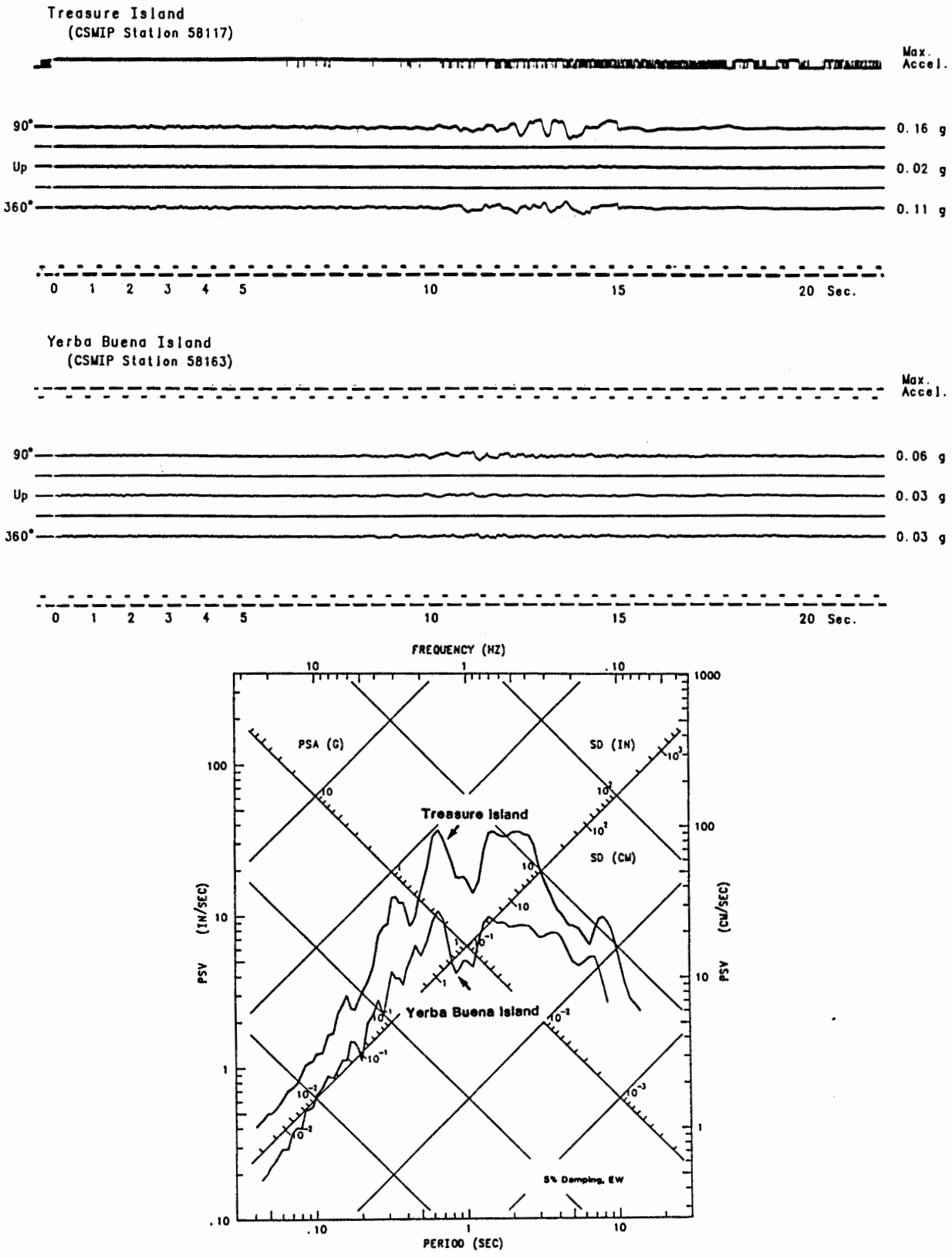

Fig. 3. Comparison of accelerations and response spectra for the Treasure Island (soft-soil site) and Yerba Buena Island (rock site). The Treasure Island spectrum is amplified by a factor between 2 to 4 for the range of periods shown.

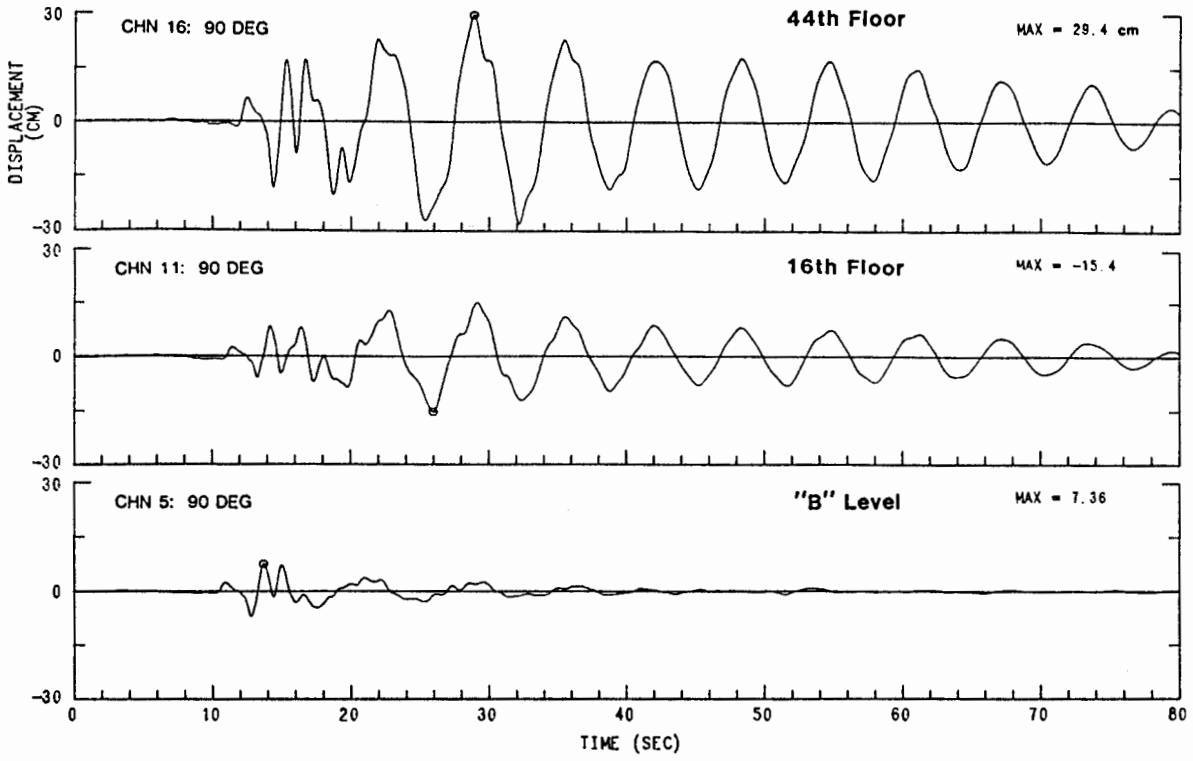

Fig. 4. Displacements computed from the accelerations recorded at the 44th floor, 16th floor, and base level in the longitudinal direction of a 47-story steel office building in San Francisco. Note that the building oscillated in free vibration with amplitude of 30 cm after the ground motion stopped.

the lateral displacement and the torsional motion of the deck. Note that the torsional motion of the bridge deck at the side span has a period of about 1 second, and the motion of the side span is larger than that of the center span. In lateral motion, the main span shows a longer period of about 7 seconds with an amplitude of about 4 cm. Studies underway will extend the analysis of the response and compare it to modelling results.

Another important record was obtained during the 5.5 M_L Upland earthquake of February 28, 1990 at the base-isolated Law and Justice Center of San Bernardino County. Several records were obtained in the building since it was instrumented in 1985, but the previous events all had very small motion at the site. As shown in Fig. 7, the peak accelerations recorded at the foundation level (below the isolators) and the basement (above the isolators) were 0.14 g and 0.05 g, respectively. The peak acceleration at the roof was 0.16 g. Comparison of the records above and below the isolators shows that high-frequency horizontal motion was filtered by the isolator, which was also observed in the records from other earthquakes. The period of the structure during this event was near 0.75 second; this is longer than the 0.6 second period present in other low-amplitude records. The differences in the horizontal motions at different levels in the structure can also be compared in the response spectra, which show a reduction at high frequency as well as amplification at the structural period.

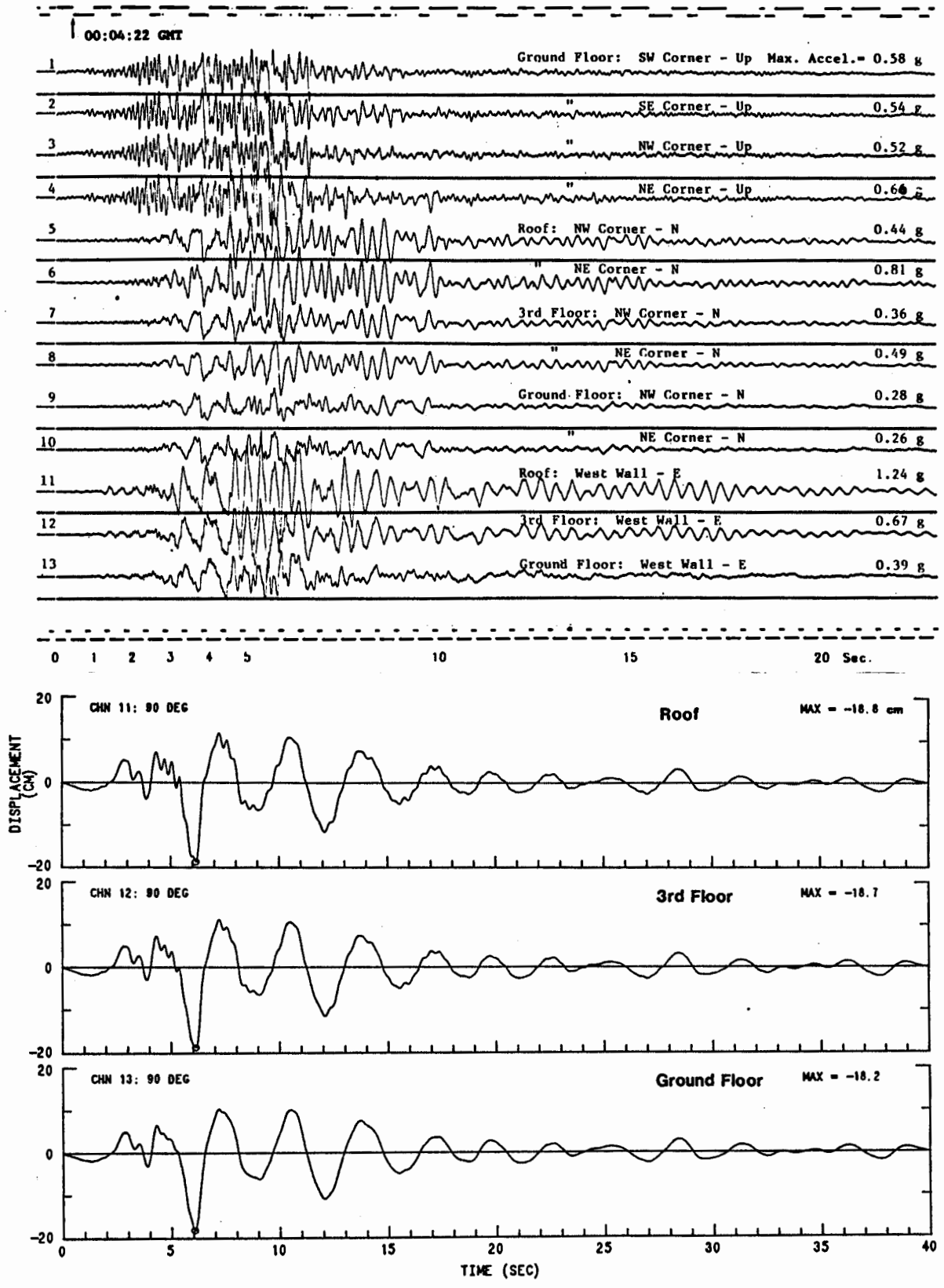

Fig. 5. Recorded accelerations from a 4-story concrete shear wall building in Watsonville (top), and the computed displacements at the roof, 3rd and ground floors in the EW direction (bottom). Note that the displacements are very similar because the building is relatively stiff. The building response is seen as the high frequency motion between 3 to 6 seconds in the roof and 3rd floor displacements.

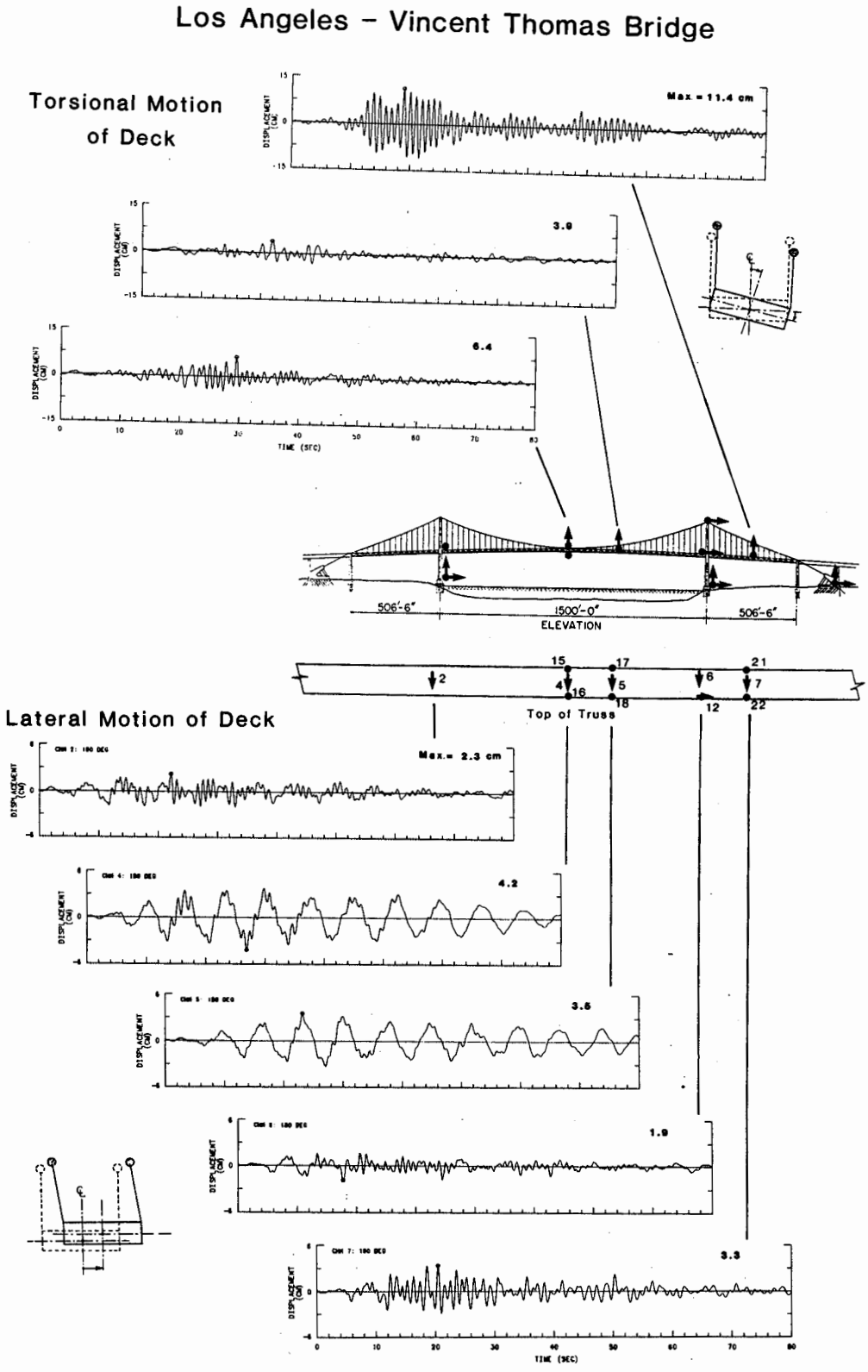

Fig. 6. The torsional and lateral displacements of the deck computed from the accelerations recorded at the Vincent Thomas bridge during the 1987 Whittier earthquake. A 7-second period can be seen in the center span lateral displacements. The torsional motion of the deck is dominated by a 1-second oscillation which has maximum displacement at the middle of the side span.

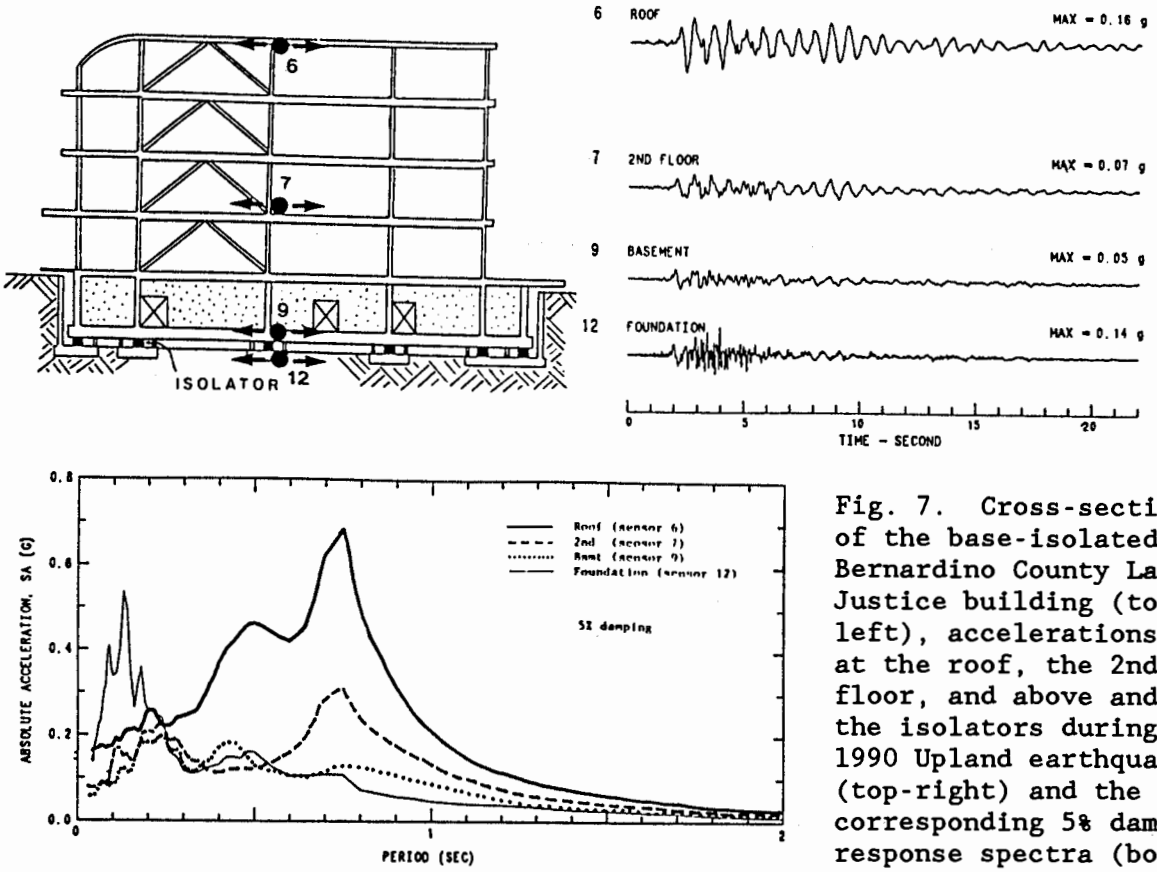

Fig. 7. Cross-section of the base-isolated San Bernardino County Law & Justice building (top-left), accelerations at the roof, the 2nd floor, and above and below the isolators during the 1990 Upland earthquake (top-right) and the corresponding 5% damping response spectra (bottom).

REFERENCES

1. Shakal, A., M. Huang, M. Reichle, C. Ventura, T. Cao, R. Sherburne, M. Savage, R. Darragh and C. Petersen (1989) "CSMIP Strong-Motion Records from the Santa Cruz Mountains (Loma Prieta), California Earthquake of 17 October 1989", Div. Mines and Geology Report No. OSMS 89-06.
2. Shakal, A., M. Huang, C. Ventura, D. Parke, T. Cao, R. Sherburne and R. Blazquez (1987) "CSMIP Strong-Motion Records from the Whittier, California Earthquake of 1 October 1987", Div. Mines and Geology Report OSMS 87-05.
3. Trifunac, M.D. and V.W. Lee (1979) "Automatic Digitization and Processing of Strong Motion Accelerograms", Report 79-15, University of Southern California, Los Angeles, California.
4. Maley, R., A. Acosta, F. Ellis, E. Etheredge, L. Foote, D. Johnson, R. Porcella, M. Salsman and J. Sitzer (1989) "U.S. Geological Survey records from the northern California (Loma Prieta) earthquake of October 17, 1989", U.S. Geological Survey Open-File Report 89-568.
5. Joyner, W. and D. Boore (1981) "Peak horizontal acceleration and velocity from strong-motion records including records from the 1979 Imperial Valley, California, earthquake", Bull. Seism. Soc. Amer., 71, 2011-2038.
6. Huang, M., T. Cao, U. Vetter and A. Shakal (1990) "Second Interim Set of CSMIP Processed Strong-Motion Records from the Santa Cruz Mountains (Loma Prieta) Earthquake of 17 October 1989", Div. Mines and Geology Report No. OSMS 90-01.

Directional Site Resonances Observed from the 1 October 1987 Whittier Narrows, California Earthquake and the 4 October Aftershock

John E. Vidale
Research Scientist, University of California at Santa Cruz

Ornella Bonamassa
Research Assistant

Heidi Houston
Research Scientist

Abstract

We present evidence that sites often resonate preferentially in a particular compass direction. The 1 October 1987 mainshock and 4 October 1987 aftershock in the Whittier Narrows, California, sequence had very different mechanisms. Nevertheless, at 8 of 11 strong motion stations for which digitized records of both events are available, the direction of strongest shaking in the two events was much more similar than would be expected from their different focal mechanisms. The coincidence of the polarizations from the two events was greatest for the frequencies at peaks in the spectra, suggesting that site amplification and directional resonances are linked. Knowledge of directional site resonances may aid in predicting the directions of damaging earthquake motions.

Introduction

The 1 October 1987 Whittier Narrows California (M_L = 5.9) earthquake and its 4 October aftershock (M_L = 5.3) created an excellent data set of strong motion recordings. These events produced nearly orthogonal radiation patterns. The mainshock had a thrust mechanism and the aftershock had a strike-slip mechanism. Observations from these two sources permit the isolation of site from source effects. Vidale (1989) showed that the 3 to 6 Hz peak accelerations of these two events are modulated by the focal mechanisms. In that study, only peak amplitudes from analog records were utilized. Since eleven records from the aftershock and numerous records from the main shock have now been digitized by the California Strong Motion Instrumentation Program (CSMIP) of the California Division of Mining and Geology, a more broadband quantitative analysis can be done.

Near-receiver geology is an important factor in determining the strength of shaking from an earthquake (Haukkson *et al.*, 1987, Malin *et al.*, 1988). Models of geology that assume homogeneous flat layers can explain some features of observed site amplification (e.g., Joyner *et al.*, 1976). For example, the amplification of 2 sec energy in the lakebed deposits in Mexico City during the 1985 Michoacan earthquake

dramatically showed the influence of thin, slow-velocity layers near the Earth's surface (e.g., Campillo *et al.*, 1989).

Patterns of amplification and duration of shaking that require lateral variations in geologic structure have also been documented (Vidale and Helmberger, 1987, 1988), and strong-motion effects of some simple large-scale structures have been investigated (Bard and Gariel, 1986, Kawase and Aki, 1989, Vidale *et al.*, 1985). However, the importance of near-receiver structures more realistic than horizontal layers has not been documented for high-frequency seismic energy. The data analyzed here indicate a need for an increased understanding of the effects of two- and three-dimensional structure near the receiver.

In this paper, to assess the prevalence of frequency- and direction-dependent station resonances, we compare the particle motions of S waves with those predicted from the earthquake focal mechanisms. It is of interest to earthquake engineers whether particular sites have a preferred direction of ground motion in a given frequency range. Initial results from Loma Prieta aftershock recordings (Bonamassa *et al.*, 1990) suggest that such effects occur for more than half the sites investigated, and that the preferred direction does not depend on earthquake location. The results below indicate that directional resonances are a general feature.

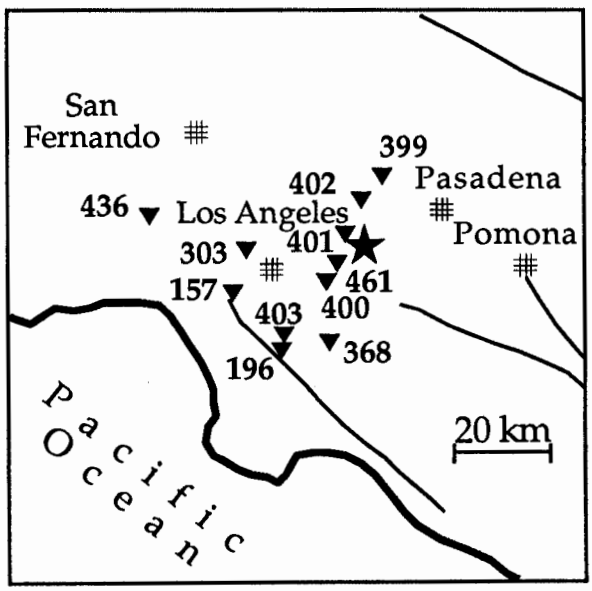

Figure 1. Map showing the location of the 11 CDMG stations. The star indicates the epicentral region of the mainshock and the aftershock, which are separated by only 2 km.

Polarization Analysis for 1 October and 4 October 1987 Whittier Narrows Events

We conduct analysis of the frequency content and polarization characteristics of the Whittier Narrows mainshock and an aftershock to understand the relative contributions of source and site to observed ground motions.

The mainshock hypocenter was located at 14.6 km depth, and the mechanism is a gently dipping thrust (Haukkson and Jones, 1989). Numerous aftershocks filled the volume from 8 to 17 km depth extending about 4 km in all directions horizontally. Bent and Helmberger (1989) analyzed the teleseismic body waves and proposed a double source; their second source is 11 km deep and 5 times larger than the first with a slightly different mechanism. It is important to consider the location and mechanism of the largest patch of moment release to understand the strong ground motions. The double source they propose is best studied with teleseismic body-waves since the strong ground motions are more complicated by the Los Angeles basin near-surface structure. We use the depth and mechanism of their second and largest source to represent the mainshock in this paper. The aftershock that occurred on 4 October 1987 was located 2 km northwest of the mainshock at a depth of 13.3 km, with a strike-slip mechanism on a vertical plane (Haukkson and Jones, 1989).

The 11 stations for which CDMG digitized strong motion records of both the mainshock and the aftershock are shown in Figure 1. The stations range from almost directly above the earthquakes to 50 km distant.

Acceleration spectra for the mainshock and aftershock are shown in Figure 2. The S waves are windowed into 4 sec and 2.5 sec segments for the mainshock and aftershock, respectively, and tapered, and then Fourier transformed. The frequency of the peak acceleration ranges from 1 Hz for station 368 (Downey) to 5-6 Hz for stations 399 (Mt. Wilson). In general, the two spectra from each of the 11 stations are similar, although the mainshock produced a higher level of acceleration.

We processed the Whittier Narrows strong motions as follows: 1) All three components of motion were filtered with a central frequency of 1, 2, 4, 8 and 16 Hz. 2) The particle motion of each filtered record is characterized by its predominant azimuth of polarization (see Vidale, 1986, and Montalbetti and Kanasewich, 1970, for details of polarization analysis). This azimuth of polarization is the equivalent to the direction of the largest excursions in a particle motion diagram. The predominant azimuth of particle motion is compared with the azimuth expected from the source and receiver locations and the focal mechanism of the earthquake.

This procedure is first illustrated in detail for station 157 (Baldwin Hills), then applied to the other ten stations. The S waves from station 157 are shown in Figure 3.

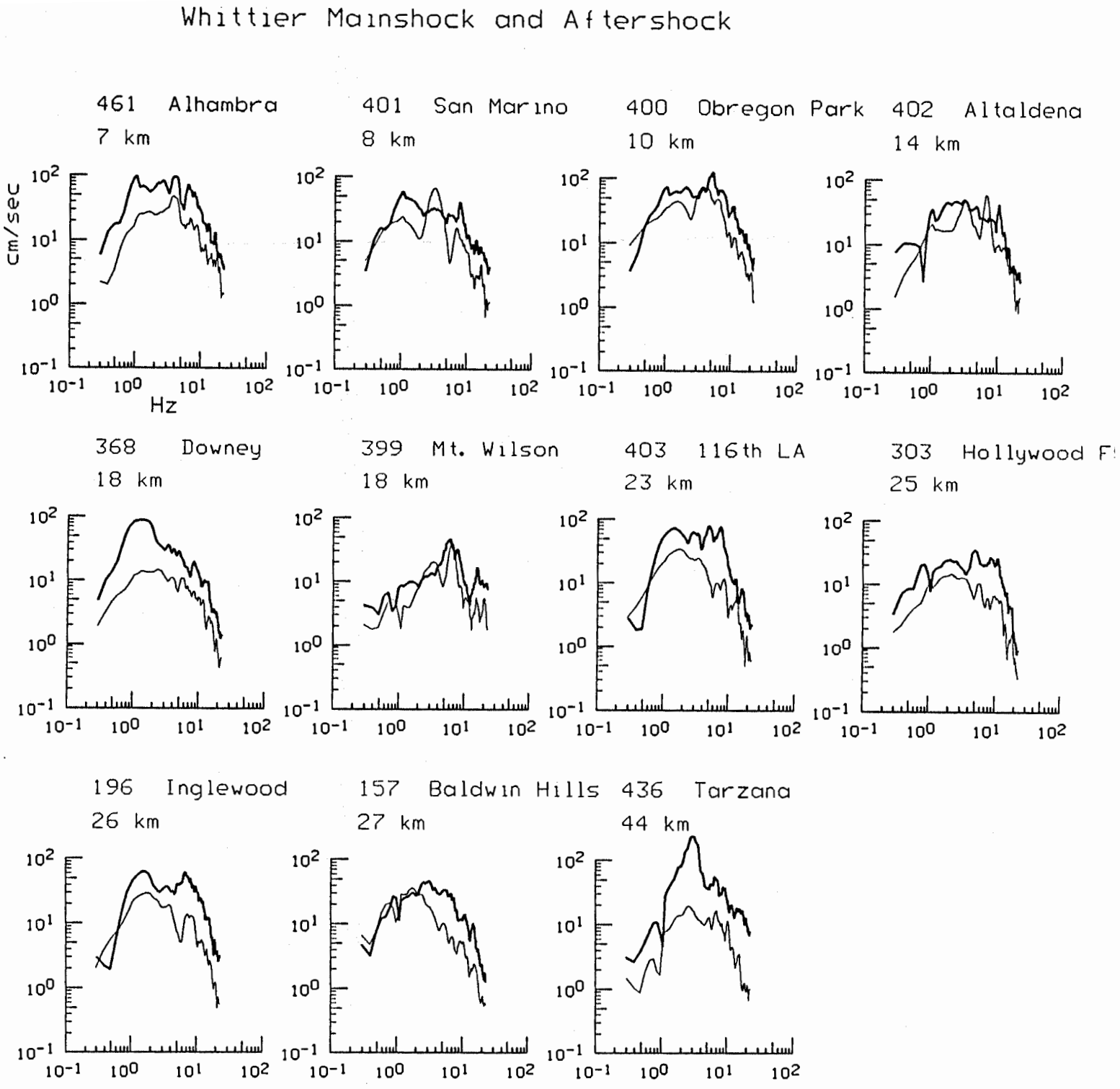

Figure 2. Comparison of acceleration spectra from October 1 mainshock (heavy lines) and October 4 aftershock (light lines) for 11 CSMIP stations. The distance in km from the epicenter is given beneath each station name. The RMS sum of the SH and SV motions is plotted.

Figure 4 shows the particle motions of the passband filtered horizontal motions at station 157, while Figure 5a shows the dominant direction of polarization in each passband. Polarization has the usual two-fold ambiguity, for example, north-south vibration has a direction of either north or south. We therefor plot polarization in the 180° range centered about north.

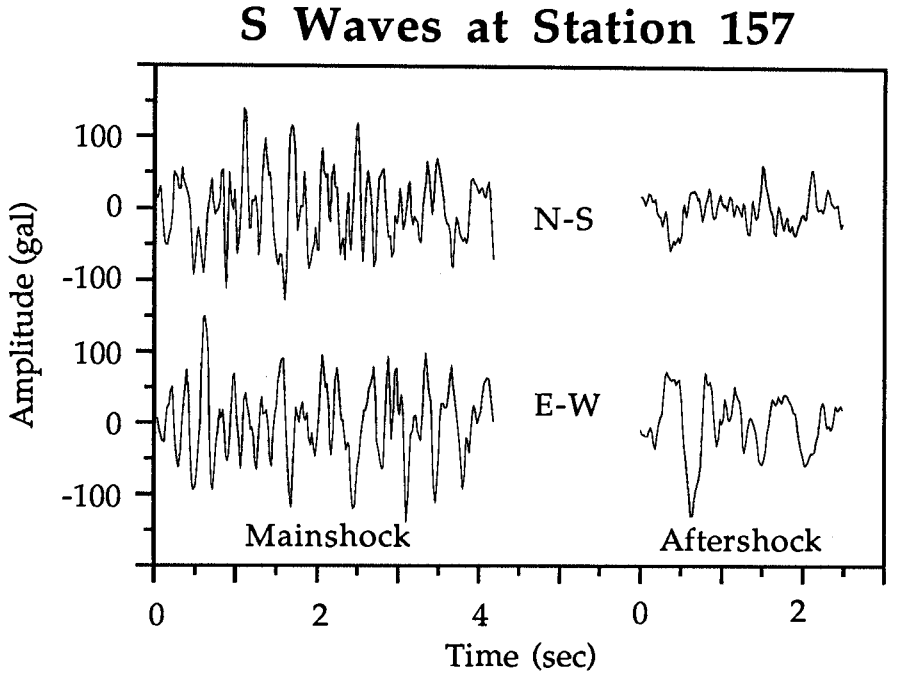

Figure 3. The windowed S waves for the mainshock and aftershock from station 157.

The polarization directions agree between the records for the two events in each pass band, but do not agree particularly well with the directions predicted by the focal mechanisms. The directions of polarization of the broadband signals shown at the right of Figure 5a are similar for the two earthquakes because the azimuths agree fairly well in the 2 and 4 Hz windows where station 157 recorded the strongest accelerations as is apparent in the spectrum in Figure 2. The polarization directions also agree between the two events in other passbands. The directions do not match well between different frequencies, however. These patterns can also be seen in Figure 4, particularly by comparing the 4 Hz and 8 Hz polarizations for the two events.

This pattern suggests that for station 157, 4 Hz shaking tends to be strong in the direction N30W, while 8 Hz shaking is strongest N75E, which is information that may be useful for earthquake engineers. This pattern also suggests that it is not the earthquake source that is controlling the polarization of the S waves at high

frequencies. The other ten stations also show similar patterns to varying extents. They are presented in order of increasing station number (i.e., random order).

Particle Motions for the Mainshock at Station 157

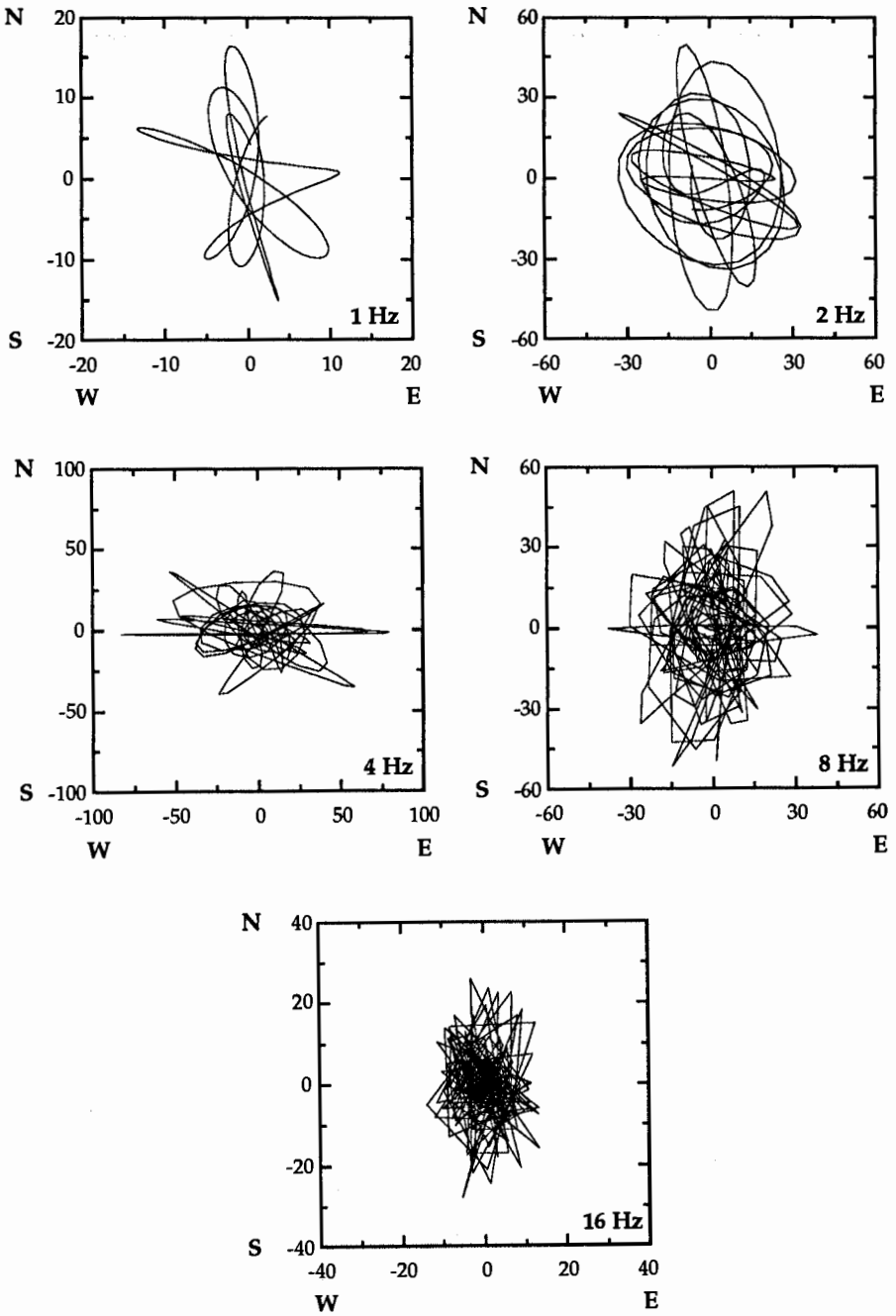

Figure 4a. Particle motion at station 157. Mainshock records bandpassed with 1, 2, 4, 8, and 16 Hz center frequencies.

Particle Motions for the 4 October Aftershock at Station 157

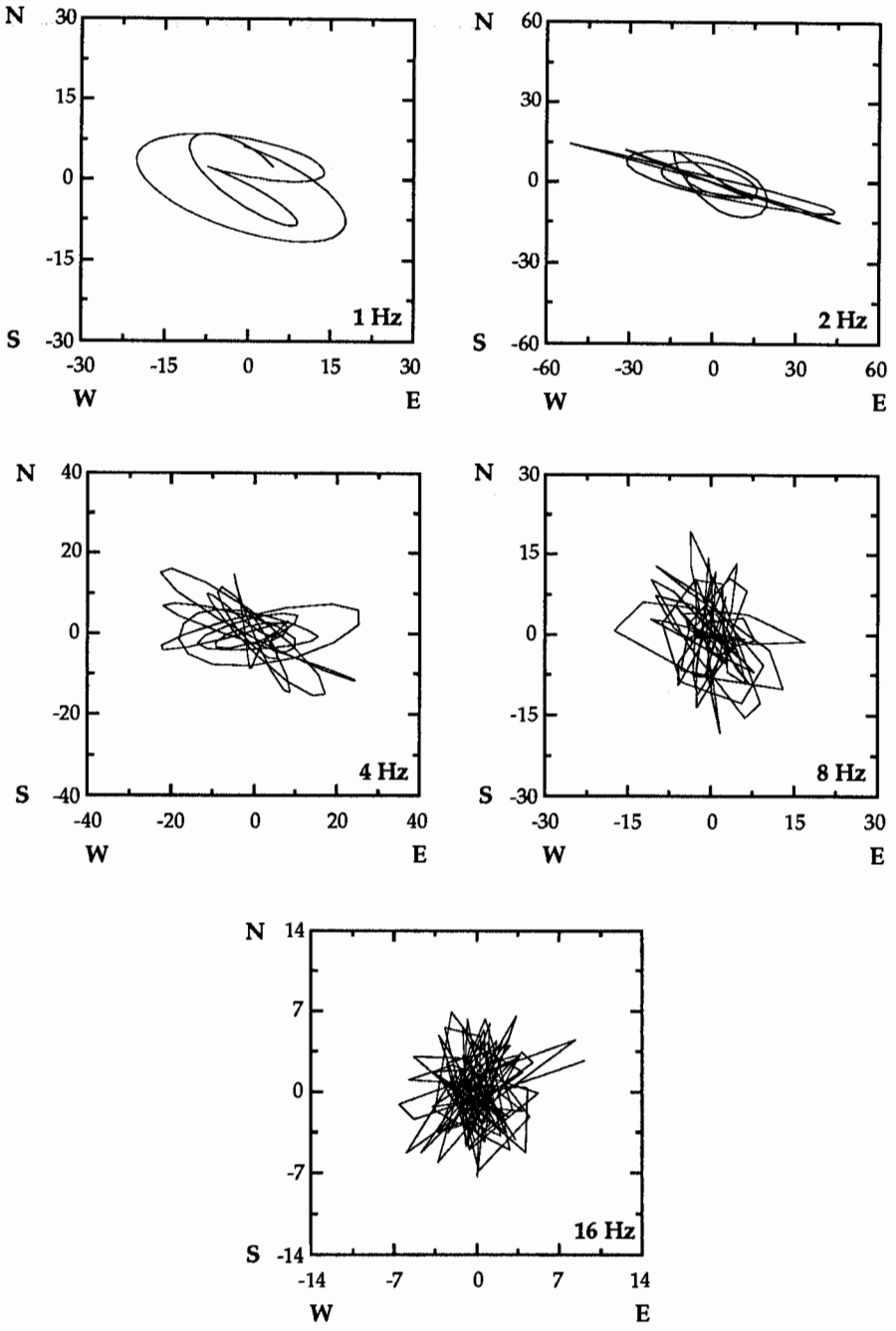

Figure 4b. Particle motion at station 157. Aftershock records bandpassed with 1, 2, 4, 8, and 16 Hz center frequencies.

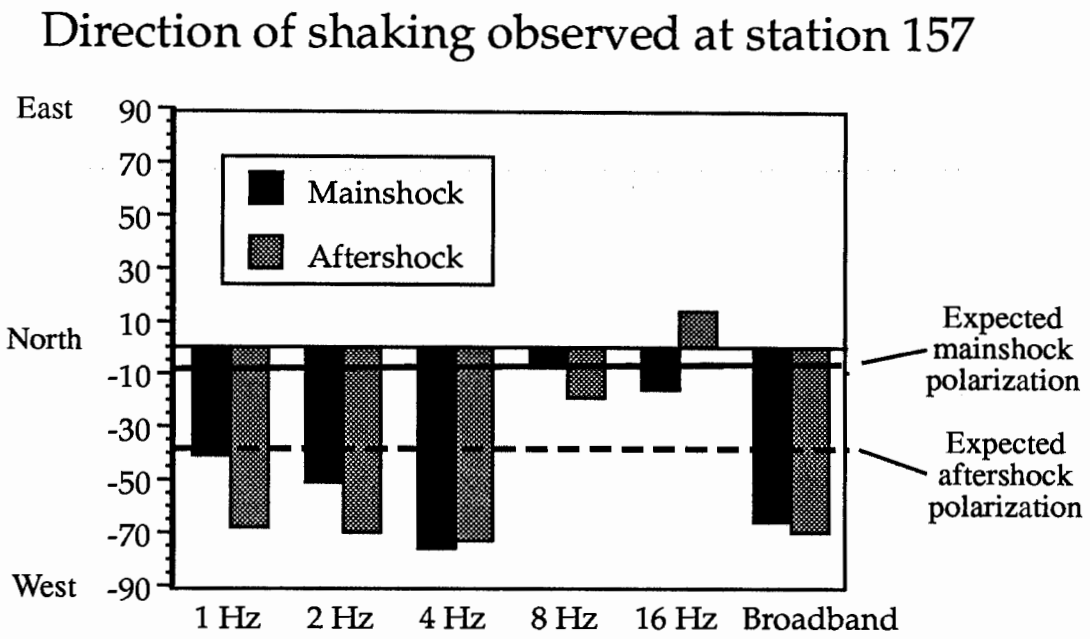

Figure 5a. The primary azimuth of particle motion during the mainshock and aftershock as a function of frequency. The solid and dashed lines indicate the azimuth of polarization expected from the focal mechanisms of the two events, and the bars indicate the polarization measured from the observations. Polarization is measured clockwise from north (north = 0°, northeast = 45°). The polarizations of the mainshock and aftershock are more similar to each other than to the predictions from their respective focal mechanisms.

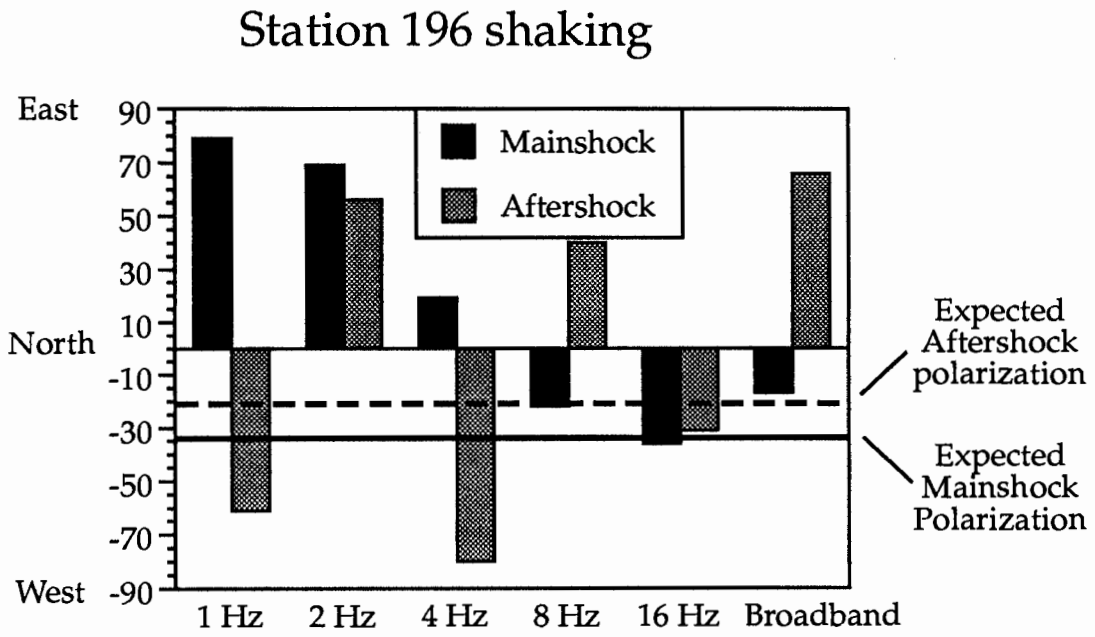

Figure 5b. The azimuth of particle motion of the mainshock and aftershock as a function of frequency for station 196. See caption for Figure 5a.

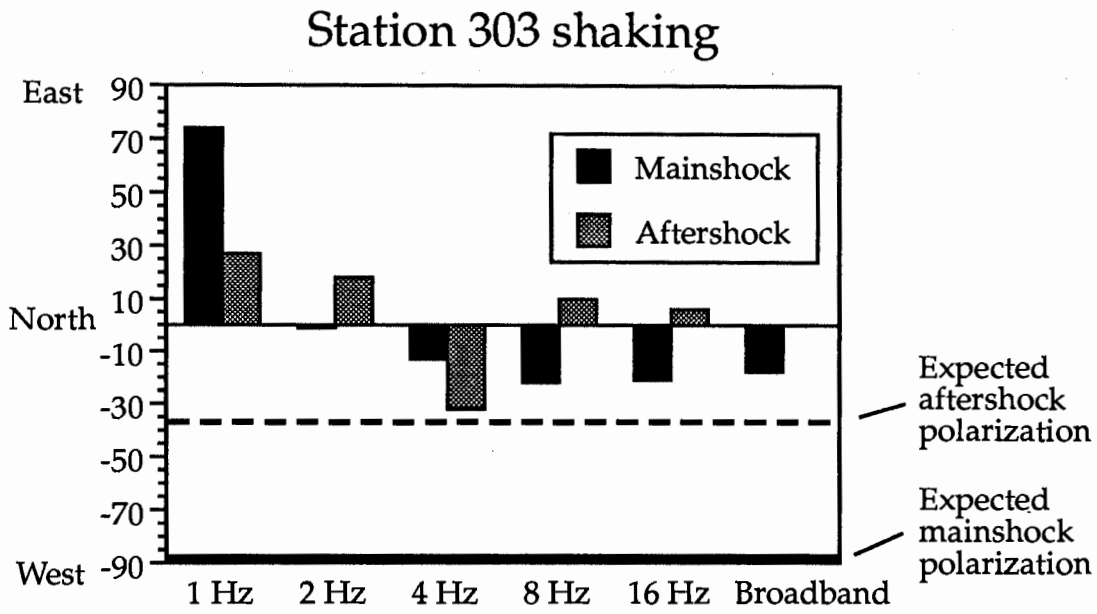

Figure 5c. The azimuth of particle motion of the mainshock and aftershock as a function of frequency for station 303. See caption for Figure 5a.

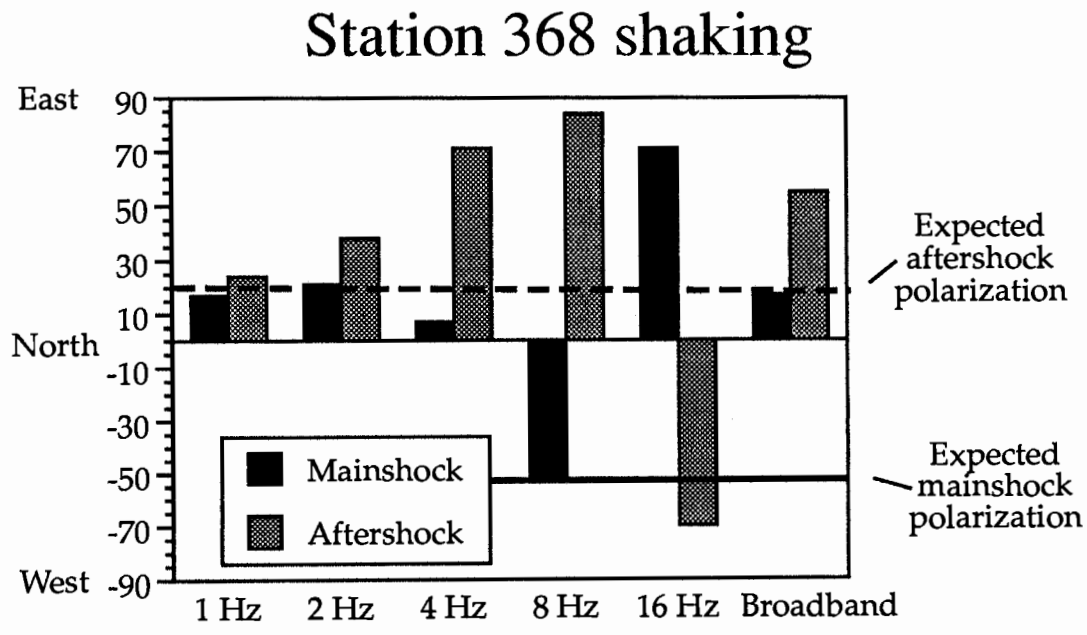

Figure 5d. The azimuth of particle motion of the mainshock and aftershock as a function of frequency for station 368. See caption for Figure 5a.

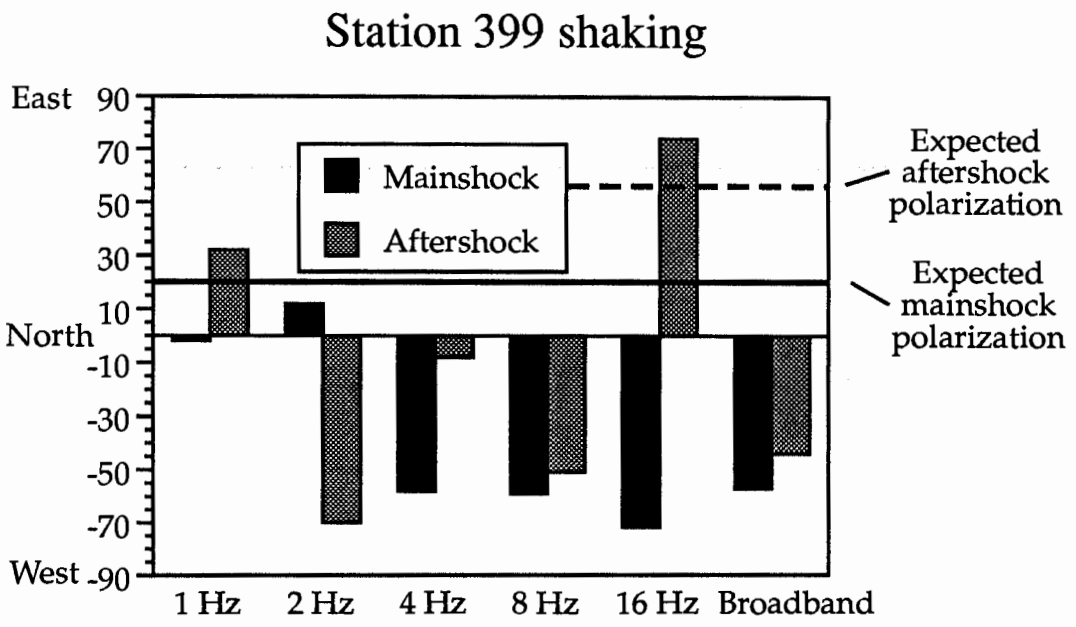

Figure 5e. The azimuth of particle motion of the mainshock and aftershock as a function of frequency for station 399. See caption for Figure 5a.

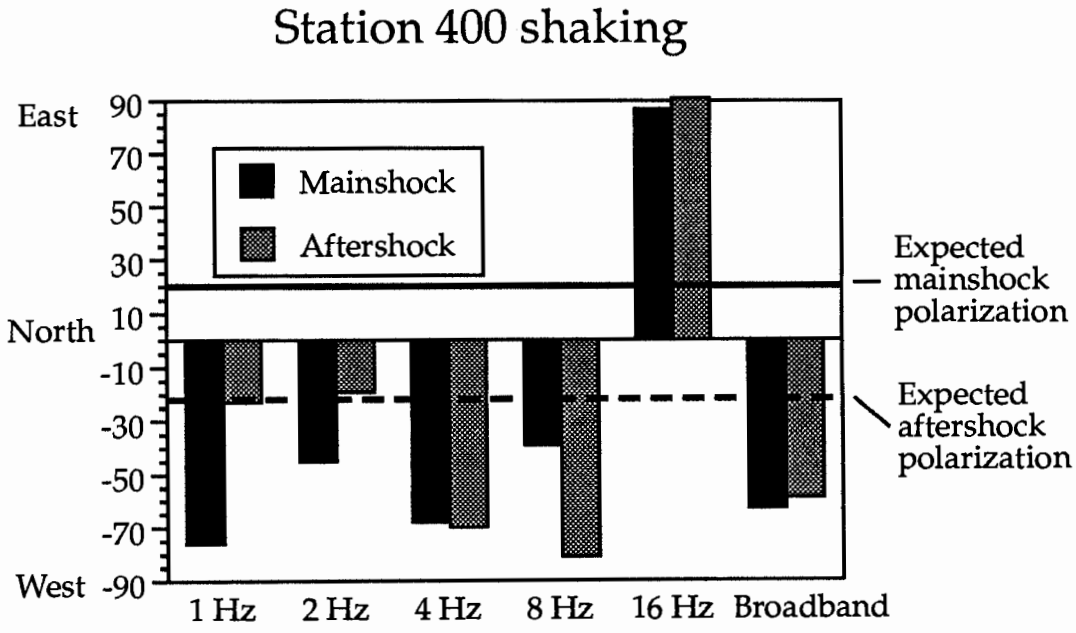

Figure 5f. The azimuth of particle motion of the mainshock and aftershock as a function of frequency for station 400. See caption for Figure 5a.

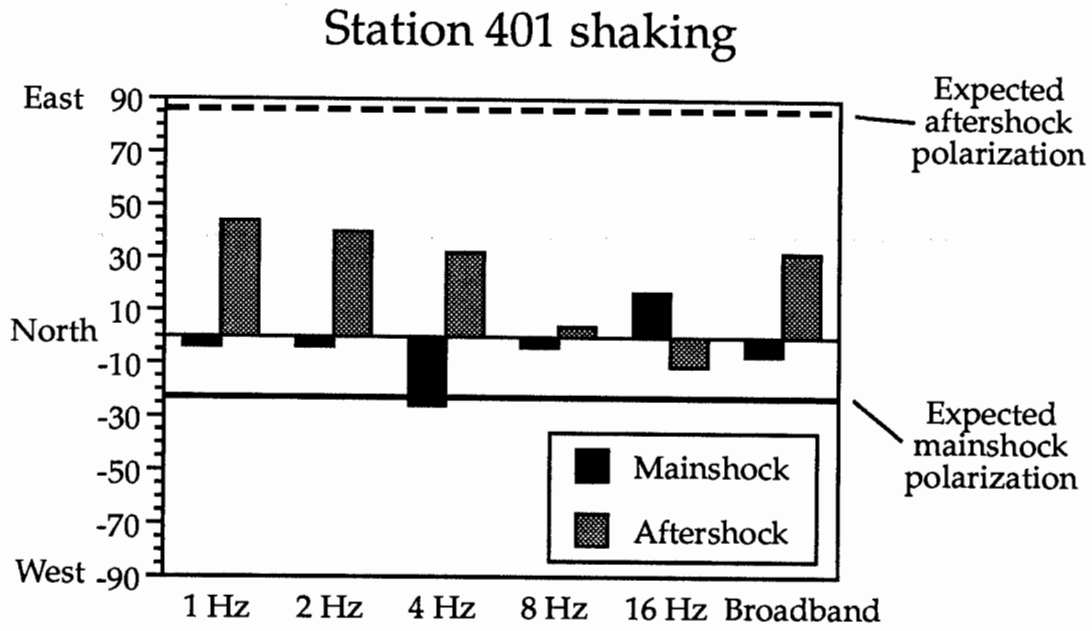

Figure 5g. The azimuth of particle motion of the mainshock and aftershock as a function of frequency for station 401. See caption for Figure 5a.

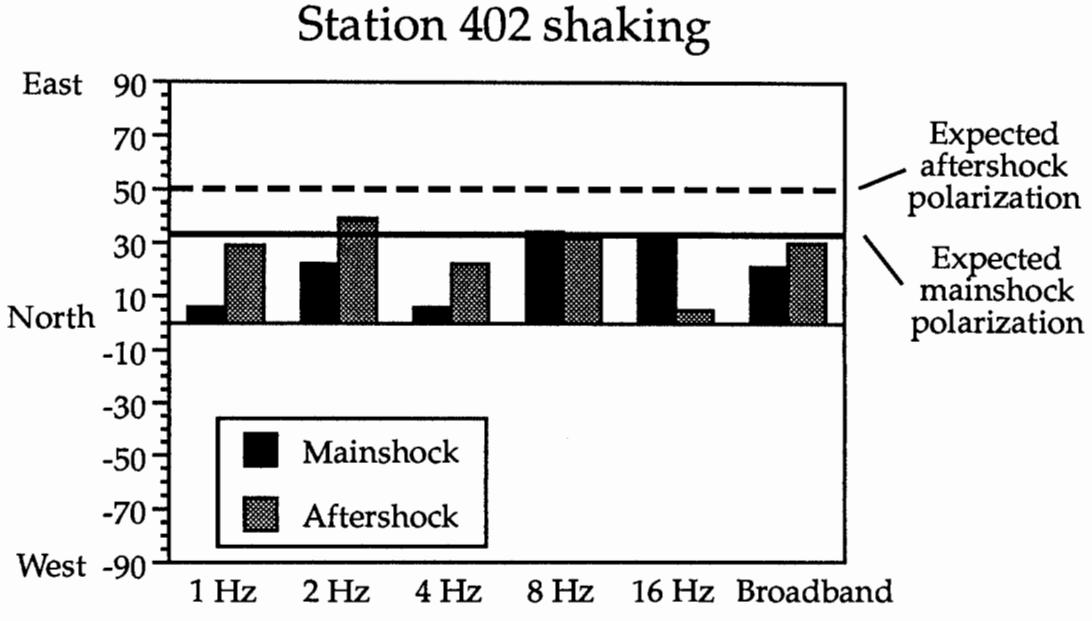

Figure 5h. The azimuth of particle motion of the mainshock and aftershock as a function of frequency for station 402. See caption for Figure 5a.

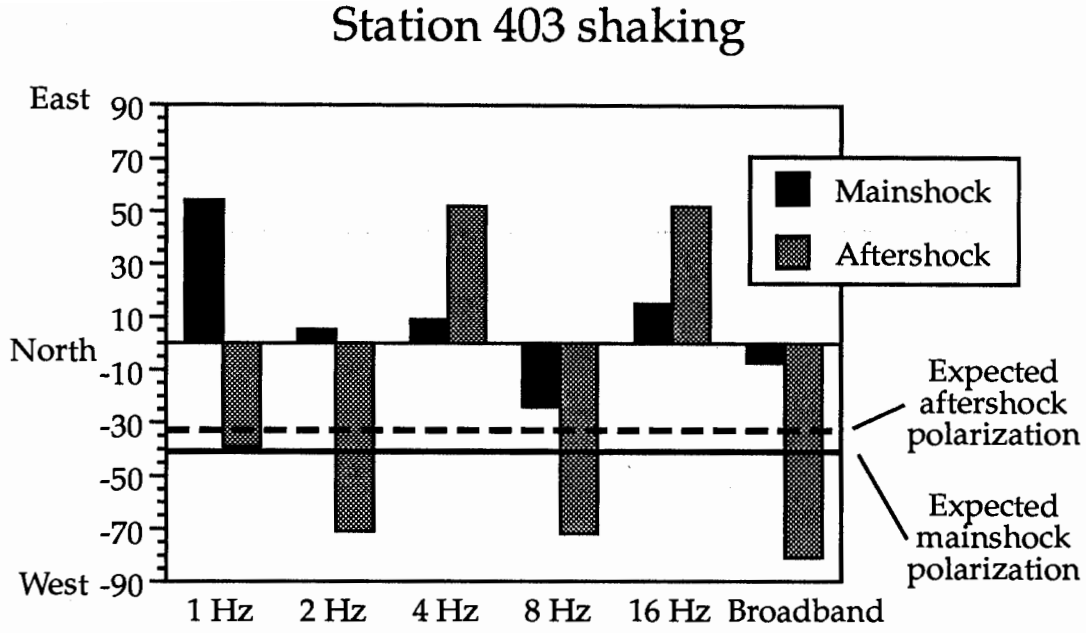

Figure 5i. The azimuth of particle motion of the mainshock and aftershock as a function of frequency for station 403. See caption for Figure 5a.

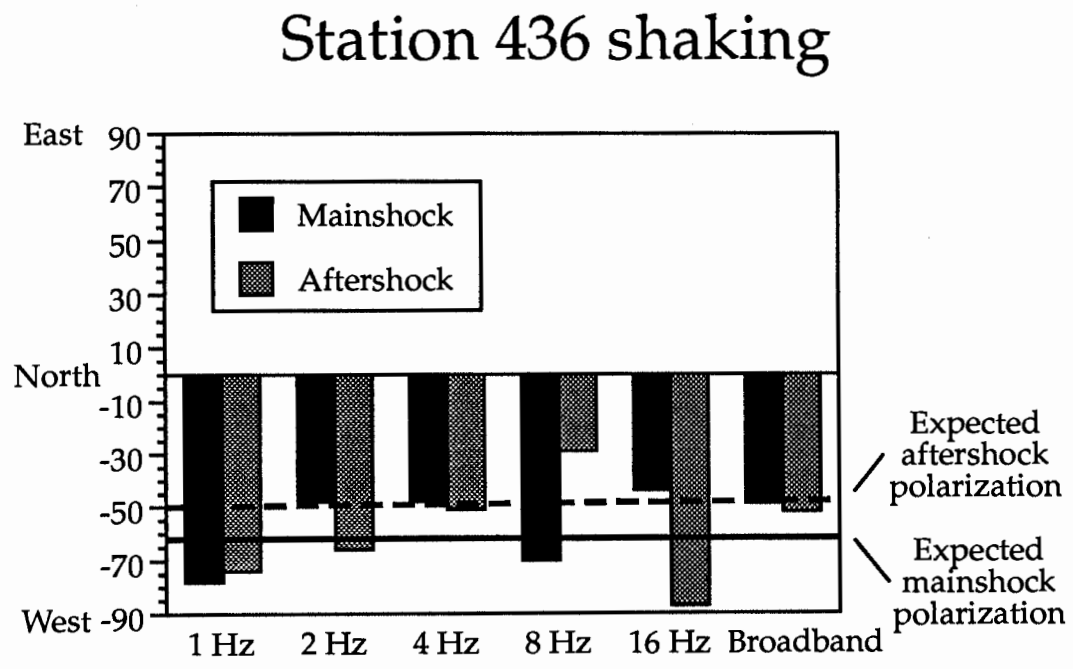

Figure 5j. The azimuth of particle motion of the mainshock and aftershock as a function of frequency for station 436. See caption for Figure 5a.

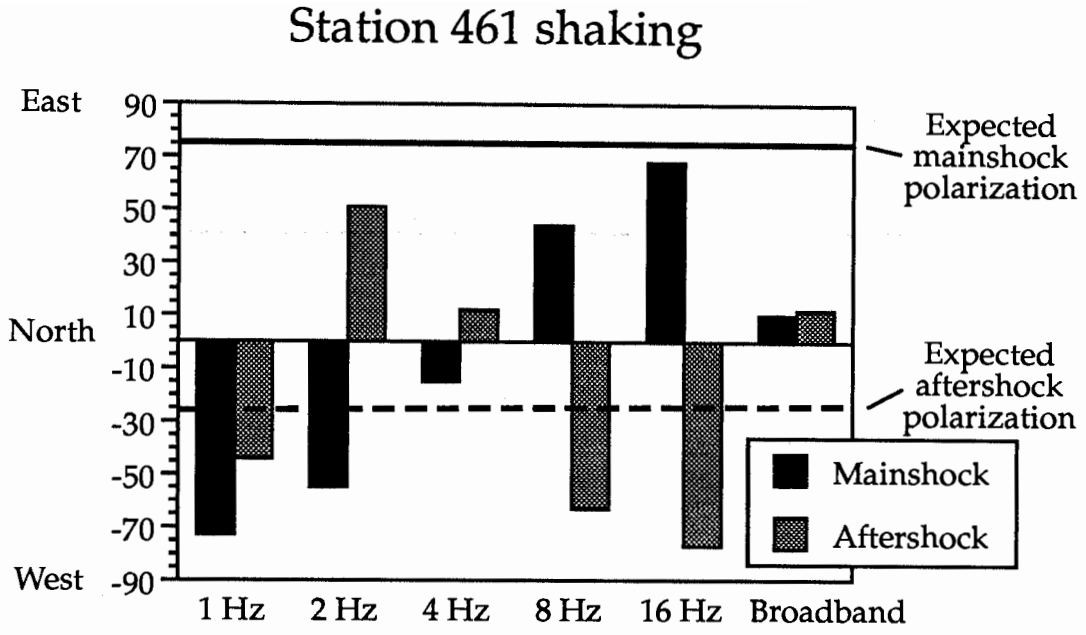

Figure 5k. The azimuth of particle motion of the mainshock and aftershock as a function of frequency for station 461. See caption for Figure 5a.

Station 196 (Inglewood) does not show agreement between the two events in broadband polarization direction, as seen in Figure 5b. Closer examination reveals some evidence for directional site effects, however. The strongest peaks in the two spectra for this station in Figure 2 lie at 2 Hz, and at this frequency the polarization directions agree between the mainshock and the aftershock. The broadband disagreement arises from stronger high frequency energy in the mainshock, but more energy at 1 Hz in the aftershock.

Figure 5c shows good agreement in the broadband polarization for station 303 (Hollywood), despite a large difference in the polarizations predicted by the focal mechanisms. The spectra for this station do not show prominent peaks.

Figure 5d, for station 368 (Downey) shows that the directions of polarization are closer to each other than expected from the focal mechanisms. The 1 Hz passband, which has the largest spectral peak for the mainshock, shows excellent agreement in polarization.

Figure 5e shows the polarization for station 399 (Mt. Wilson). The polarization directions for the two events agree in most pass bands, but again do not agree particularly well with the directions predicted by the focal mechanisms. The azimuths agree fairly well in the 4 and 8 Hz windows where station 399 recorded the strongest accelerations (see Figure 2), and thus again the directions of polarization shown at the right of Figure 5e are very similar for the two earthquakes.

Station 400 (Figure 5f, Obregon Park) has good agreement in polarization direction at 4 Hz, where there is a peak in the spectra. The predicted directions from the focal mechanism are not similar to the observed directions.

Station 401 (Figure 5g, San Marino) does not have good agreement in polarization direction, although even greater disagreement in polarization direction is predicted by the focal mechanism. Different peaks appear in the spectra of the mainshock and aftershock, but no particular pattern is seen.

Station 402 (Figure 5h, Altadena) shows excellent agreement, even better than is predicted from the focal mechanisms. These signals seem coherently polarized at all frequencies, and close to the predicted directions.

Station 403 (Figure 5i, 116th St., Los Angeles) shows poor agreement in polarization direction despite the prediction of good agreement from the focal mechanisms.

Station 436 (Figure 5j, Tarzana) shows excellent agreement in the dominant direction of polarization, perhaps controlled by the sharp peak at 3 Hz. The mainshock and the aftershock are predicted to have a similar direction of polarization. This suggests that the discrepancy between the anomalous amplification seen in Tarzana from the mainshock and the more normal aftershock spectra is *not* due to a difference in the polarization of the incident S waves, which might have resulted in different levels of amplification at Tarzana in the two events.

Station 461 (Figure 5k, Alhambra) shows excellent agreement in broadband polarization direction despite the prediction of orthogonal motion from the focal mechanisms. The spectra are relatively flat.

Figure 6 shows that eight (157, 303, 368, 399, 400, 402, 436, 461) of the eleven stations have similar polarizations for the mainshock and the aftershock. This suggests that a majority of the stations may have a characteristic direction of polarization, which does not change from event to event.

Previous work (Vidale, 1989) on the Whittier Narrows sequence suggests that the focal mechanism controls peak acceleration at a site, but the data presented here indicate that in many cases, the azimuth of polarization of the motion in the range 1-16 Hz depends on the site. In addition, in several cases, including stations 157, 196, 368, 399, 400, 436, the most similarity between the mainshock and aftershock polarizations is in the pass band where spectral peaks appear, suggesting that the geologic features that enhance amplitudes in a particular frequency band also have a preferred direction of particle motion. The 11 stations span a wide range of surficial geology from hard rock to soft sediment, summarized in Table 1, suggesting that these directional resonances are probably a common feature.

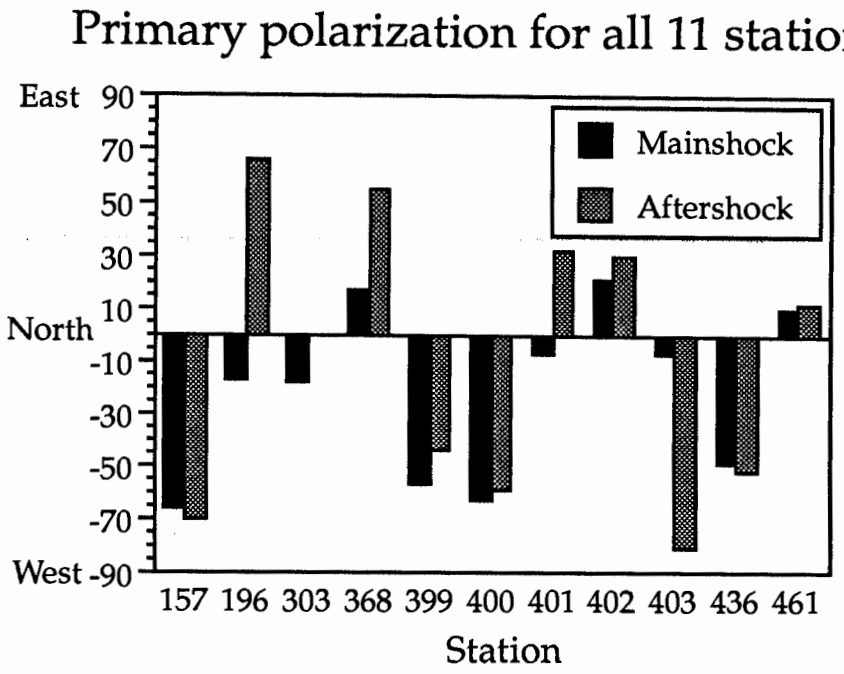

Figure 6. Observed directions of the strongest polarization of the broadband signal for acceleration records from the Whittier Narrows mainshock and aftershock for 11 stations. The predicted polarizations from the first-motion focal mechanisms do not agree as well. Polarizations are measured clockwise from north.

The present study provides results that complement those of Bonamassa *et al.* (1990). Bonamassa *et al.* (1990) find that S waves from 11 aftershocks of the Loma Prieta earthquake recorded at a dense 6-station 3-component array in the Santa Cruz mountains show directional resonances. The resonances vary within the array on a scale of 25 meters, but persist for a given station for a range of earthquake locations and expected S-wave polarizations. The rapid variation across the array suggests very near-surface structure is causing the resonances. The present study has higher quality stations that are situated in a wider range of surficial geologies, suggesting that these resonances are a common occurrence.

The most likely explanation for these azimuthal patterns is that particle motion in one compass direction is amplified compared to the motion in other directions. The specific geological structures that cause this amplification are not yet known. Surface topography seems unlikely, as Buchbinder and Haddon (1990) estimate only small S-wave azimuthal anomalies due to topography. The most likely structures are strong lateral variation in the S-wave velocity in the top 10's of meters, where velocity can be very low.

Conclusions

Three-component seismic recordings for 8 of 11 stations of the Whittier Narrows earthquake sequence show that in the frequency range from 1 to 16 Hertz, there is a

preferred direction of ground motion, which we term "directional resonance" that does not depend on the polarization of the shear waves expected from the focal mechanism. The study of Bonamassa et al. (1990) also finds directional resonances and suggests that the preferred direction also does not depend on the earthquake location. The coincidence of the polarizations from the two events was greatest for the frequencies at peaks in the spectra, suggesting that site amplification and directional resonances are linked. This study has focused on S waves since they carry the largest amplitude motions in the near-field and are of interest to earthquake engineers.

These preliminary conclusions drawn from good data for various sites in the Los Angeles area suggest that in-depth analysis of the processes that control directional resonances is necessary. Earthquake engineers as well as seismologists will benefit from knowledge of the strength of the characteristic resonance at a site and the area over which it is coherent.

Acknowledgements

This work was supported by the California Department of Conservation, Division of Mines and Geology, Strong Motion Instrumentation Program under contract number OSMS 8-8068. The contents of this paper were developed under a contract from the California Department of Conservation, Division of Mines and Geology, Strong Motion Instrumentation Program. However, those contents do not necessarily represent the policy of the agency, and you should not assume endorsement by the State Government. Support for this work has been provided in part by a grant from the W.M. Keck Foundation, and the Institute of Tectonics, University of California, Santa Cruz.

References

Bard, P.-Y., J.C. Gariel, 1986. The seismic response of two-dimensional sedimentary deposits with large vertical velocity gradients, *Bull. Seism. Soc. Am.*, **76**, 343-360.

Bent, A.L., and D.V. Helmberger, 1989. Source complexity of the 1 October 1987 Whittier Narrows Earthquake, *J. Geophys. Res.*, **94**, 9548-9556.

Blakeslee, S.N., 1989. Studies in near-surface, crustal and fault-zone attenuation: borehole analysis of Parkfield earthquakes, *Ph.D. Thesis*, University of California at Santa Barbara.

Bonamassa, O., J.E. Vidale, S.Y. Schwartz, 1990. Observations of directional site resonances from the Loma Prieta earthquake sequence, in preparation for *Bull. Seism. Soc. Am...*

Buchbinder, G.G.R., and R.A.W. Haddon, 1990. Azimuthal anomalies of short period P-wave arrivals from Nahanni aftershocks, N.W.T., Canada and effects of surface topography, *Bull. Seism. Soc. Am.*, in press.

Campillo, M., J.C. Gariel, K. Aki, and F.J. Sánchez-Sesma, 1989. Destructive strong ground motion in Mexico City: source path and site effects during the great 1985 Michoacán earthquake, *Bull. Seism. Soc. Am.*, **79**, 1718-1734.

Haukkson, E., and L. Jones, (1989). The 1987 Whittier Narrows Earthquake sequence in Los Angeles, southern California, seismological and tectonic analysis, *J. Geophys. Res.*, **94**, 9569-9590.

Haukkson, E., T.-L. Teng, T.L. Henyey, 1987. Results from a 1500 m deep, three-level downhole seismometer array, *Bull. Seism. Soc. Am.*, **77**, 1883-1904.

Joyner, W.B., R.E. Warrick, and A.A. Oliver, III, 1976. Analysis of seismograms from a downhole array in sediments near San Francisco Bay, *Bull. Seism. Soc. Am.*, **66**, 937-958.

Kanamori, H., 1979. A semi-empirical approach to prediction of long-period ground motions from great earthquakes, *Bull. Seism. Soc. Am.*, **69**, 1645-1670.

Kawase, H. and K. Aki, 1989. A study on the response of a soft basin for incident S, P, and Rayleigh waves with special reference to the long duration observed in Mexico City, *Bull. Seism. Soc. Am.*, **79**, 1361-1382.

Malin, P.E., J.A. Waller, R.D. Borcherdt, E. Cranswick, E.G. Jensen, and N. Van Schaak, 1988. Vertical seismic profiling of Oroville microearthquakes: velocity spectra and particle motion as a function of depth, *Bull. Seism. Soc. Am.*, **78**, 401-420.

Montalbetti, J.R., and E.R. Kanasewich, 1970. Enhancement of teleseismic body phases with a polarization filter, *Geophys. J. R. astr. Soc.*, **21**, 119-129.

Vidale, J.E., 1986. Complex polarization analysis of particle motion, *Bull. Seism. Soc. Am.*, **76**, 1393-1406.

Vidale, J.E., 1989. Influence of focal mechanism on peak accelerations for the Whittier Narrows, Ca. earthquake and an aftershock, *J. Geophys. Res.*, **94**, 9607-9615.

Vidale, J.E., and D.V. Helmberger, 1987. Path effects in strong motion seismology, chapter in volume of *Methods of Computational Physics*, Bruce Bolt, ed., 267-319.

Vidale, J.E., and D.V. Helmberger, 1988. Elastic finite-difference modeling of the 1971 San Fernando, Ca. earthquake, *Bull. Seism. Soc. Am.*, **78**, 122-142.

Table 1 : Stations co-ordinates and geology

Station	Latitude	Longitude	Directional Resonance	Surficial Geology
157	34.01	118.36	Yes	Fill over shale, sandstone
196	33.90	118.28	No	Terrace deposits
303	34.09	118.34	Yes	Alluvium (130 m) over sandstone, shale
368	33.92	118.17	Yes	Deep alluvium
399	34.22	118.06	Yes	Quartz Diorite
400	34.04	118.18	Yes	Alluvium
401	34.11	118.13	No	Alluvium
402	34.18	118.10	Yes	Alluvium
403	33.93	118.26	No	Terrace deposits
436	34.16	118.53	Yes	Shallow alluvium (10 m) over sandstone, shale
461	34.07	118.15	Yes	Alluvium

STRENGTH AND DUCTILITY DEMANDS FOR SDOF AND MDOF SYSTEMS SUBJECTED TO WHITTIER NARROWS EARTHQUAKE GROUND MOTIONS

H. Krawinkler
Professor of Civil Engineering, Stanford University

A. Nassar
Research Assistant, Stanford University

ABSTRACT

This paper summarizes parts of a project that is concerned with an evaluation of the damage potential of the October 1, 1987 Whittier Narrows ground motions. The discussion focuses on strength and ductility demands imposed by these ground motions on single degree of freedom (SDOF) and multi-degree of freedom (MDOF) systems. In the SDOF study, bilinear as well as stiffness degrading models are evaluated. A procedure is presented that permits the evaluation of strength demands for MDOF systems based on inelastic strength demand spectra of SDOF systems.

INTRODUCTION

Proper seismic design implies that strength and deformation capacities of structures should exceed the demands imposed by severe earthquakes with an adequate margin of safety. This simple statement is difficult to implement because both demands and capacities are inherently uncertain and dependent on a great number of variables. Moreover, more knowledge has to be acquired on the relative importance of different demand and capacity parameters and on the methods of incorporating these parameters in design without unduly complicating the design process. For these and many other reasons, code design is presently based on simplified procedures that have no transparent relation to many of the demand and capacity parameters that dominate the seismic response of structures.

A desirable long-range objective of research in earthquake engineering is to provide the basic knowledge needed to permit a simple but explicit incorporation of relevant demand and capacity parameters in the design process. To this end, much work needs to be done. Identification and evaluation of relevant ground motion and seismic demand parameters is one aspect of this work. To this date the earthquake engineering profession has not succeeded in identifying and quantifying a set of ground motion and seismic demand parameters that is sufficiently complete, yet simple enough, to permit capacity/demand based code design. In this context, a demand parameter is defined as a quantity that relates seismic input (ground motion) to structural response. Thus, it is a response quantity, obtained by filtering the ground motion through a linear or nonlinear structural filter. A simple example of a demand parameter is the acceleration response spectrum, which identifies the strength demand for an elastic SDOF system. Considering that most structures behave inelastically in a major earthquake, it is evident that this parameter alone is insufficient to describe seismic demands.

The Whittier Narrows earthquake provided an extensive set of ground motion records and damage information. It is the objective of this study to utilize the CSMIP ground motion data to evaluate basic seismic demand parameters, search for patterns in their characteristics, study the

attenuation of the parameters, and use the demand information together with capacity information on several types of code designed structures to assess the damage potential of the Whittier Narrows ground motions. The early results of this study have been summarized in [Krawinkler and Nassar, 1989]. The discussion presented here focuses an evaluation of strength and ductility demands, with an emphasis on MDOF systems. In order to put this issue in perspective it is necessary first to identify the objectives of demand and capacity based seismic design, a design approach that shows much potential for improvement of present design practice.

DEMAND AND CAPACITY BASED SEISMIC DESIGN

Good seismic design implies that structural capacities should exceed demands imposed by earthquakes with a sufficient margin of safety to provide adequate protection, with due consideration given to the uncertainties inherent in demands and capacities. Demands are response quantities that affect capacities and can be computed from ground motion and structural system characteristics, and include, amongst others, elastic strength demand, $F_{y.e}$, inelastic strength demands, $F_y(\mu)$, ductility demand, μ, strength reduction factors, $R_y(\mu) = F_{y.e}/F_y(\mu)$, and cumulative damage demands, of which energy demands are a subset. Definitions of these terms are given in [Krawinkler and Nassar, 1989].

Capacities are limiting values of the same response quantities, employed to assure adequate safety against failure. From the aforementioned quantities, ductility, or more specific, local or element ductility, appears to be the fundamental capacity parameter. If an element fails in a non-ductile mode (e.g., connections, or columns under axial compression), its ductility capacity is 1.0 or smaller. If an element exhibits ductile behavior (e.g., flexural hinging in beams), its ductility capacity is larger than 1.0. The magnitude of the ductility capacity of an element is a matter of structural behavior and will depend also on cumulative damage demands. Explicit consideration of cumulative damage demands (e.g., hysteretic energy dissipation) in design is possible but may unduly complicate the design process. Due consideration can be given to these demands by modifying the ductility capacity for strong motion duration, energy dissipation demands, or other cumulative damage parameters.

If <u>ductility</u> is used as a basic capacity parameter for design, then <u>strength</u> becomes a dependent quantity than can be derived from the criterion that ductility capacity must exceed ductility demand. This is believed to be the intent of code design, but the implementation in present codes is implicit and nontransparent. Explicit consideration of ductility capacity in design is feasible, as has been pointed out in many recent, and some old, technical papers. A framework for ductility based design has recently been proposed [Osteraas and Krawinkler, 1990]. Implementation of this design procedure requires, amongst other, much more information on seismic demands.

The Whittier Narrows earthquake has provided an extensive ground motion data set from a single earthquake, permitting statistical studies as well as an evaluation of attenuation of relevant seismic demand parameters. A total of 33 CSMIP ground motions recorded in this earthquake are used in this study to evaluate these parameters for SDOF and MDOF systems.

SEISMIC DEMANDS FOR SDOF SYSTEMS

A great number of demand parameters have been investigated in this study, with some of the results summarized in [Krawinkler and Nassar, 1989].and presented, wherever possible, in terms of spectra that vary with epicentral distance. Initially the analysis was performed with bilinear SDOF systems with 10% strainhardening and 5% damping. Recently the analysis was repeated with stiffness degrading systems in order to evaluate the effect of stiffness degradation on important demand parameters. A typical comparison of strength demands for bilinear and stiffness degrading systems is shown in Fig. 1. The stiffness degradation model used in this analysis was a modified Clough model illustrated in Fig. 2.

The general conclusion from this part of the study is that stiffness degradation of the type represented by the modified Clough model does not have a dominant effect on most of the important demand parameters. This can be seen in the example presented in Fig. 1. The illustrated inelastic strength demand spectra for μ = 2, 3, and 4, which apply for an epicentral distance of 10 km and are developed from a regression analysis, differ very little between the bilinear and stiffness degrading model. Comprehensive results of the evaluation of SDOF seismic demands will be presented soon in a report to be submitted to CDMG.

EFFECT OF HIGHER MODES ON SEISMIC DEMANDS FOR MDOF SYSTEMS

The previous discussion has focused on the nonlinear dynamic response of SDOF systems. Unfortunately, most real structures are MDOF systems affected by several translational and torsional modes. For elastic MDOF systems, combination of modal responses using SRSS, CQC, or other approaches, provides reasonable estimates of peak dynamic response characteristics. For inelastic MDOF systems, modal superposition cannot be applied with any degree of confidence. Thus, it becomes a matter of much interest to find out if and how the demand predictions for SDOF systems can be applied to MDOF structures.

In the pilot study summarized here it is assumed that only translational response needs to be considered; torsion is neglected. Thus, structures are modeled two-dimensionally. A series of structures are designed and subjected to the 33 ground motions used in the SDOF response study. Of primary interest are strength and ductility demands since they are basic design parameters that can be compared directly to counterparts in the SDOF study.

The following assumptions are made in the design of the MDOF structures:

- Only structures with 2, 5, 10, 20, 30, and 40 stories are considered. Equal mass is assumed for each story and the height of each story is taken as 12 ft.

- Structures are modeled as single bay frames and are of one of the following two types: "Column Hinge" model, from here on called CH model (Fig. 3(a)), or "Beam Hinge" model, from here on called BH model (Fig. 3(b)). A clear distinction is made between these two models, as significant differences in the response are expected. The CH model is used to model braced frames (or moment frames with column plastic hinges) in which story mechanisms can develop; the BH model is used to model structures in which mechanisms involve the full structure.

- The strengths of the members are tuned in a manner so that mechanisms develop simultaneously in every story under the UBC88 seismic lateral load pattern. Thus, under this load pattern the lateral load - lateral deflection response is bilinear. A strain hardening ratio of 10% is assumed at each plastic hinge location, resulting in a bilinear load deflection response that resembles that of the bilinear SDOF model without stiffness degradation, which was employed as one of the models of the SDOF study.

- The member stiffnesses in each story are tuned in a manner so that under the UBC88 seismic load pattern the interstory drift in every story is identical, resulting in a straight line deflected shape. As a consequence, the first mode shape of all structures is close to a straight line. Furthermore, the stiffnesses are tuned in a manner so that the first mode period of each structure is equal to the UBC88 code period of $0.002h_n^{2/3}$ for braced frames. This tuning is done also for the BH model in order to permit a direct comparison of dynamic analysis results between CH and BH models. Pertinent data for the first five elastic modes of the CH models are presented in Table 1. The periods for the BH models are the same for the first mode but deviate slightly for higher modes because of difficulties in stiffness tuning. As a consequence the modal masses also differ slightly. For the first two modes a damping of 5% critical is assumed in the time history analysis.

- The base shear strength, V_y, is varied for each structure and ground motion record in a manner so that it is identical to the inelastic strength demand $F_y(\mu)$ of the corresponding first mode period SDOF system for ductilities of either 2, 3, or 4.

The last assumption is critical for the intended comparison of SDOF and MDOF seismic demands. Because modal superposition is hardly feasible for inelastic MDOF systems, it is desirable to utilize SDOF demand estimates to predict MDOF demands. The inelastic strength demands for target ductilities can be evaluated for SDOF systems as discussed in [Krawinkler and Nassar, 1989], with typical results shown in Fig. 1. The question to be answered is how different the ductility demands for the MDOF systems are if the base shear strength of the MDOF system is identical to the inelastic strength demand of the SDOF system for the prescribed ductility. Or even better, the question to be answered is how large should the base shear strength of the MDOF system be [assuming the code prescribed seismic load pattern] in order to limit the maximum ductility in the MDOF system to a certain prescribed value. The results discussed next provide a partial answer to these questions.

The model structures, with their strength tuned as discussed in the preceding paragraphs, were subjected to the 33 CSMIP ground motions using a modified version of the DRAIN-2D analysis program. Results for mean values of ductilities obtained from the analyses with the 33 records are illustrated in Figs. 4 to 7.

Figure 4 shows the means of the story ductilities for each story of CH models with a base shear strength V_y equal to the inelastic strength demand $F_y(2)$ corresponding to a ductility of 2 for the SDOF system with a period equal to the first natural period of the MDOF structure. From here on the SDOF ductility is called the target ductility. If the MDOF system would respond like a SDOF system, the story ductility would also be 2 in every story. Clearly this is not the case, as expected, because of higher mode participation. For structures of ten stories and less the deviations from the SDOF target ductility of 2 are moderate, for taller structures the deviations

become very large. These large deviations for tall structures come as no surprise as the Whittier Narrows ground motions had very low energy content at periods exceeding one second and, therefore, the inelastic strength demand $F_y(\mu)$ for long period SDOF systems, which is used as base shear strength for the MDOF systems, is very small. As a consequence, higher mode effects become dominant for tall structures subjected to Whittier Narrows ground motions, more so than for other ground motions. Because of this peculiarity of the Whittier Narrows ground motions, no general conclusions can or should be drawn on seismic demands for long period structures, and emphasis from here on is on 2 to 10 story structures.

Figure 5 shows the means of the story ductilities for CH models with a target ductility of 4 (i.e., these structures are designed for a base shear strength $V_y = F_y(4)$), and Figures 6 and 7 show the results for target ductilities of 2 and 4, respectively, for BH models with 2, 5, and 10 stories. At the time of writing, the results for the 20, 30, and 40 story BH models are not yet available. The results in Figures 4 to 7 show consistent trends that can be summarized as follows:

- Except for the 2-story models, the story ductility demands are higher than the target ductility in the bottom and top stories, and are close to or smaller than the target ductilities in the middle stories. Thus, the UBC88 seismic design load pattern does not create an equal ductility demand for all stories (it probably was not intended to do so); ductility demands are concentrated in top and bottom stories.

- For the five and 10 story buildings the story ductility demands are higher in the top story than in the bottom story even though all stories yield simultaneously under static loads conforming to the code seismic load pattern. Thus, if the strength of all stories is fine-tuned to the code seismic load pattern, high upper story ductilities have to be expected. This indicates that a closer look should be taken at the presently used seismic load pattern.

- The ductility demands for the CH model is consistently higher than the demands for the BH model even though both models are designed for the same base shear strength. This is more evident from Figs. 8 and 9, which show the maximum ductility demands for all stories and the ductility demands for the first story, respectively. Again, each presented value is the mean obtained from the results of 33 time history analyses. The disadvantage of the CH models, in which individual story mechanisms can form, is evident. However, for the range of direct comparison, i.e., 2 to 10 story buildings, the difference between the two models is not as overpowering as often argued in defense of the need for strong column - weak girder design.

Figures 8 and 9 illustrate also the differences between SDOF and MDOF ductility demands. The base shear strength of the MDOF systems, V_y, was taken equal to the inelastic strength demand, $F_y(\mu)$, of the SDOF system with the period of the fundamental MDOF mode and ductilities of $\mu = 2$, 3, or 4. Thus, values of $\mu = 2$, 3, and 4 are target ductilities, and deviations from these targets are due to higher mode effects. As the two figures show, the deviations exhibit consistent trends, being small for two story CH and BH models, moderate for five and ten story CH and BH models, and becoming large for CH models of more than ten stories. Since the ductility demands for the MDOF systems are usually larger than the target ductilities, the implication is that the base shear strength of the MDOF systems must be increased in order to limit the ductility demand to the desired target values. The question is by how much. The following discussion provides preliminary answers.

For SDOF systems, the parameter that relates elastic to inelastic strength demands is the strength reduction factor $R_y(\mu) = F_{y.e}/F_y(\mu)$. It is a convenient design parameter as it permits, in concept, the derivation of a design strength spectrum from an acceleration response (elastic strength demand) spectrum. Although it is arguable whether it is the right parameter for this purpose, it is used here to address the question posed. From the regression analysis performed with the 33 Whittier Narrows records used in this study it was found that the strength reduction factor is not very sensitive to epicentral distance, thus, this factor can be represented by distance independent mean and mean+σ values. These values, plotted versus period, are shown in Fig. 10. The figure shows trends similar to those reported by others but the R-factors are larger than is usually assumed, an issue that is not important in the context of this discussion.

The advantage of using strength reduction factors, which are strength demand ratios, is that they are dimensionless parameters that do not depend on the severity of ground motions and can be utilized to evaluate relative strength demands. Their utilization for the 2, 5, and 10 story model structures is illustrated in the $R_y(\mu)$ versus μ plots shown in Figs. 11 to 13. The points shown on each graphs are obtained by using, as ordinates, the mean strength reduction factors for μ = 2, 3, and 4 of the SDOF system with the period of the first mode of the MDOF system (these values define the relative strength of the SDOF and MDOF models), and as abscissa, the ductilities of the SDOF and MDOF models. Connecting the three data points for each model with straight lines gives approximate R-μ relationships for the SDOF as well as MDOF models. Figures 11 to 13 show that for 2-story buildings the R-μ relationships for MDOF systems are very close to that of the SDOF system, but they deviate by increasing amounts as the number of stories increases.

Within the limitation of the approximate nature of the straight-line interpolation, Figs. 11 to 13 provide the information needed to assess the required increase in strength for MDOF systems compared to the SDOF system of first mode period, in order to limit the story ductility in the MDOF systems to the target value of the SDOF system. For instance, the R-factor for the 10-story BH model with a target ductility of 3 is approximately equal to 3.5, whereas the R-factor of the SDOF system is 4.2. Thus, the base shear strength of the 10-story BH model should be increased by a factor of about 4.2/3.5 = 1.2 compared to the inelastic strength demand $F_y(3)$ of the SDOF system. If the less desirable CH model is used, this factor becomes about 4.2/3.2 = 1.3.

The foregoing discussion points out a procedure that can be employed to derive design strength demands for MDOF systems from inelastic strength demand spectra of SDOF systems. The few numerical results shown cannot be generalized without a much more comprehensive parameter study. The parameters that need to be considered include the frequency content of the ground motions (which may be greatly affected by local site conditions), the hysteretic characteristics of the structural models (strainhardening, stiffness and strength degradation, etc.), and the dynamic characteristics of the MDOF models (periods, mode shapes, and modal masses of all important modes). Furthermore, it must be pointed out that the R-μ relationships for MDOF systems developed here are based on ductility demands in the first story. In several cases the maximum ductility does not occur in the first story, but at the top of the structures. This issue is not considered here, but can be addressed through modifications of the distribution of design story forces over the height for structures without stiffness discontinuities (regular structures) and through dynamic analysis studies for irregular structures.

CONCLUSIONS

In the context of long range research objectives directed towards improvements of seismic design, the following conclusions can be drawn:

- Consistent protection against failure requires that ductility capacity, which may be modified for cumulative damage effects, becomes the basic design parameter.
- The strength of structures is a dependent quantity that depends on the specified ductility capacities.
- For SDOF systems the required strength for specified ductilities can be evaluated from statistical studies of ground motion response of representative hysteretic systems, and can be represented in terms of inelastic strength demand spectra.
- For MDOF systems the required base shear strength must be modified compared to the SDOF inelastic strength demand to account for higher mode effects. A procedure for implementing this modification is presented in this paper.

ACKNOWLEDGEMENTS

The contents of this paper were developed under contract OSMS 8-8533 with the California Department of Conservation, Division of Mines and Geology, Strong Motion Instrumentation Program. However, these contents do not necessarily represent the policy of that agency, and you should not assume endorsement by the State Government. Additional financial support was provided by the John A. Blume Earthquake Engineering Center at Stanford University.

REFERENCES

1. Krawinkler, H., and Nassar, A., 1989. "Damage Potential of the Whittier Narrows Earthquake Ground Motions," SMIP89, Proceedings of the Seminar on Seismological and Engineering Implications of Recent Strong-Motion Data, California Department of Conservation, Sacramento, California, May 1989.

2. Osteraas, J., and Krawinkler, H., 1990. "Strength and Ductility Considerations in Seismic Design," John A. Blume Earthquake Engineering Center Report, Department of Civil Engineering, Stanford University, to be published in June 1990.

Table 1. Modal Periods and %Mass for Column Hinge (CH) Models

	2-STORY		5-STORY		10-STORY		20-STORY		30-STORY		40-STORY	
MODE	T (sec)	% MASS	T (sec)	% MASS	T (sec)	% MASS	T (sec)	% MASS	T (sec)	% MASS	T (sec)	% MASS
1	0.217	90.0	0.431	81.8	0.725	79.4	1.220	78.1	1.653	77.8	2.051	77.8
2	0.089	10.0	0.176	11.4	0.288	11.2	0.475	11.0	0.636	10.9	0.781	10.8
3			0.111	4.1	0.181	4.1	0.294	4.1	0.391	4.1	0.479	4.0
4			0.082	1.9	0.133	2.1	0.214	2.1	0.282	2.1	0.345	2.1
5			0.064	0.8	0.106	1.2	0.169	1.3	0.221	1.3	0.269	1.3

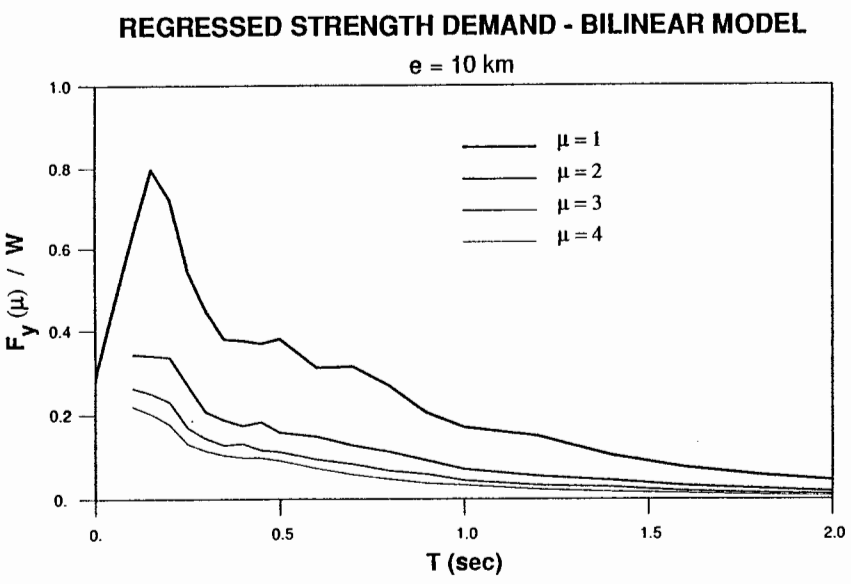

(a) Bilinear Model

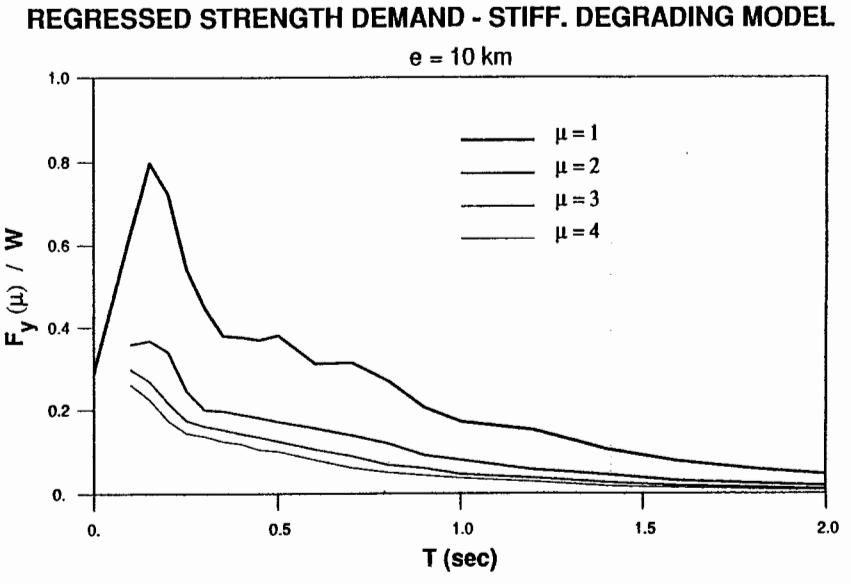

(b) Stiffness Degrading Model

Fig. 1 Elastic and Inelastic Strength Demand Spectra for Bilinear and Stiffness Degrading SDOF Systems

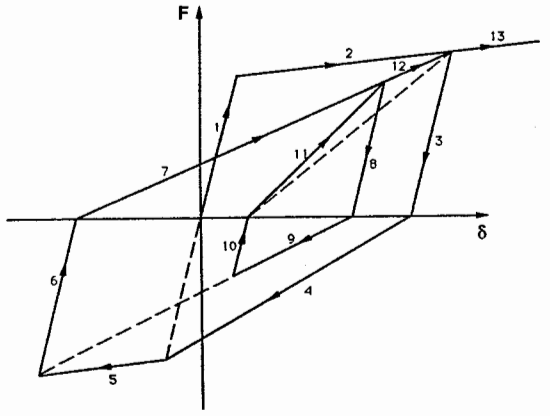

Fig. 2 Modified Stiffness Degrading Clough Model

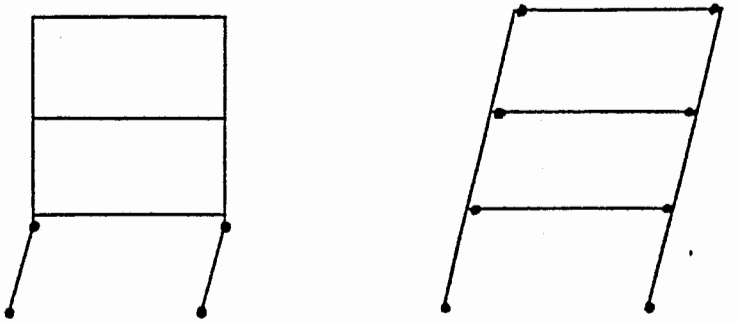

(a) Column Hinge (CH) Model (b) Beam Hinge (BH) Model

Fig. 3 Types of Structures Used in MDOF Study

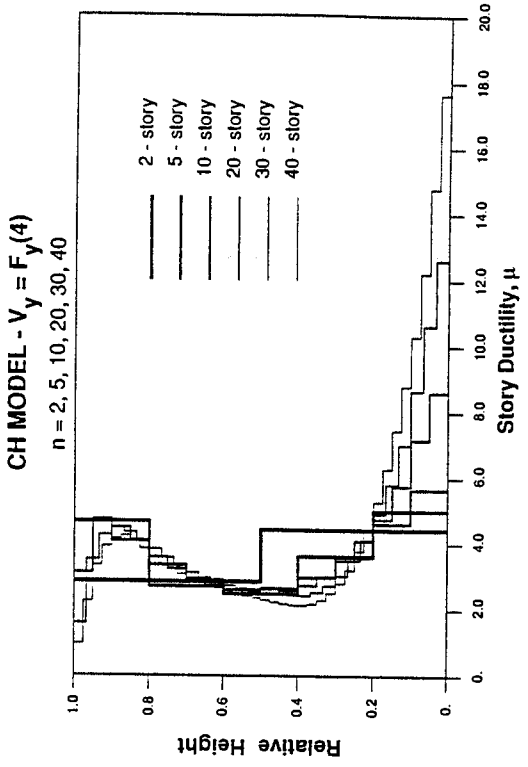

Fig. 5 Story Ductilities for CH Models with Target Ductility of 4

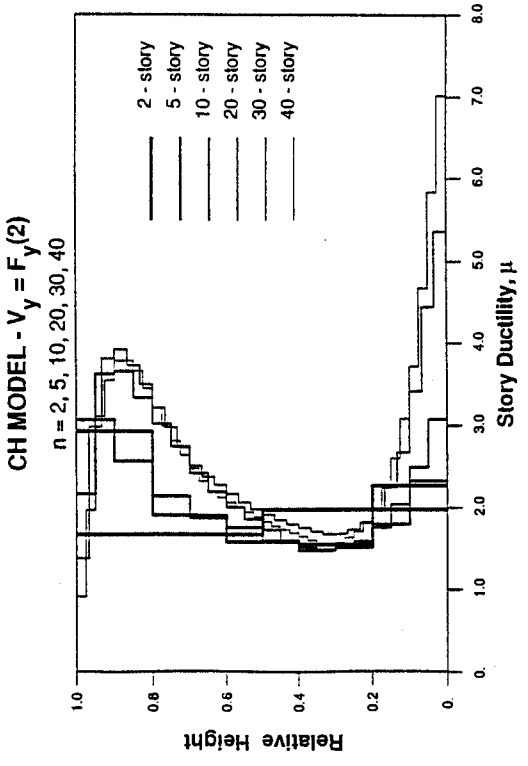

Fig. 4 Story Ductilities for CH Models with Target Ductility of 2

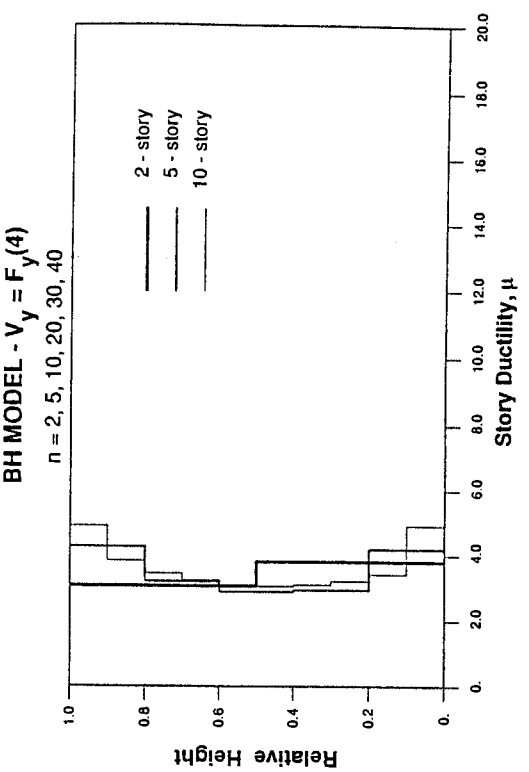

Fig. 7 Story Ductilities for BH Models with Target Ductility of 4

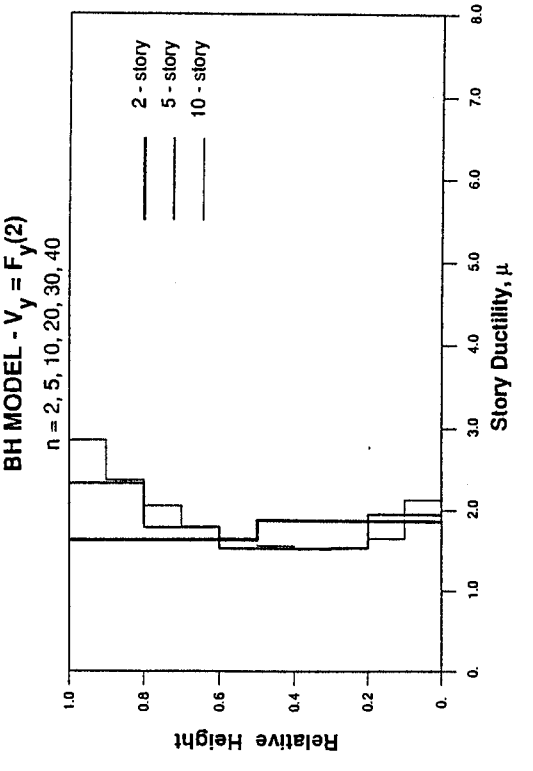

Fig. 6 Story Ductilities for BH Models with Target Ductility of 2

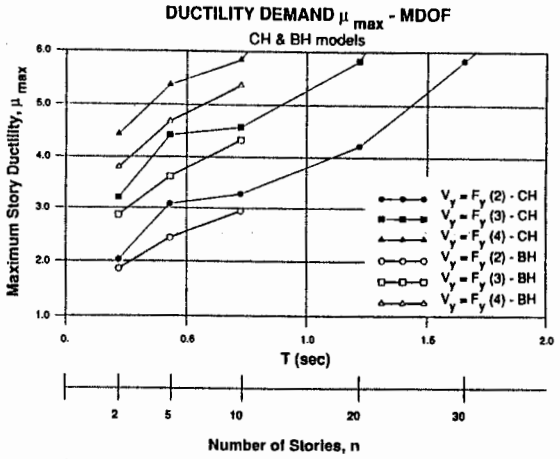

Fig. 8 Max. Story Ductilities for CH and BH Models

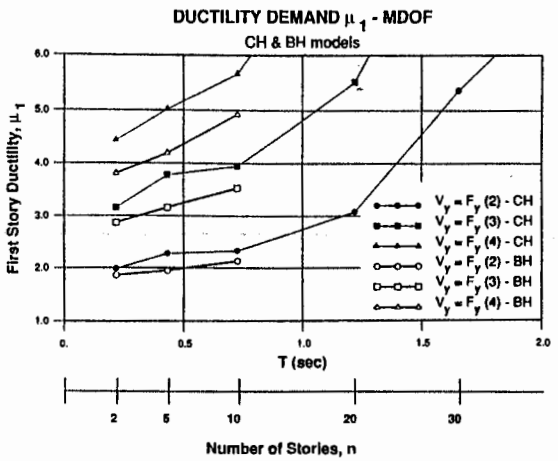

Fig. 9 Bottom Story Ductilities for CH and BH Models

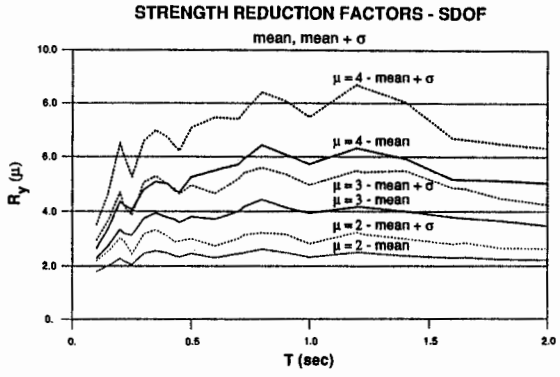

Fig. 10 Strength Reduction Factors for Bilinear SDOF Systems

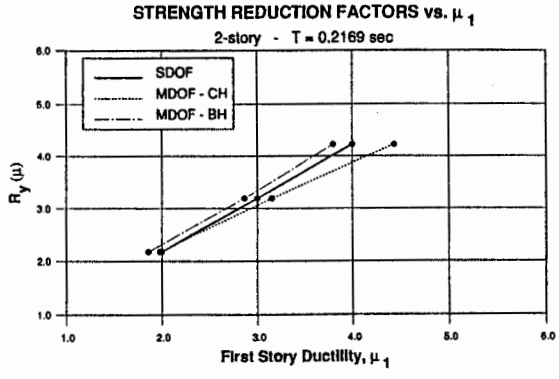

Fig. 11 R-μ Relationships for 2-Story CH and BH Models and Corresponding SDOF System

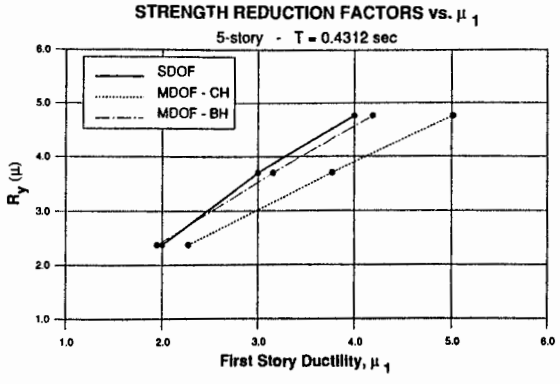

Fig. 12 R-μ Relationships for 5-Story CH and BH Models and Corresponding SDOF System

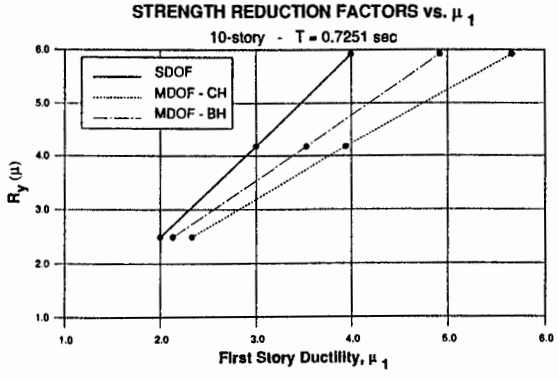

Fig. 13 R-μ Relationships for 10-Story CH and BH Models and Corresponding SDOF System

AN EVALUATION OF UNREINFORCED MASONRY WALL PERFORMANCE

JON D. RAGGETT AND CHRISTOPHER ROJAHN

ABSTRACT

The objective of this study is to evaluate the assumption that there is no amplification of ground motion at the top of unreinforced masonry walls. Strong-motion records at the top and bottom of shear walls for one unreinforced masonry building, and four reinforced concrete buildings were analyzed. Accelerations at the top of reinforced concrete shear walls typically did not exceed 1.31 times ground accelerations. The unreinforced masonry building was damaged during the motions analyzed making results unreliable for predicting future motions.

OBJECTIVE

The objective of the ATC-27 project is to review and analyze existing strong-motion data from instrumented buildings to evaluate the assumption that there is no amplification of ground motion at the top of unreinforced masonry walls (in the direction parallel to the wall). The assumption is of concern because it may not be appropriate for multi-story buildings, especially those with large window openings in the wall.

SELECTION OF INSTRUMENTED BUILDINGS AND EARTHQUAKES TO ANALYZE

The principal sources of strong-motion records from buildings are California Strong-Motion Instrumentation Program (CSMIP): Seismic engineering Branch, USGS; and the California Institute of Technology (CIT). The buildings instrumented by the USGS or CIT typically were high-rise steel or concrete frame structures. Furthermore, the instrumentation was designed (for the USGS and CIT studies) primarily to obtain gross building movement, not relative movement within a building. Included in the CSMIP data base are a sufficient number of low-rise and moderate-rise shear wall buildings that are of value to this study. Furthermore, those buildings are sufficiently well instrumented so that relative motions between parts of the buildings (for example, between the top and bottom of shear walls) can be determined. Consequently, all building motions analyzed were from the CSMIP data base of strong-motion records.

The first, and obvious, building selected was the Old Gilroy Firehouse, the only unreinforced masonry building for which detailed strong-motion records are available. The building is shown with instrument location, in Figure 4.1. In-plane instrumentation does exist, at the top and bottom of the north wall, for this structure. Strong-motion records are available for this building from the Loma Prieta Earthquake 10/17/89.

No other strong-motion records are available, at this time, for this or other unreinforced masonry structures. Therefore, strong-motion records from other buildings having similar characteristics as typical unreinforced masonry buildings were sought.

For this study, unreinforced masonry buildings typically 1) are rectangular in plan, 2) are 4-stories or less tall, 3) have perimeter shear walls with or without openings, and 4) have flexible wood frame horizontal diaphragms at the floor levels and at the roof. Instrumented buildings having similar characteristics, for which strong-motion records exist, were sought. In particular, records were sought only from those buildings that had in-plane shear wall motions recorded.

Other buildings studied included the following: Second, the four-story Pacific Telephone Building in Watsonville, again, for the Loma Prieta Earthquake, 10/17/89, was studied. By its proportions, the building is a bit too "high rise" but it does have perimeter shear walls (of reinforced concrete) with many openings. It also has, which is not great for this study, rigid concrete floor diaphragms. It is hoped something can be learned about in-plane deformations of shear walls with openings. See Figure 4.2.

Third, the Marshall Electronics Group Building in Milpitas was included. Strong-motion records exist for this building for the Loma Prieta earthquake, 10/17/89, as well, and were analyzed. This building is a two-story reinforced concrete tilt-up structure with large openings around the entire perimeter. It has a plywood, on wood frame, roof diaphragm. The second floor structure consists of concrete fill on metal deck on open-web steel joists. This second floor diaphragm is perhaps stiffer than desired compared to a wood diaphragm, but it is still far more flexible than a cast-in-place concrete diaphragm. Again, this structure was selected because the analysis of in-plane deformations of shear walls with openings would hopefully be rewarding. See Figure 4.3 for a simple description of the building and the instrumentation plan.

Fourth, the Glorietta K Warehouse in Hollister was selected to be studied. Strong-motion records for the Loma Prieta earthquake 10/17/89, the Morgan Hill Earthquake 4/24/84, and the Hollister earthquake 1/26/86 were studied. The Glorietta K Warehouse is a typical, one-story concrete tilt-up warehouse with a wooden panelized roof structure. There are very few openings in the entire building. See Figure 4.4 for a simple description of the building and the instrumentation plan.

And fifth, the Interstate Van Lines building in Redlands was studied. Records for this building from the Palm Springs Earthquake 7/8/86 were studied. This is another warehouse, very similar to the Glorietta K Warehouse. See Figure 4.5 for a simple description of the building and the instrumentation plan.

PRELIMINARY ANALYSIS PROCEDURE USED

It is to be remembered that the objective of this study is to evaluate the assumption that there is no in-plane amplification of motion from top to bottom of unreinforced masonry walls. with this objective in mind, the following bits of information were obtained for the analysis of each input (ground motion)/output (structure motion) pair of time histories: peak input acceleration, peak output acceleration, peak input displacement, peak output displacement, peak and RMS relative displacement, and best-fit single-degree-of-freedom dynamic response characteristics. Those dynamic response characteristics are those coefficients C1, C2, and C3 such that C1*A(t) + C2*V(t) + C3*D(t) fits AG(t), the input (ground) acceleration, in a least-squares sense

where

A(t)	output acceleration relative to input acceleration;
V(t)	output velocity relative to input velocity; and
D(t)	output displacement relative to input displacement.

All functions are a function of time, t. The natural frequencies, damping ratios, and participation factors can be readily obtained from the best-fit coefficients C1, C2, and C3. The procedure used is similar to that which was described by Raggett J. and Rojahn C. in "Use and Interpretation of Strong-Motion Records From Highway Bridges", FHWA-RD-78-158, Fed Highway Admin., Wash DC, October 1978.

Although the specific objective of the study was to evaluate in-plane motions at the top of walls relative to motions at the base of walls, all response motions were analyzed relative to the ground motions, for the instrumented buildings and earthquakes identified.

DISCUSSION OF RESULTS

Discussed are preliminary findings of the analyses of in-plane motions recorded for the five buildings described earlier. First will be a summary of in-plane motion analyses for the four reinforced concrete shear wall buildings that have similar expected dynamic response characteristics to unreinforced masonry buildings. It it is assumed that the modulus of elasticity for

unreinforced brick is 1,2000,000 psi, and that for reinforced concrete is 3,000,000 psi, then reinforced concrete building relative displacements could be multiplied by 2.5 to be approximations of similarly proportioned unreinforced masonry buildings. Included in this summary are a series of ratios:

Accel Ratio = (peak response acceleration)/(peak ground acceleration)

Disp Ratio = (peak response displacement)/(peak ground acceleration)

Rel Disp Ratio=(peak relative disp)/(peak ground displacement)

All three ratios give a sense of the degree to which the wall is following the ground motions as a rigid body. See the summary on Table 4.1 Shown on Figures 4.6 to 4.11 are typical displacement time histories, one for each direction, for each of the buildings sampled, starting one second before the maximum relative displacement was recorded.

Some observations from the tabulated results and sampled time histories follow:

1. For all time histories presented, the response displacement is very similar in shape and magnitude to the ground displacement.

2. The peak roof acceleration for the Pacific Telephone building is substantially greater than the peak ground acceleration. This building is much more of a "high-rise" building and is probably the least representative of typical unreinforced masonry buildings.

3. Most buildings are on flexible soil material. Note the very long ground motion periods for all cases.

4. Base rocking components have not been identified yet in the Pacific Telephone Building response and the Marshal Electronics group building response. Base rocking cannot be identified in the other responses.

For all cases, best-fit dynamic response characteristics made little sense. Best-fit coefficients were identified, but natural frequencies, damping ratios, and participation factors derived from the best-fit coefficients made little physical sense. This exists for two reasons. First, it was attempted to identify dynamic response characteristics from small differences between

two time histories (very similar input and output time histories). In such cases huge variations in dynamic response characteristics cause minor variations in the response. Therefore, response analyses, relative to the input, produce unreliable results. Second, a single-degree-of-freedom linear elastic model does not appear to be a very good approximation to the observed behavior. A linear elastic model is a model of convenience (it is easy to formulate and solve) and it is very appropriate for wall behaved flexible structures (such as high-rise building steel frames). It simply is not a particularly good model of low-rise, shear-wall, building behavior.

This leads to the potentially most substantive but most frustrating analysis, that of the Old Gilroy Firehouse (the only true unreinforced building analyzed).

One pair of records exists that is capable of being analyzed to determine in-plane wall flexibility; the east-west motion (transverse) motion of the north wall of the building. It should be noted that this is not the north wall of the main building proper, but is the north wall of the 20-foot unreinforced masonry addition to the main building proper. The addition is loosely attached to the main building (the full height joint connecting the two is a grouted joint, but one that is cracked throughout). Nonetheless, it is still an unreinforced masonry wall with in-plane strong motion instrumentation top and bottom. See Figure 4.12 for the input, output, and relative displacement time histories and pertinent peak values for this input/output pair of time histories.

The peak value ratios are rather startling

Accel Ratio =	1.453
Disp Ratio =	1.107
Rel Disp Ratio =	1.328

From the record it is obvious that there is significant flexibility in the wall (and an undetermined amount of base rocking). Furthermore, it is obvious that the top of the wall is not following, even remotely, the wall base motion. Note that the peak relative displacement of the top of the wall to the base is a whopping 12.904 cm! It is hard to imagine an unreinforced masonry building distorting this much over a height of about 30 feet without damage, and herein lies the frustration. There is, in fact, a large crack (about 1/2 inch permanent opening) extending down from the parapet to a second floor window on the north wall. Obviously, there was significant cracking on this wall; and therefore, a large relative roof-to-ground displacement could be expected. This does taint the results, however, and

makes the records of little value for use in predicting unreinforced masonry wall performance in anything less than damaging levels. Note that the peak ground acceleration was 0.285 g.

PRELIMINARY CONCLUSIONS

Based upon the preliminary analyses made, in-plane distortions of concrete (and presumably unreinforced masonry) shear walls with and without modest openings, are not expected to be large relative to absolute ground displacements. Peak-roof-to-peak ground acceleration ratios of 1.31 or less have been observed for one and two story shear walls (the 1.31 was for a tilt-up wall building with large openings). For a 4-story "high-rise" concrete shear wall type building this acceleration ratio was as high as 3.118. Typically, however, for a shear wall type walls, for low-rise buildings, an acceleration ratio of 1.31 or less was observed.

Unreinforced masonry "walls" run the full range from a solid one-story shear wall, to a frame, typical of many store fronts. An unreinforced masonry frame (or wall with such large openings that it behaves like a frame) will of course be very flexible. It also will be very weak, and should not be relied upon to resist seismic loads. The dynamic response characteristics of the structural reinforcements would then govern predicted and future responses.

A preliminary conclusion of this study so far is that the assumption that there is no amplification of ground motion at the top of unreinforced masonry walls (in the direction parallel to the wall) is a reasonable assumption for normally proportioned unreinforced masonry walls. This does not mean, however, that building motions in general parallel to shear walls are not amplified. Quite to the contrary, building motions in general are greatly amplified, between shear walls because the horizontal diaphragms are so flexible, and at the same time, are so heavily loaded by those walls perpendicular to the isolated motion.

As an example, consider the transverse motions of the Marshall Electronics Group building. Shown on Figure 4.13 are the building peak accelerations, conservatively assumed here to act simultaneously. For this preliminary analysis, consider this to be a reasonable (but conservative) approximation to the true overall peak response. Assuming the modal response shown, the overall building base shear is 1.73 times the overall building base shear that would have occurred had the building moved with the ground without amplification. For this case, the overall building base shear based upon in-plane wall distortions alone

would have been 1.23 times the overall base shear that would have occurred had the building moved with the ground without amplification. This too is far below the actual, expected, peak base shear. Obviously, the overall building response amplification has little to do with end wall flexibility. This behavior is expected to be similar for most unreinforced masonry buildings with flexible wooden, horizontal diaphragms.

BUILDING	PEAK GROUND ACCEL(g)	DIRECT	ACCEL RATIO	DISP RATIO	REL DISP RATIO
INTERSTATE	.037	LONG	1.036	1.025	0.185
	.037	LONG	1.038	.994	0.170
	.042	TRANS	1.101	1.046	0.267
	.042	TRANS	.914	.998	0.309
GLORIETTA	.360	LONG	.965	1.029	0.053
	.360	LONG	1.057	1.064	0.084
	.238	TRANS	1.4120	.999	0.070
	.252	TRANS	.993	.990	0.042
MARSHALL	.090	TRANS	1.252	.986	0.038
	.100	TRANS	1.310	.974	0.030
PACIFIC BELL	.253	TRANS	3.118	1.042	0.237
	.272	TRANS	1.524	1.068	0.162

TABLE 4-1

PEAK ROOF/GROUND RATIOS

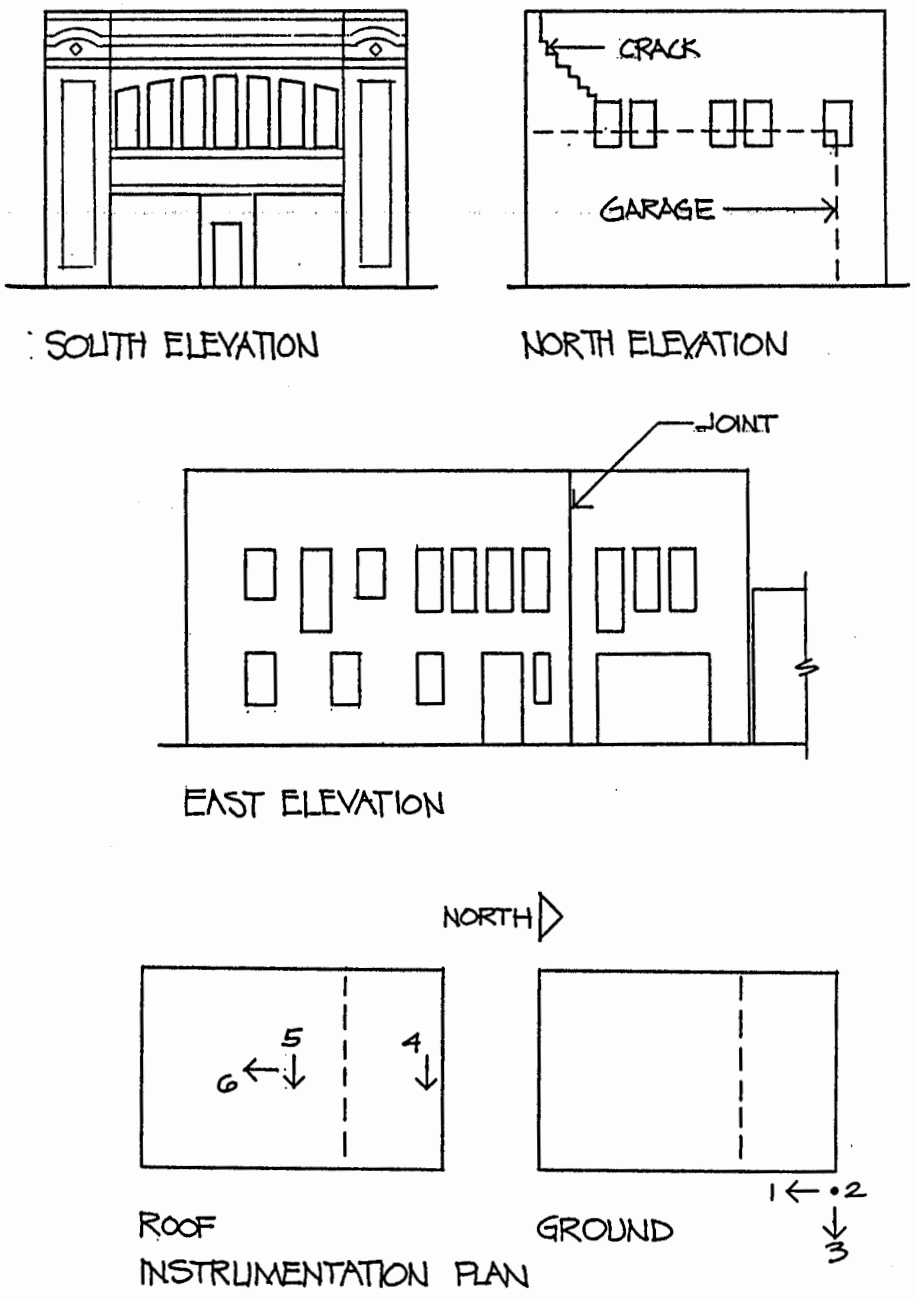

FIGURE 4.1
ELEVATIONS AND INSTRUMENTATION PLANS - OLD GILROY FIREHOUSE

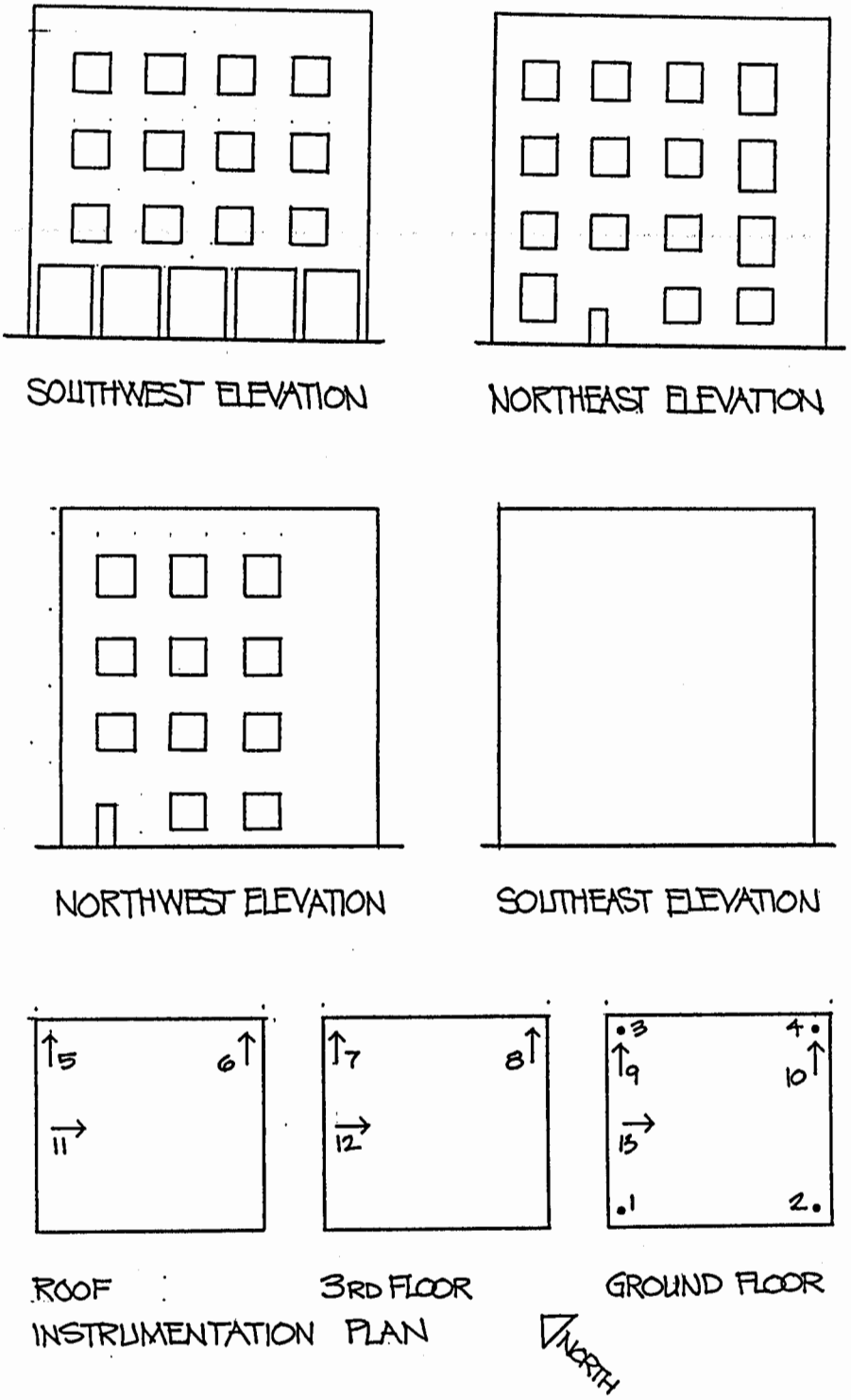

FIGURE 4.2 ELEVATIONS AND INSTRUMENTATION PLANS PACIFIC TELEPHONE BUILDING

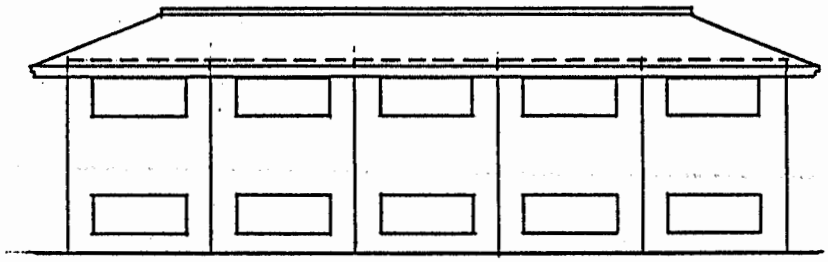

EAST ELEVATION (OTHERS SIMILAR)

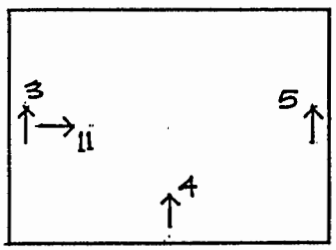

ROOF

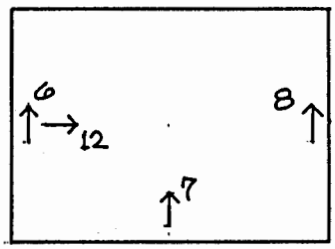

SECOND FLOOR

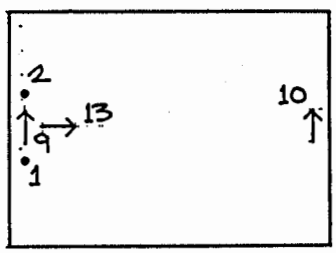

GROUND FLOOR
INSTRUMENTATION PLAN

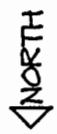

FIGURE 4.3
ELEVATIONS AND
INSTRUMENTATION PLANS
MARSHALL ELECTRONICS
GROUP BUILDING

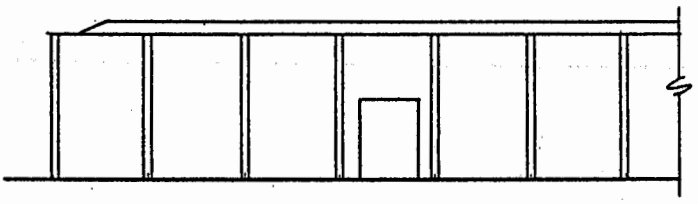

TYPICAL ELEVATION

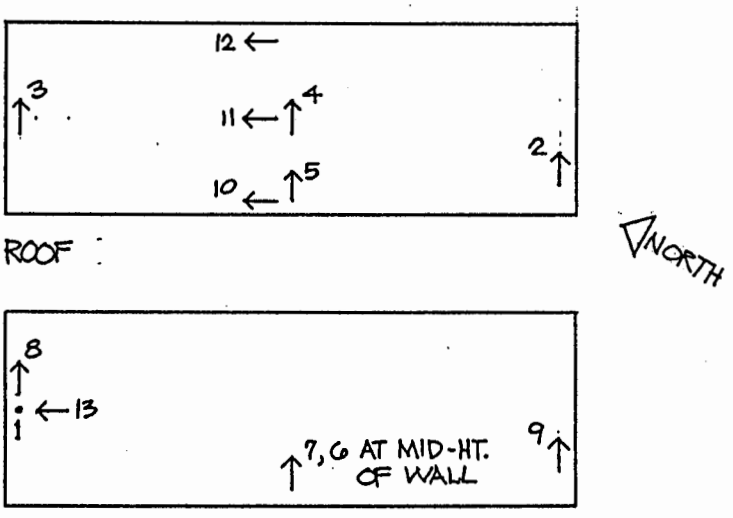

INSTRUMENTATION PLAN

FIGURE 4.4
ELEVATIONS AND
INSTRUMENTATION PLANS
GLORIETTA K WAREHOUSE

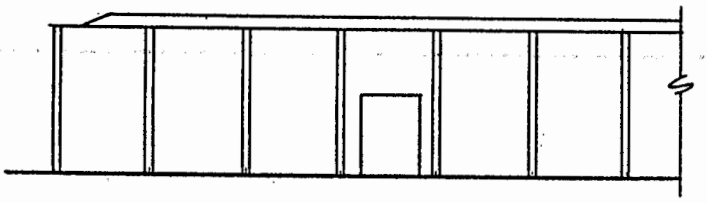

TYPICAL ELEVATION

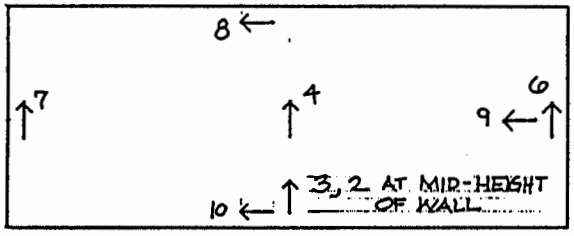

ROOF

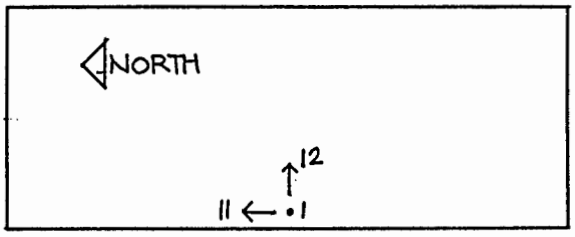

GROUND FLOOR
INSTRUMENTATION PLAN

FIGURE 4.5
ELEVATIONS AND
INSTRUMENTATION PLANS
INTERSTATE VAN LINES
BUILDING

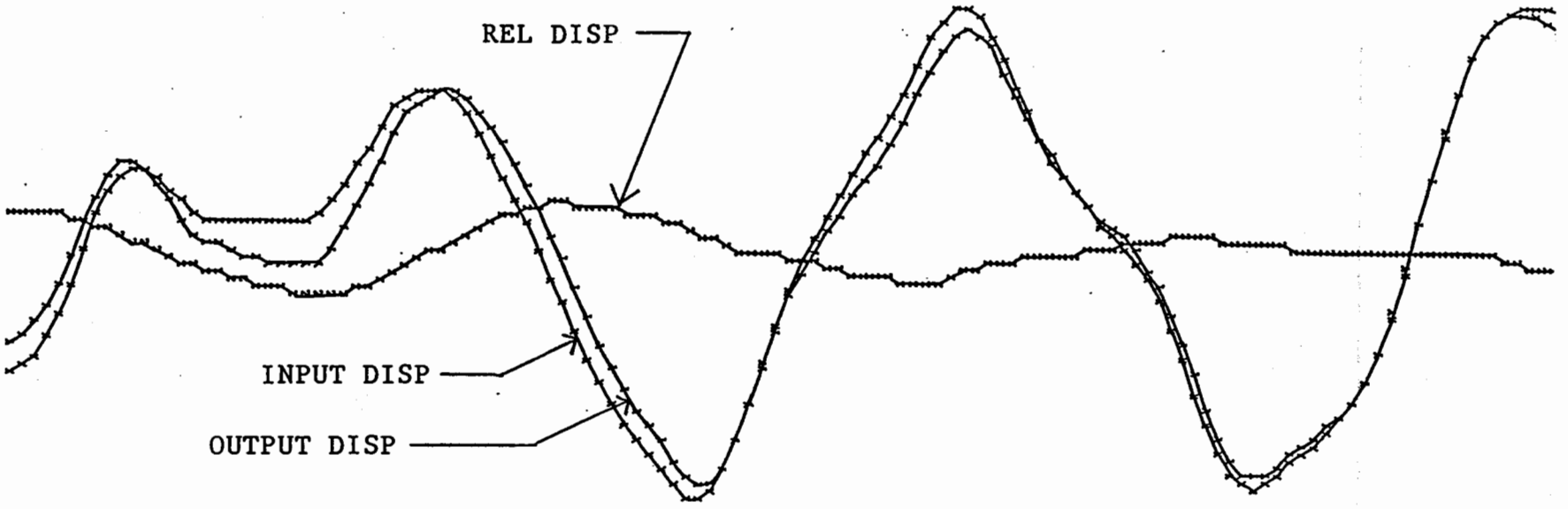

INTERSTATE VAN LINES WAREHOUSE
PALM SPRINGS EARTHQUAKE 7/8/86
INPUT CHANNEL NUMBER 11
OUTPUT CHANNEL NUMBER 10
MAX Y ACCEL (CM/SEC/SEC)= 38.021
MAX X ACCEL (CM/SEC/SEC)= 36.646
MAX Y DISP (CM)= .322
MAX X DISP (CM)= .324
MAX REL DISP(CM)= .055
RMS REL DISP (CM)= .017
MAX X, Y,OR Z DISP (CM) = .324
START TIME (SEC)= 21.360
FINISH TIME (SEC)= 26.360

FIGURE 4.6

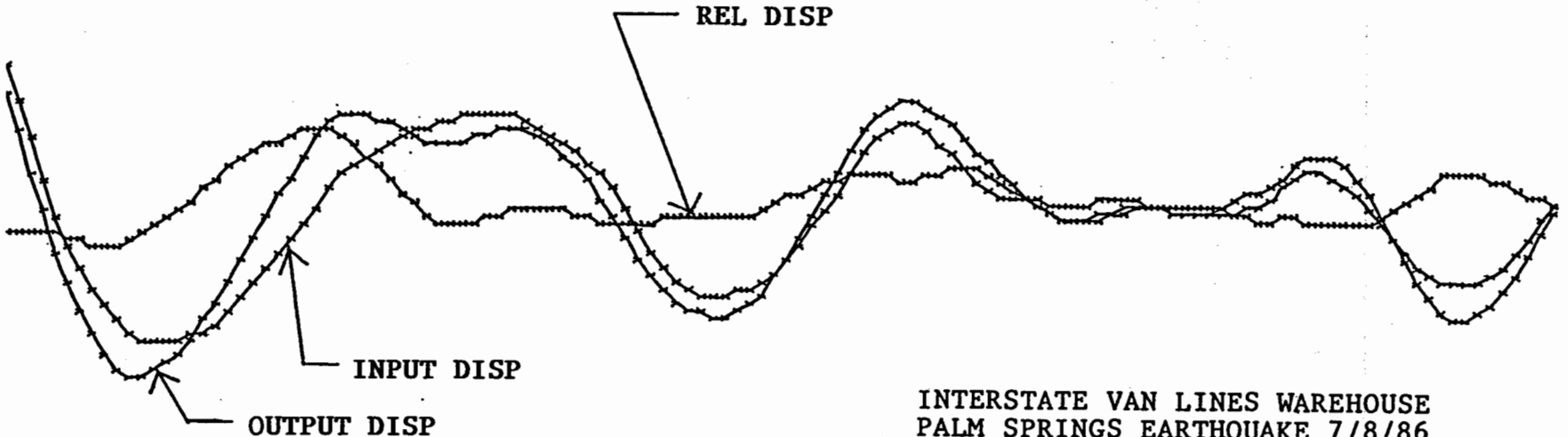

INTERSTATE VAN LINES WAREHOUSE
PALM SPRINGS EARTHQUAKE 7/8/86
INPUT CHANNEL NUMBER 12
OUTPUT CHANNEL NUMBER 7
MAX Y ACCEL (CM/SEC/SEC)= 45.739
MAX X ACCEL (CM/SEC/SEC)= 41.534
MAX Y DISP (CM)= .497
MAX X DISP (CM)= .475
MAX REL DISP(CM)= .127
RMS REL DISP (CM)= .044
MAX X, Y,OR Z DISP (CM) = .497
START TIME (SEC)= 27.940
FINISH TIME (SEC)= 32.940

FIGURE 4.7

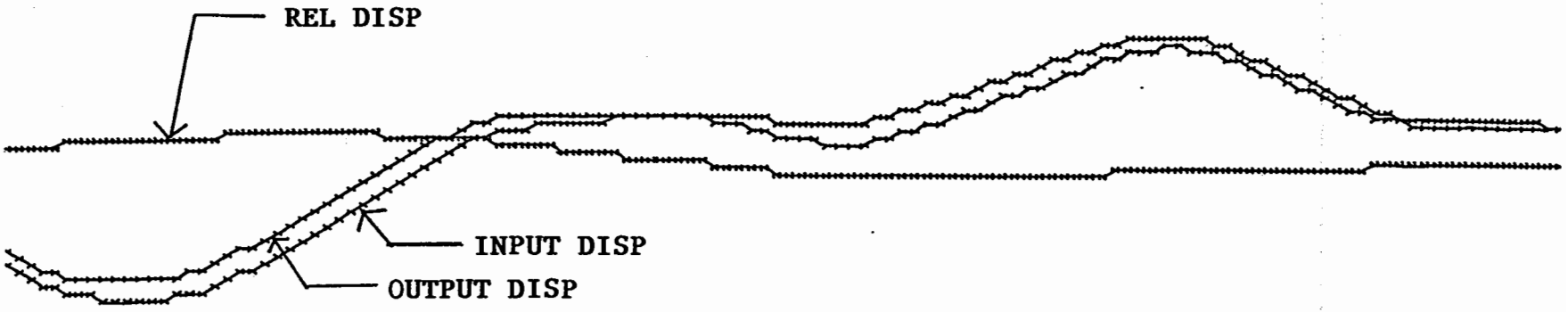

FIGURE 4.8

GLORIETA WAREHOUSE
LOMA PRIETA EARTHQUAKE 10/17/89
INPUT CHANNEL NUMBER 13
OUTPUT CHANNEL NUMBER 10
MAX Y ACCEL (CM/SEC/SEC)= 372.841
MAX X ACCEL (CM/SEC/SEC)= 352.852
MAX Y DISP (CM)= 18.366
MAX X DISP (CM)= 17.260
MAX REL DISP(CM)= 1.456
RMS REL DISP (CM)= .499
MAX X, Y,OR Z DISP (CM) = 18.366
START TIME (SEC)= 20.060
FINISH TIME (SEC)= 25.060

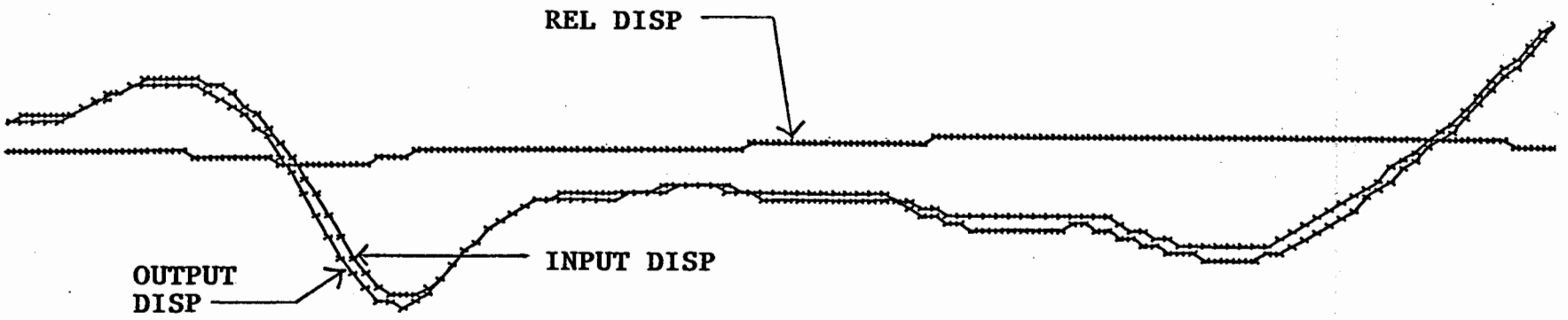

GLORIETTA WAREHOUSE
LOMA PRIETA EARTHQUAKE 10/17/89
INPUT CHANNEL NUMBER 9
OUTPUT CHANNEL NUMBER 2
MAX Y ACCEL (CM/SEC/SEC)= 261.539
MAX X ACCEL (CM/SEC/SEC)= 233.504
MAX Y DISP (CM)= 21.597
MAX X DISP (CM)= 21.626
MAX REL DISP(CM)= 1.519
RMS REL DISP (CM)= .372
MAX X, Y,OR Z DISP (CM) = 21.626
START TIME (SEC)= 11.060
FINISH TIME (SEC)= 16.060

FIGURE 4.9

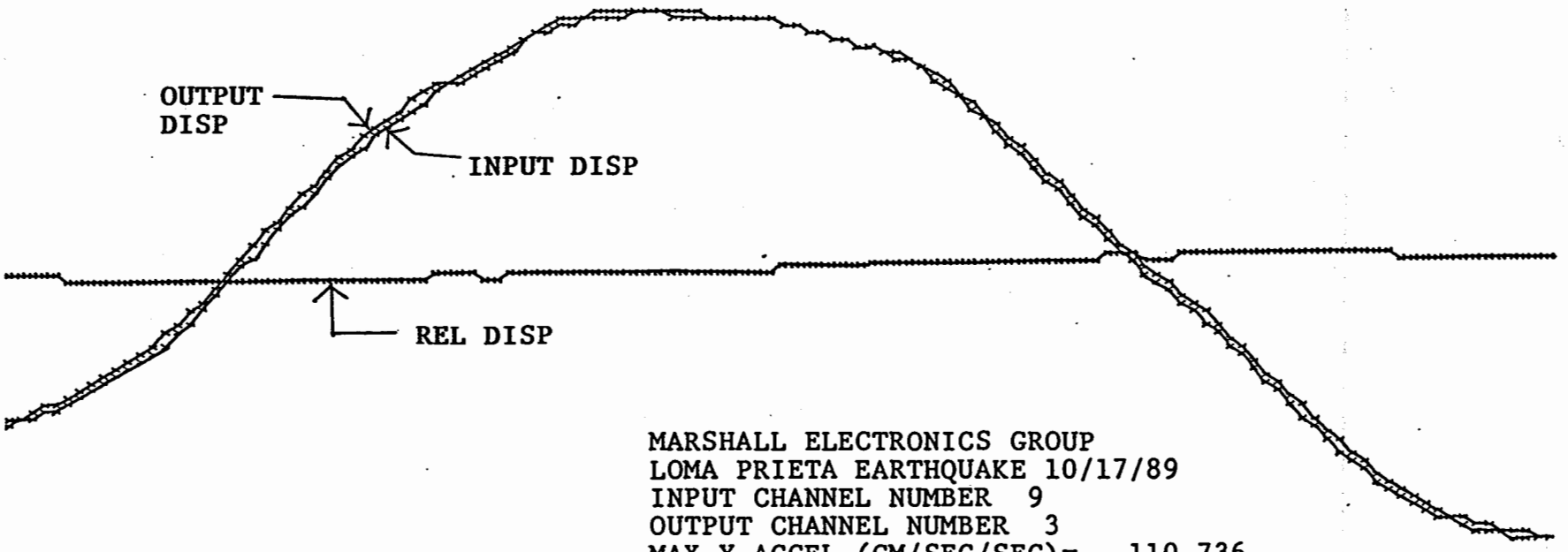

FIGURE 4.10

MARSHALL ELECTRONICS GROUP
LOMA PRIETA EARTHQUAKE 10/17/89
INPUT CHANNEL NUMBER 9
OUTPUT CHANNEL NUMBER 3
MAX Y ACCEL (CM/SEC/SEC)= 110.736
MAX X ACCEL (CM/SEC/SEC)= 88.421
MAX Y DISP (CM)= 23.814
MAX X DISP (CM)= 24.161
MAX REL DISP(CM)= .926
RMS REL DISP (CM)= .301
MAX X, Y,OR Z DISP (CM) = 24.161
START TIME (SEC)= 12.560
FINISH TIME (SEC)= 17.560

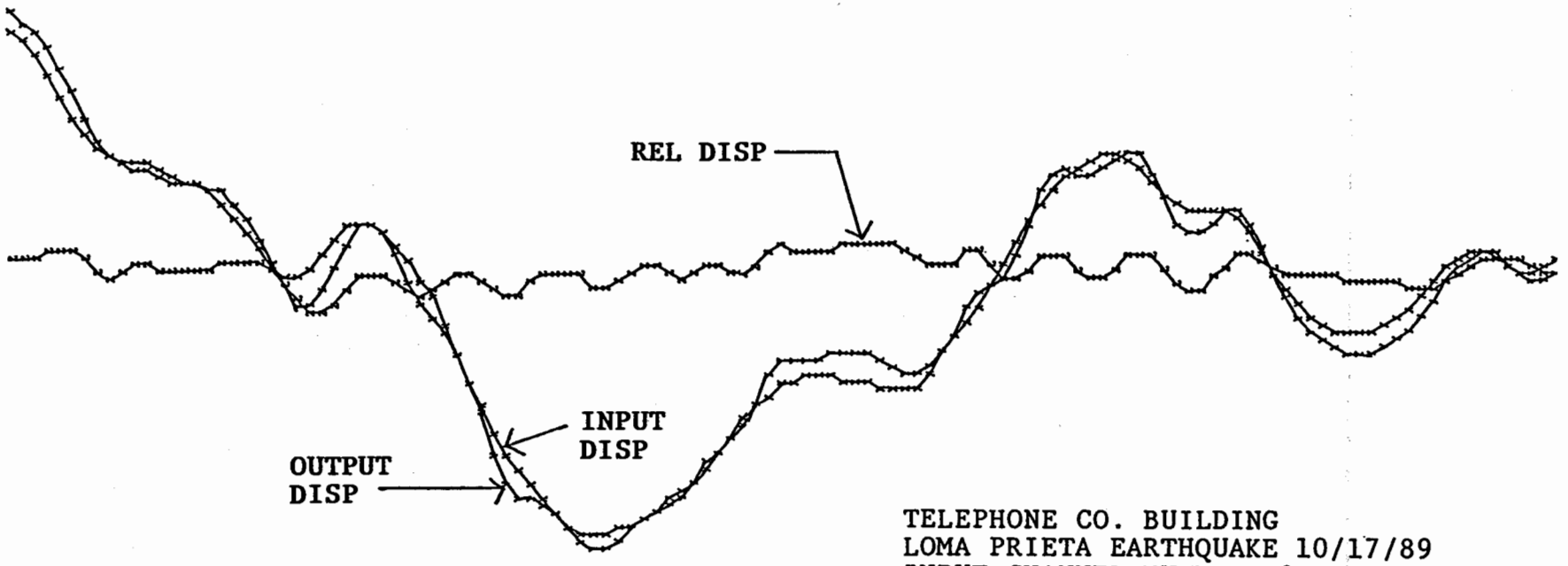

TELEPHONE CO. BUILDING
LOMA PRIETA EARTHQUAKE 10/17/89
INPUT CHANNEL NUMBER 9
OUTPUT CHANNEL NUMBER 5
MAX Y ACCEL (CM/SEC/SEC)= 406.604
MAX X ACCEL (CM/SEC/SEC)= 266.776
MAX Y DISP (CM)= 9.562
MAX X DISP (CM)= 8.953
MAX REL DISP(CM)= 1.447
RMS REL DISP (CM)= .305
MAX X, Y,OR Z DISP (CM) = 9.562
START TIME (SEC)= 4.720
FINISH TIME (SEC)= 9.720

FIGURE 4.11

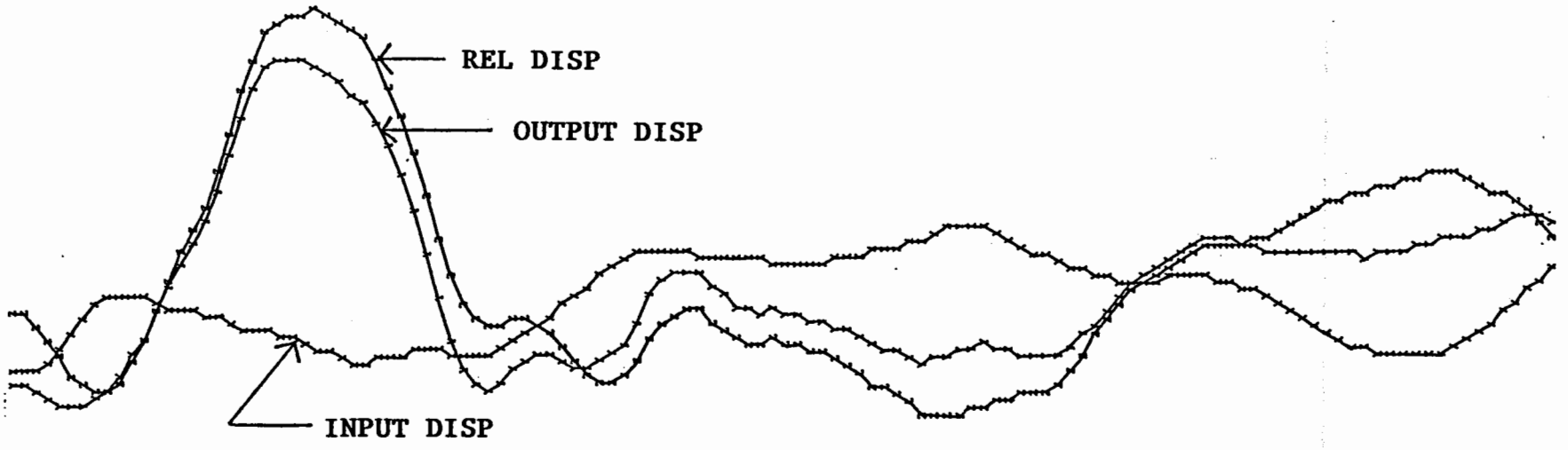

OLD GILROY FIREHOUSE
LOMA PRIETA EARTHQUAKE 10/17/89
INPUT CHANNEL NUMBER 3
OUTPUT CHANNEL NUMBER 4
MAX Y ACCEL (CM/SEC/SEC)= 406.464
MAX X ACCEL (CM/SEC/SEC)= 279.742
MAX Y DISP (CM)= 10.753
MAX X DISP (CM)= 9.716
MAX REL DISP(CM)= 12.904
RMS REL DISP (CM)= 2.966
MAX X, Y,OR Z DISP (CM) = 12.904
START TIME (SEC)= 4.860
FINISH TIME (SEC)= 9.860

FIGURE 4.12

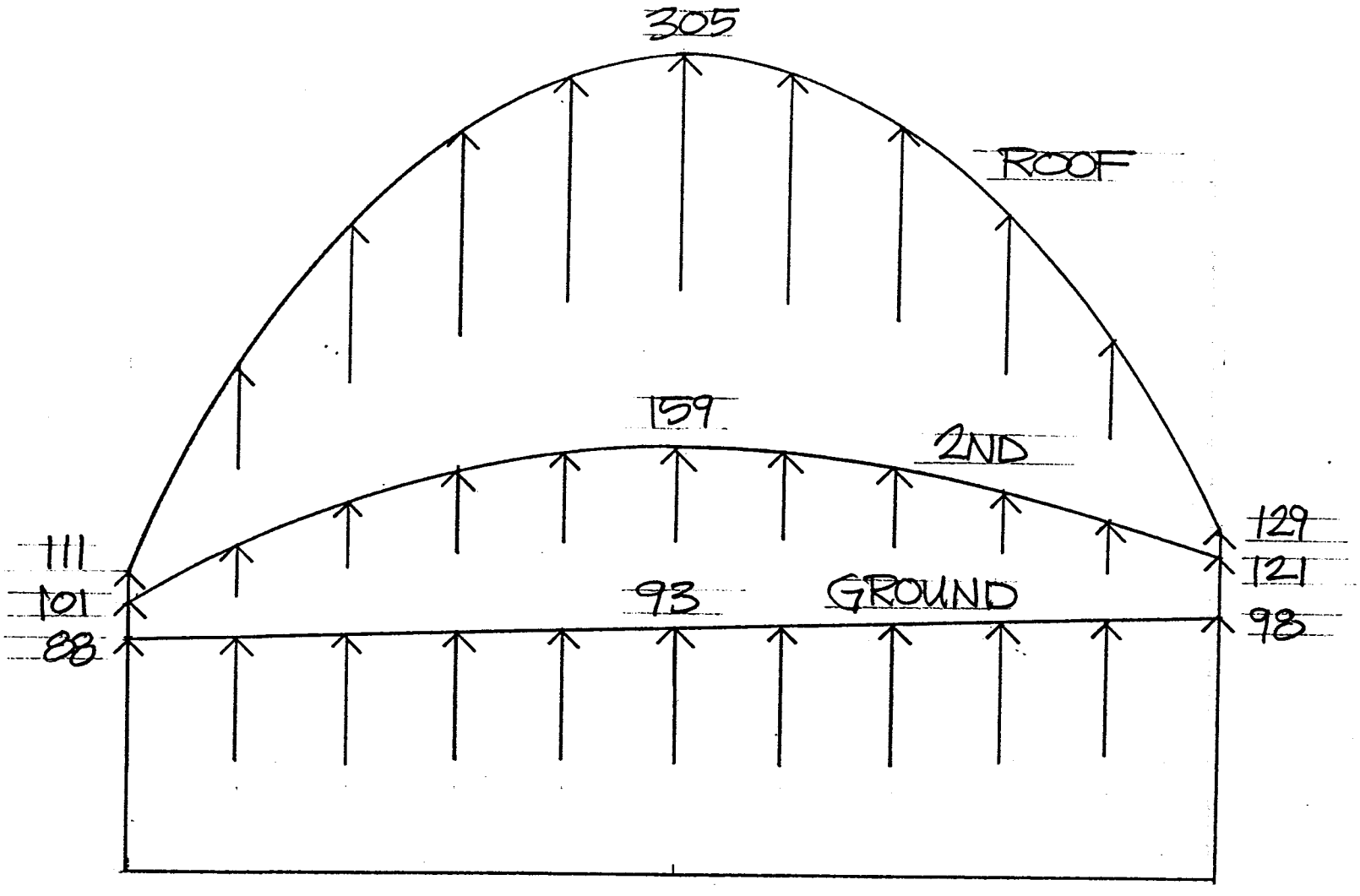

FIGURE 4.13
ENVELOPE OF PEAK ACCELERATIONS (CM/SEC^2)
MARSHALL ELECTRONICS GROUP BLDG.

INTERPRETATION OF PAINTER STREET OVERCROSSING RECORDS TO DEFINE INPUT MOTIONS TO THE BRIDGE SUPERSTRUCTURE

K. Romstad
Professor of Civil Engineering, University of California, Davis

B. Maroney
Graduate Student, University of California, Davis
Senior Bridge Engineer, California Department of Transportation

ABSTRACT

This paper discusses portions of a study utilizing the strong motion data obtained from twenty sensors on and near the Painter Street Overcrossing in Rio Dell, California. Particular attention is paid to the influence abutment behavior has on measured response in the three directions of motion of the bridge superstructure. Previous studies have shown that transverse modes of vibration predicted by ambient testing may not reflect behavior during seismic events. The study also focusses on the influence of direction of input boundary motions to be used in analytical models to predict bridge response.

DESCRIPTION OF BRIDGE AND INSTRUMENTATION AND RECORDED DATA

The Painter Street Overcrossing, California bridge number 04-0236, (see Fig. 1) is a continuous two span cast-in-place prestressed post-tensioned concrete box girder bridge located near Rio Dell over Highway 101. The structure has unbalanced spans of 146 and 119 feet and is 52 feet wide. Both end diaphragm abutments and the two-column bent are skewed at 39 degrees. The bent spans 38 feet measured along the centerline of the skewed cross sections and is monolithically connected top and bottom to the footings and superstructure respectively. The columns are approximately 20 feet in height. The abutments have been constructed on top of fill material to provide appropriate vertical clearance over Highway 101 below. The west abutment rests on a neoprene bearing strip which is part of a designed thermal expansion joint. All of the foundations are supported on driven 45 ton concrete friction piles. The bridge is typical of numerous bridges in California spanning two or four lane separated highways.

The Painter Street Overcrossing was instrumented in 1977 by the California Division of Mines and Geology as part of the California Strong Motion Instrumentation Program (CSMIP). The bridge site was instrumented with twenty strong accelerometers capturing various motions on and off the bridge as shown in Fig. 1. Channels 12, 13 and 14 measure free field motions (longitudinal, vertical and transverse to the bridge axis respectively) near the bridge site. At the east end of the bridge, triaxial sets of sensors are located both on the embankment (15, 16, 17) and on the end of the bridge deck (9, 10, 11) so that relative motion between the embankment and the deck could be assessed.

A triaxial set of sensors (1, 2, 3) is also located at the base of the bent's north column to aid in assessing soil-structure interaction. A transverse sensor (7) is located at the base of the deck adjacent to the center bent and vertical sensors are located at midspan of the east (8) and west (6) spans on the north side of the deck. Torsion of the bridge deck cannot be directly assessed since only the north edge of the bridge deck is instrumented.

Since the overpass was instrumented, it has been shaken by six earthquakes starting with the large (6.9ML) Trinidad offshore earthquake of November 8, 1980 at 72 km from the site. The second earthquake was a smaller (4.4ML) event on December 16, 1982 only 15 km from the site. The other events ranged from 5.1 to 5.5 ML at 27 to 61 km. The six earthquakes are summarized in Table 1. Observation of the free field data in Table 1 shows that the maximum vertical accelerations are less than fifty percent of the maximum transverse accelerations and less than

twenty five percent of the maximum longitudinal accelerations. However, the maximum vertical accelerations measured by sensors six and eight on the north end of the deck at the middle of the spans generally equal to or exceed the maximum transverse acceleration measured by sensor 7 of the deck at bent #2. The largest bridge accelerations were caused by caused by the relatively small Rio Dell earthquake of 12/16/82. Unfortunately the free field sensors did not record this event.

TABLE 1 Earthquakes Recorded by Painter Street Instrumentation

Earthquake	Date	Mag. (ML)	Epicent. Distance (km)	Maximum Ground Acceleration C12	C13	C14	Maximum Bridge Acceleration C6	C7	C8
Trinidad	11/08/80	6.9	72	.15g	.03g	.06g	.34g	-	.25g
Rio Del	12/16/82	4.4	15	-	-	-	.39g	.43g	.59g
Cape Mendocino	08/24/83	5.5	61	-	-	-	.27g	.22g	.16g
Event #1	11/21/86	5.1	32	.46g	.08g	.16g	.24g	.26g	.33g
Event #2	11/21/86	5.1	26	.15g	.02g	.12g	.21g	.36g	.29g
Cape Mendocino	07/31/87	5.5	28	.15g	.04g	.09g	-	.34g	.27g

REVIEW OF PREVIOUS WORK

Gates and Smith (1982) performed a comprehensive series of ambient vibration tests on 57 bridges in California in an effort to improve dynamic modeling of bridges. Included in this series of tests were the Meloland Road Overcrossing (Br. No. 58-215) and the Painter Street Overcrossing (Br. No. 4-236). At the time of this study the 1979 Imperial Valley Earthquake had shaken the Meloland Road Overcrossing and it was possible for them to compare natural periods obtained from the ambient vibration tests with the interpretations of the data from the 1979 Imperial Valley Earthquake. They stated "Examination of the results shows that the bridge responds differently to earthquake motions than to ambient vibrations due to the changing soil parameters. It is apparent that even though no inelastic reinforced concrete action took place in the bridge during the earthquake, the abutments experienced the effects of non-linear soil behavior. The abutments acted much looser during the larger excitation of the earthquake than under ambient vibration conditions." They presented the first transverse bridge natural frequency from the ambient results as 3.42 Hz compared to 2.49 Hz from the earthquake result.

Werner, Beck and Levine (1987) studied the strong motion data obtained from the 26 accelerometers installed at the Meloland Road Overcrossing during the 1979 Imperial Valley Earthquake. They used a system identification methodology to assess the seismic response characteristics of the bridge. In their concluding remarks they noted "the abutments and embankments were seen to be the major contributors to the transverse response characteristics of the bridge, whereas the deck structure dominated the MRO's vertical response characteristics." They also presented results indicating modal damping ratios ranging from 0.06 to 0.08 were identified during strong seismic excitation.

Werner, Beck and Nisar (1990) recently presented results comparing the behavior of the Meloland Road Overcrossing during free vibration response following "quick release" tests started from two different initial displacement positions, and the earthquake data from the 1979 Imperial Valley Earthquake. Their data shows significant differences in the transverse response similar to the differences first noted by Gates and Smith (1982). In particular the displacement of the abutments relative to the center of the span is much larger during the real earthquake event and the first transverse natural frequency is much smaller. They also noted a significant increase in the modal damping ratio during the real earthquake compared to the field test program.

Crouse, Hushmand and Martin (1987) performed experimental and analytical studies to determine dynamic soil-structure characteristics of a single-span, prestressed concrete bridge with monolithic abutments supported by spread footings. The experimental program revealed the presence of four modes in the frequency band between 0 to 11 Hz. Three of the modes represented primarily bending and twisting modes of the deck with measured modal damping ratios of 0.020 to 0.035. A fourth mode at 8.2 Hz was primarily in the transverse direction incorporating considerable soil-structure interaction and yielded a measured modal damping ratio of 0.15.

Wilson (1986) studied accelerograms obtained on the San Juan Bautista 156/101 Separation Bridge during the 6 August 1979 Coyote Lake earthquake. The bridge consists of six spans with the abutments and bents skewed at 34.8° with respect to the bridge deck. The main shock produced a magnitude $M_L = 5.9$ with a maximum ground acceleration of 0.12g at an epicentral distance of 26km. To model the actual field behavior of the bridge it was necessary to place a linear translational spring in the longitudinal direction of the bridge. One significant conclusion of the study showed that the modal damping ratio for the dominantly longitudinal fundamental mode approximately doubled during the strong motion phase from 4 to 8 seconds compared to the initial value of 5.4 percent. At low levels of vibration it was inferred one might reasonably expect 3 to 6 percent damping in the fundamental mode. This indicates certain energy dissipation mechanisms are activated at higher levels of response. Damping in the second horizontal mode ranged from 7.3 to 13.4 percent during five time segments of the record evaluated.

Maroney, Romstad and Chajes (1990) presented results from data obtained during six different earthquake events at the instrumented Painter Street Overcrossing. It was only possible to capture the actual measured natural frequencies and superstructure accelerations by using a relatively soft transverse spring at each abutment. Fixing the abutments resulted in a computed first transverse natural period of 0.16 seconds compared to the measured transverse period of 0.28 seconds. The results of that study indicating the importance of appropriately modeling the abutment served as the motivation for this study.

OBSERVED BEHAVIOR OF PAINTER STREET OVERCROSSING

Table 2 presents the complete set of maximum accelerations from all sensors for earthquakes 4, 5 and 6 arranged by direction. These are simply listed here because they contain essentially complete data sets including free field and sensor 7. In each direction the free field motion is given first followed by the base of pier motion. The remaining channels are then listed in sequential order from the west abutment fill to east abutment fill.

TABLE 2. Maximum Accelerations from Earthquakes 4, 5 and 6

	Longitudinal Max. Accel. (g/100)					Transverse Max. Accel. (g/100)							Vertical Max. Accel. (g/100)							
	Channel					Channel							Channel							
Earthquake	12	1	18	11	15	14	3	20	4	7	9	17	13	2	19	5	6	8	10	16
11/21/86*	46	27	45	40	40	16	13	30	23	26	23	23	8	8	18	10	23	33	25	11
11/21/86**	15	11	17	19	17	12	12	25	25	35	30	22	2	5	6	5	20	29	14	4
07/31/87	15	11	20	21	17	9	10	17	18	34	25	26	4	6	19	5	-	26	11	5

Longitudinal Motion

It is interesting to note the maximum longitudinal accelerations on the abutment fill (15 and 18) and on the structure (11) are essentially the same as the free field motion (12) for all earthquakes. This may indicate the bridge is moving as a rigid body with the ground in the longitudinal direction. Figure 2 presents the Fourier Amplitude Spectra for the longitudinal free field motions and the longitudinal sensor on the fill at the east abutment. Although the frequency content is somewhat smoother on the fill, there is no general amplification through a broad frequency range. This spectra is representative of the other earthquake records for the longitudinal motions. Fourier

Spectra at sensors 11 and 15 are generally very similar. Surprisingly, the longitudinal motion at the base of the pier (3) is consistently attenuated relative to all other longitudinal motion.

Vertical Motion

All vertical sensors on the fill (16 and 19) and bridge (5, 6, 8 and 10) are amplified relative to the free field (13) and base of pier (2) except sensor 5 on the west bridge abutment. This is probably due to the bearing strip which exists at the base of this abutment. This influence is rather dramatically demonstrated by viewing the acceleration response spectra for the vertical sensor 19 on the fill and sensor 5 adjacent to it, but on the bridge, shown in Figure 3. The motion is attenuated for all periods less than 0.33 seconds. The opposite effect can be seen by viewing Figure 4 showing the same two spectra for vertical sensor 16 on the fill and vertical sensor 10 on the bridge at the east abutment. At this abutment the vertical motion is generally amplified on the bridge abutment relative to the fill.

Transverse Motion

In the transverse direction, Table 2 shows all sensors on the abutment fill (17 and 20) and on the structure (4, 7 and 9) are considerably amplified relative to the free field (14) and base of pier motion (3). Figure 5 shows average Fourier Amplitude Spectra for all recorded transverse free field motions, base of pier motions, and on the fill and on the bridge abutment at the east end. The free field and base of pier motions are similar indicating very little soil-structure interaction. However, the motion in the free field, on the abutment fill and on the bridge abutment are significantly different in dicating relative motion between all three locations. This has considerable implication for analytical modeling.

Transverse motions are also quite different at the two abutments because of the difference in the construction of the two abutments. The influence of the bearing strip and shear keys at the west abutment can be seen in Figure 6 by observing the transverse time history of acceleration motions as the waves arrive first at the west abutment, then the free field station and then the east abutment. Inspecting sensor 4 on the abutment above the bearing strip and shear key shows very eratic motion with the arrival of the first strong wave. Similar behavior can be observed at sensor 4 in every recorded motion. In some instances the acceleration appears to hold relatively constant, indicating either sliding or plastic resistance in the abutment, and in other instances dramatic reversals in direction occur indicating impacting has occurred.

ABUTMENT BOUNDARY CONDITIONS

The interpretation of recorded data at other bridge sites and this brief description of the recorded data at Painter Street indicates the actual load-deformation behavior of the Painter Street abutment system is extremely complicated to model due to factors such as the

1) interaction of soil, piles, footings, shear keys, abutment backwall, abutment wingwalls, bearing strip,
2) nonlinearities due primarily soil stress-strain characteristics, opening and closing of gaps (impacts), friction surfaces,
3) time effects such as long term prestress shortening, thermal state relative to original thermal state, lockup of gaps caused by foreign materials,
4) coupling of longitudinal and transverse motion due to skew effects,
5) "effective mass" of the wingwall/backfill system, and
6) material, frictional and radiation damping.

Stiffness resistance to deformation at the abutments may be described by a complex system of springs reflecting soil, pile, concrete and interaction properties. Figures 7 and 8 shows plan and elevation views of the abutment system with schematic springs attached approximating resistance of individual elements to longitudinal motion (global X) of the bridge deck. Similar models have been constructed for transverse (global Z) and vertical (global Y) resistance.

At both abutments the "simple beam" wingwalls are not monolithically connected to the abutment backwall or its foundation. Over the height of the wingwalls an effectively pinned connection exists with respect to moment about the vertical global Y axis. The transfer of shear from the

backwall to the wingwalls in the transverse global Z direction is one directional in that resistance the movement of the wing wall out from the centerline of the bridge is resisted once the joint filler is crushed to transfer the load. However, the connection offers no resistance to movement of the wingwall toward the longitudinal centerline of the bridge except frictional resistance at the base of the wingwall where it rests on the abutment backwall footing. At this location the wingwalls and abutment backwall footing are separated by 1/4" of expansion joint filler. The same pinned joint interrupts the transfer of load to the wingwalls and back to the rear piles in the longitudinal global X direction until one inch of expansion joint filler is sufficiently crushed. Once the joint filler is sufficiently compressed resistance forces between the wingwalls, rear pile caps, rear piles and soil can be developed when the deck is moving into the backfill material.

At the base of the west abutment there is not a monolithic connection between the abutment backwall and the abutment footing. The backwall and the foundation are separated by a 1/4" neoprene bearing strip. Shear keys effectively bound the abutment backwall in the case of gross relative displacements in both transverse directions and in the skewed longitudinal direction such that the backwall is keyed against moving into the soil. The abutment backwall and the transverse shear keys are separated by one inch of expansion joint filler. In the skewed longitudinal direction the abutment backwall and the shear key at the time of construction were separated by one inch of expansion joint filler; however the separation at any time since the original construction is a function of the time effects noted. Friction and shear stiffness of the bearing strip offer the only load path to the footing from the abutment backwall prior to the expansion joint filler being compressed sufficiently to transfer compressive stresses.

A 39 degree skew at both abutments forces the normal and shear abutment resistance to be defined at an angle to the global axes. Movement of the abutment backwall into the abutment backfill in the global X direction is resisted by passive soil forces normal to the abutment backwall and frictional forces parallel to the abutment backwall which have components in the global X and Z directions.

Figure 9 presents an articulated set of longitudinal components of the springs in series and in parallel at west abutment where the bearing strip is located. The springs can be combined to represent a single nonlinear spring in the longitudinal direction. Similar models have constructed for the global Y and Z directions. The complete assembled set can be combined to form a coupled set of six degree of freedom nonlinear springs at a point on the abutment backwall if a stick model is employed, or a coupled set of distributed nonlinear springs at nodal points along the abutment backwall if the deck is modeled as a plate system. Due to space limitations herein only the longitudinal springs at the west abutment will be described.

Conceptually we will describe the mechanisms by thinking of the bridge deck moving into, or away, from the backfill material. A portion of the deck load will transfer through the stiffness K_{bw} of the abutment backwall above the abutment footing to the bearing strip of stiffness K_{bs}. Initially this portion of the deck load will then be transferred into the soil through the piles, K_p, and passive resistance against the cap, K_{cf}, and through the friction where the wingwall rests on the cap, $K_{ww/cf}$. The portion of the deck load not transferred to the footing from the backwall will directly transfer from the backwall to the soil through $K_{bw/s}$ representing the distributed resistance of the entire backwall area about the abutment footing. This stiffness is represented by the relatively confined soil behind the abutment backwall and the unconfined soil on the roadway side of the wall.

The load transferred to the wingwall will be distributed to the surrounding soil medium through cohesion and frictional resistance of the soil confined between the wingwalls, $K_{ww/si}$, and unconfined outside the wingwalls, $K_{ww/so}$, the horizontal component, K_{wwl}, of the normal and frictional resistance of the thickness at the base of the wingwall, the resistance of the soil to the thickness of the wingwall above the rear footing, K_{wwu}, the passive resistance to the cap, K_{cr}, and the piles, K_p, at the rear footing for the wingwalls.

Discontinuities or "gaps" at the abutment backwall/wingwall connection, D_{ww}, and abutment backwall/pilecap connection, D_{cf}, are also identified in Figure 9. The displacement D_{ww} is the deformation of the backwall required to engage the wingwall directly and D_{cf} is the deformation of the base of the backwall required to engage the pilecap directly through its shear key. Closure and opening of these gaps will result in major instantaneous stiffness discontinuities which should be observable in the recorded data.

INFLUENCE OF THREE DIRECTIONS OF MOTION ON PREDICTED RESPONSE

Elastic response spectra and time history analysis of the Painter Street Overcrossing have been carried out as part of this study using all three direction of ground motion. The comparisons of the measured results and the predicted results are only fair at this point, and space prohibits showing many of the comparisons. The clear nonlinear behavior in the abutment region and substantial differences in damping between modes makes elastic analysis almost a qualitative comparison. Table 3 is presented to demonstrate the significance both the vertical and transverse free field motions have on the accelerations at stations 6, 7 and 8. Clearly both directions of motion contribute significantly to the vertical accelerations 6 and 8 on the north edge of the deck at the middle of each of the spans. As expected, the transverse acceleration at the bent is dominantly contributed by the transverse input motion.

Table 3 Maximum Response Spectrum Predictions of Superstructure Accelerations

Earthquake	Free Field Input Direction	Center West Span (ft/sec^2) Vertical Acc 6	Center East Span (ft/sec^2) Vertical Acc 8	Center Bent Span (ft/sec^2) Transverse Acc 7
4	Vertical (13)	6.7	9.2	1.3
	Longitudinal (12)	0.3	0.4	0.0
	Transverse (14)	9.2	7.6	12.6
5	Vertical (13)	2.2	2.4	0.5
	Longitudinal (12)	0.0	0.0	0.0
	Transverse (14)	8.5	6.8	12.1
6	Vertical (13)	3.5	4.1	0.8
	Longitudinal (12)	0.0	0.0	0.0
	Transverse (14)	7.8	5.9	11.2

SUMMARY AND CONCLUSIONS

Relatively short span bridges exhibit considerable soil-structure interaction in the abutment area due to nonlinear soil behavior, gaps in abutment construction, bearing strips. It appears the phenomenon cannot be observed by ambient and quick release field testing. Damping varies significantly between modes depending upon the level of soil-structure interaction present in the mode. Elastic modeling is unlikely to provide other than qualitative information on the peak forces in bridges dominated by soil struction interaction in the abutment area.

ACKNOWLEDGEMENTS

The contents of this report were developed under a contract from the California Department of Conservation, Division of Mines and Geology, Strong Motion Instrumentation Program. However, these contents do not necessarily represent the policy of that agency nor endorsement by the State Government. The authors greatly appreciative the support of the California Department of Transportation, Office of Structures, for the use of the computer time and facilities in conducting this study.

REFERENCES

Chen, M. and Penzien, J., "Nonlinear Soil-Structure Interaction of Skew Highway Bridges," Report No. UCB/EERC-77/24, Earthquake Engineering Research Center, University of California, Berkeley, August, 1977.

Crouse, C. B., Hushmand, B., and Martin, G. R., "Dynamic Soil-Structure of a Single Span Bridge", Earthquake Engineering and Structural Dynamics, Vol. 15, 1987, pp. 711-729 .

Douglas, B.M., Maragakis, E.A., Vrontinos, S. and Douglas, B.J., "Analytical Studies of the Static and Dynamic Response of the Meloland Road Overcrossing," Proceedings of the Fourth U.S. National Conference on Earthquake Engineering, Palm Springs, Ca., Vol. 1, 1990, pp. 987-996.

Gates, J.H. and Smith, M.J., "Verification of Dynamic Modeling Methods by Prototype Excitation," Report No. FHWA/CA/SD-82/07, California Department of Transportation, Office of Structures Design, Sacramento, Ca., November, 1982.

Lam, I. and Martin, G., "Seismic Design of Highway Bridge Foundations", FHWA/RD-86/101, Earth Technology Corporation, Long Beach, Ca., June 1986.

Levine, M.B. and Scott, R.F., "Dynamic Response Verification of a Simplified Bridge-Foundation Foundation Model," ASCE, Journal of Geotechnical Engineering, Vol. 115, No. 2, February, 1989, pp. 246-260.

Maragakis, E., "A Model for the Rigid Body Motions of Skew Bridges," Report No. EERL 85-02, California Institute of Technology, 1985.

Maragakis, E., Thornton, G., Saiidi, M. and Siddharthan, R., "A Simple Non-Linear Model for the Investigation of the Effects of the Gap Closure at the Abutment Joints of Short Bridges," Earthquake Engineering and Structural Dynamics, Vol. 18, 1987, pp. 1163-1178.

Maroney, B., Romstad, K.M. and Chajes, M.J., "Interpretation of Rio Dell Freeway Response During Six Recorded Earthquake Events," Proceedings of the Fourth U.S. National Conference on Earthquake Engineering, Palm Springs, Ca., Vol. 1, 1990, pp. 1007-1016.

Werner, S.D., Beck, J.L. and Levine, M.B., "Seismic Response Evaluation of Meloland Road Overpass Using 1979 Imperial Valley Earthquake Records," Earthquake Engineering and Structural Dynamics, Vol. 15, 1987, pp. 249-274.

Werner, S.D., Beck, J.L. and Nisar, A., "Dynamic Tests and Seismic Excitation of a Bridge Structure," Proceedings of the Fourth U.S. National Conference on Earthquake Engineering, Palm Springs, Ca., Vol. 1, 1990, pp. 1037-1046.

Wilson, J. C., "Analysis of the Observed Seismic Response of a Highway Bridge," Earthquake Engineering and Structural Dynamics, Vol. 14, 1986, pp. 339-354.

Wilson, J. C., "Stiffness of Non-Skew Monolithic Bridge Abutments for Seismic Analysis", Earthquake Engineering and Structural Dynamics, Vol. 16, 1988, pp. 867-883.

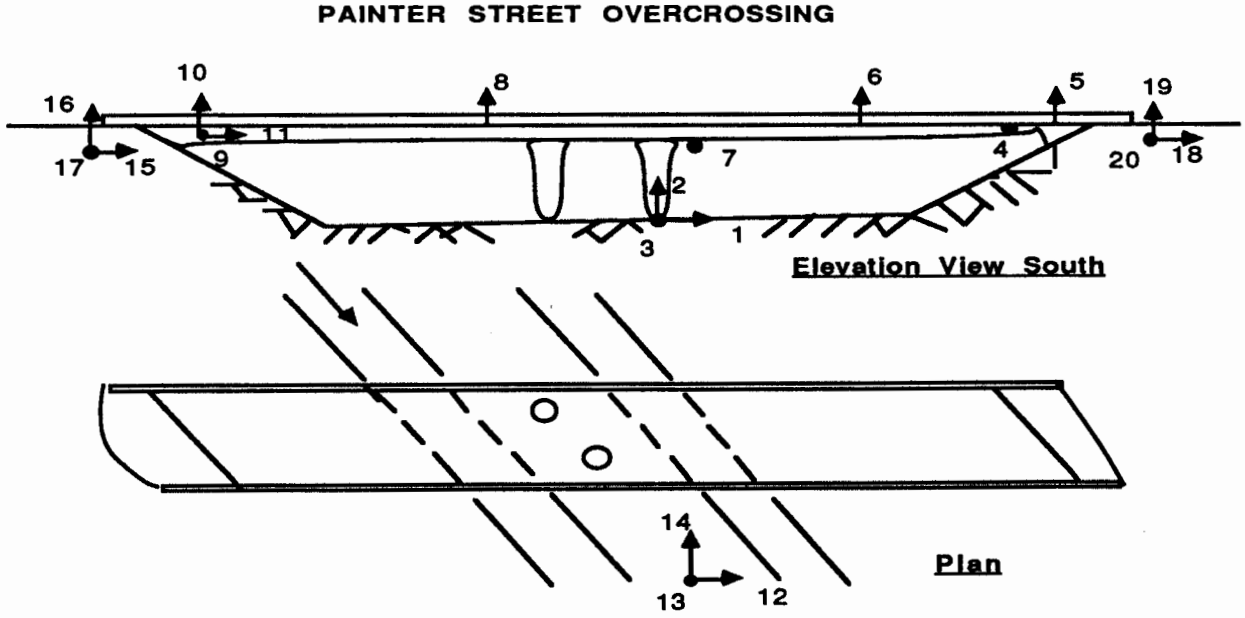

Figure 1 Superstructure and Instrumentation for Painter Street Overcrossing

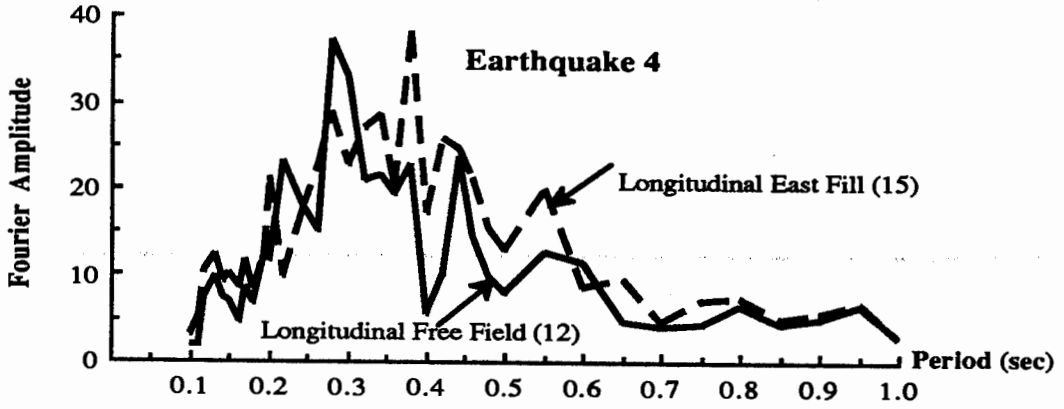

Figure 2 Fourier Amplitude for Longitudinal Motion at Sensors 12 and 15

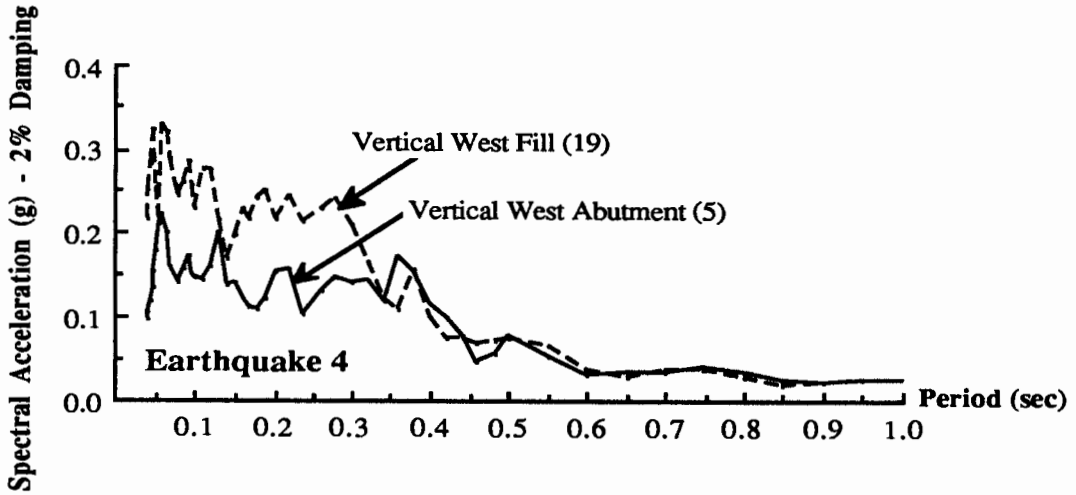

Figure 3 Acceleration Spectra for Vertical Sensors 5 and 19 at West Abutment

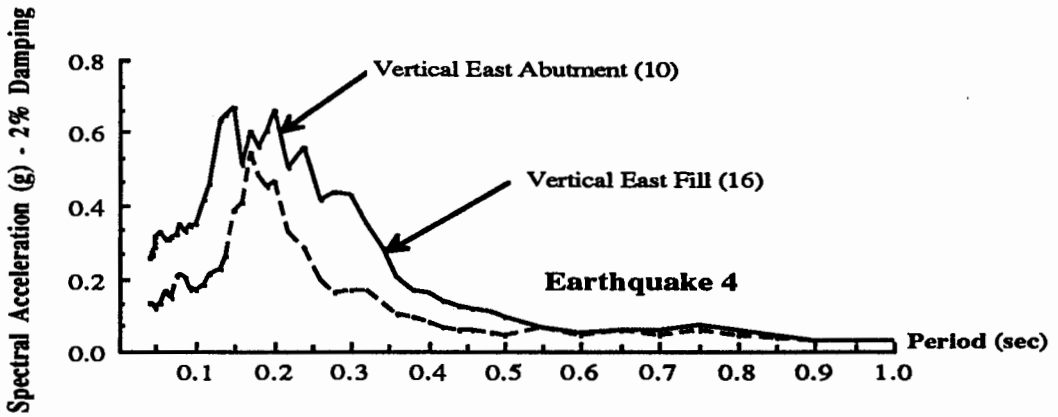

Figure 4 Acceleration Spectra for Vertical Sensors 10 and 16 at East Abutment

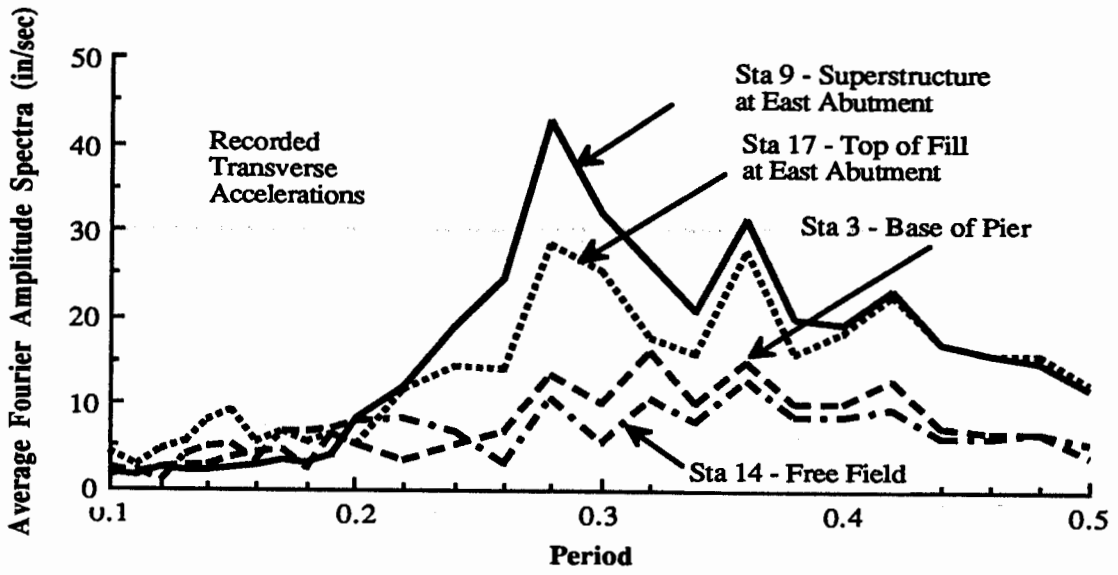

Figure 5 Average Fourier Amplitude Spectra for All Recorded Motions at 14, 3,17 and 9

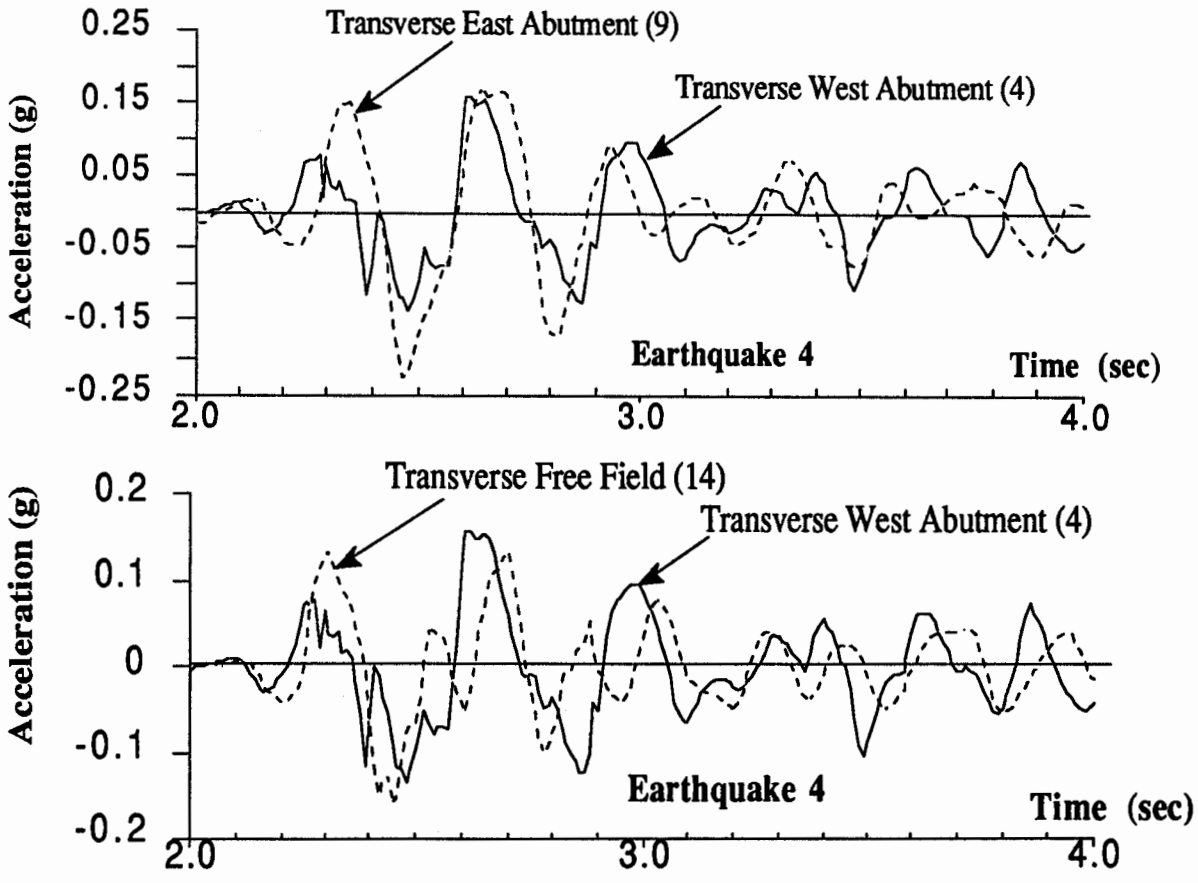

Figure 6 Recorded Transverse Time History Motions at 4, 9 and 14 During Earthquake 4

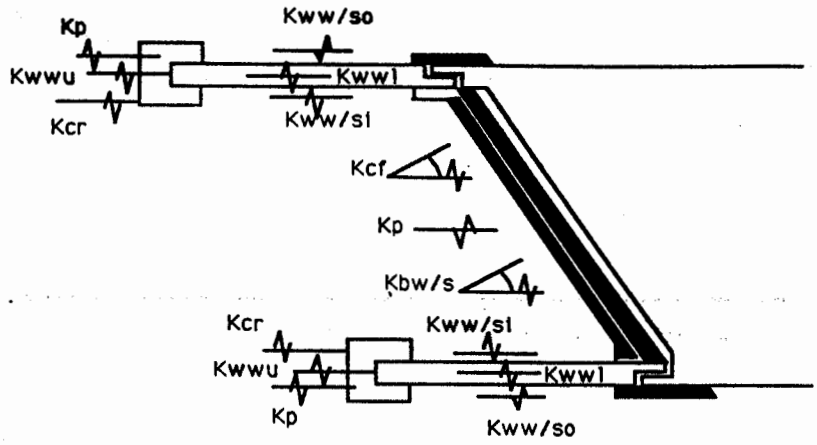

Figure 7 Plan View of Longitudinal West Abutment Resisting Elements

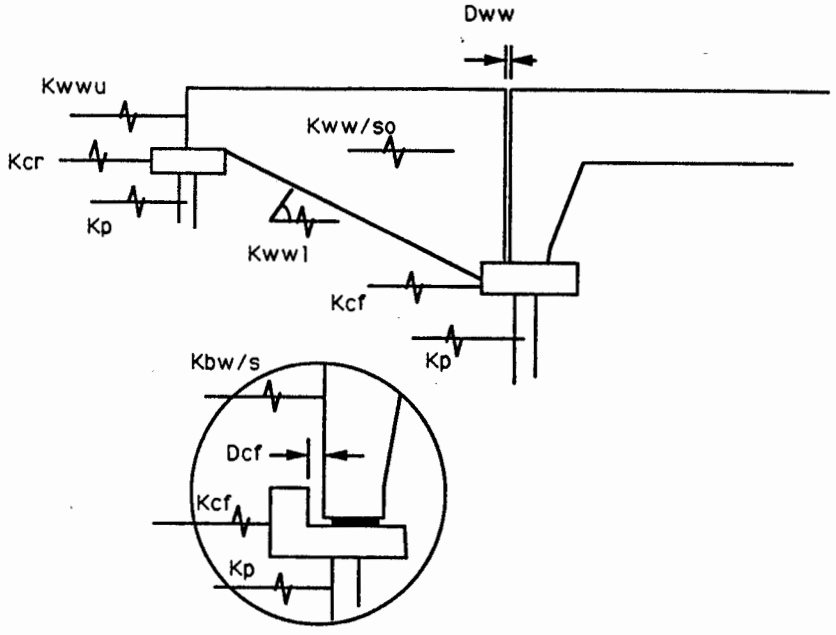

Figure 8 Elevation View of Longitudinal West Abutment Resisting Elements

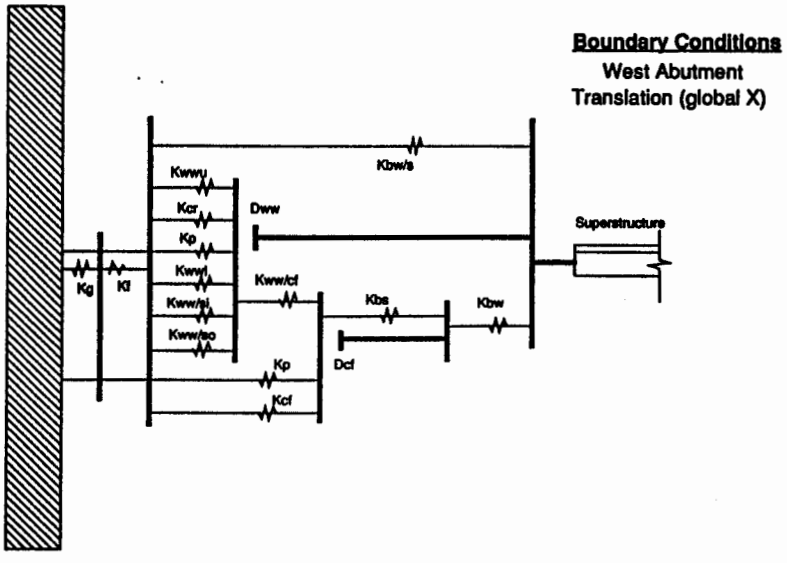

Figure 9 Schematic Representation of Longitudinal West Abutment Active Spring Elements

EVALUATION OF LATERAL FORCE PROCEDURES FOR BUILDINGS

Gregory L. Fenves
Assistant Professor
Department of Civil Engineering
University of California at Berkeley

ABSTRACT

The recent edition of building codes for earthquake resistant design specify a dynamic analysis procedure for computing lateral forces on buildings with irregular plan or vertical irregularities. This paper presents the use of the instrumented response of two buildings to strong ground motion for determining vibration properties and distribution of lateral forces. The two buildings were selected for the irregular features in their configuration, and the results illustrate the difference in lateral force distribution for type of building and amplitude of earthquake response.

INTRODUCTION

The determination of lateral earthquake forces acting on a building is a critical part of earthquake resistant design. The lateral forces depend on the dynamic characteristics of the building (mass, stiffness, strength, damping, and energy absorption) and the characteristics of the ground motion (amplitude, frequency content, and duration). The detailed modeling and analysis of a building for computing lateral forces is not practical, particularly in the early stages of a design. The current lateral force requirements developed by SEAOC [7] and incorporated in the 1988 Uniform Building Code [5] prescribe two methods for determining lateral forces:

- Static Lateral Force Procedure — Compute the maximum base shear using a design ground motion spectrum and distribute the base shear over the height of the building.

- Dynamic Lateral Force Procedure — Using a ground motion spectrum and a mathematical model of the building, compute the internal forces and displacements of the building from a response spectrum or time history analysis. For most buildings the response may be scaled such that the base shear is not greater than the base shear determined from the static lateral force procedure.

The dynamic lateral force procedure is a new requirement from earlier versions of the code. The new provisions recognize the poor earthquake performance of buildings with irregular configuration compared to buildings with regular configuration. The dynamic lateral force procedure is mandatory for buildings with a configuration that would invalidate the assumption that the response is primarily due to the fundamental mode of vibration, which is inherent in the static lateral force procedure.

The Applied Technology Council committee 3-06 report, now incorporated in the NEHRP recommended provisions [6], introduced the concept of building configuration for determining lateral forces on buildings. An irregular configuration has significant discontinuities in the mass or stiffness of the lateral force resisting system, or eccentricity of mass or stiffness. For the purpose of evaluating configuration, structural irregularities are classified by features in the vertical direction or in plan; the code provides lists of specific irregular features. Other characteristics of the building and ground motion may invalidate the use of the static lateral force procedure, such as participation of higher vibration modes, different lateral force resisting systems in orthogonal directions, and directional effects of the ground motion, particularly in buildings with closely coupled vibration modes. Although the dynamic analysis provisions for buildings with irregular configurations is a positive development in seismic design, the equivalent lateral force procedure is not always rational even for buildings with uniform mass and stiffness because of the contributions of the higher vibration modes [1] or because of torsional response.

The purpose of this study is to use the recorded earthquake response of buildings to determine the distribution of lateral forces and compare the distribution to the building code provisions. This paper presents an evaluation of the earthquake response of two buildings.

SELECTION OF INSTRUMENTED BUILDINGS

Seventy-one building/earthquake records from the California Strong Motion Instrumentation Program (CSMIP) of the Division of Mines and Geology were examined for configuration and earthquake response that may be characteristic of irregular buildings. Several parameters were collected for each building/earthquake including in the preliminary screening: number of stories and story heights, aspect ratio in plan, peak acceleration amplification factors between the roof and ground in each principal direction, classification of vertical and plan irregularity according to the code definitions [5,7], and observation of torsion, higher mode contributions or beating in the response records. Most the buildings instrumented by CSMIP are regular, however twelve buildings have at least one irregular feature, of which four had two irregular features. Two buildings were selected for detailed study; coincidentally both are hospitals.

BUILDING ONE — FOUR STORY HOSPITAL

The four story medical center is located in South San Francisco. Figure 1 shows the structural configuration of the building. The gravity load system consists of a lightweight concrete slab on metal decking supported by floor beams. The lateral force resisting system is a structural steel moment resisting frame. The foundation for each column consists fifty to seventy foot piles; grade beams connect the pile caps and support an eight inch slab. The building is instrumented with eleven acceleration transducers at the locations shown in Figure 1.

The CSMIP documentation [2,4] describes the first floor walls as a "shear walls," which would constitute an vertical irregularity because of the abrupt

change in stiffness of the lateral force resisting system. Examination of the building plans, however, show that the wall is an architectural barrier and there is no structural connection between the wall and the moment resisting frame (there is transverse support for the wall) so there is no vertical irregularity in the lateral force resisting system. One of the interesting features of the earthquake response is whether the wall participates in resisting lateral forces as a nonstructural component; the earthquake response records shed some light on this question. In plan, the re-entrant corners are approximately 15% of the length in the longitudinal direction which is on the borderline of constituting a plan irregularity [5,7].

At the beginning of the study response records were available for the 1984 Morgan Hill earthquake [4]. During the course of the study, the instruments triggered in the 1989 Loma Prieta earthquake and the processed response records have just become available [2].

Morgan Hill Earthquake

The unprocessed records are shown in Figure 2(a) and the peak total accelerations are listed in Table 1. Figures 3 and 4 show two sets of the transmissibility functions for total acceleration in each direction: (i) between the roof and ground level; and (ii) the second level and ground. The transmissibility functions are the ratio of the Fourier transform of the corrected acceleration records computed over two time windows. The first time window, zero to fifteen seconds, shows the response before the strong response, and the second time window, fifteen to forty seconds contains the strong ground motion and response. The transmissibility functions for frequencies less than one-half Hertz have not been considered in the interpretation.

The vibration periods and damping ratios for the lower mode in each direction are obtained using the half-power bandwidth method; the values are tabulated in Table 2. The periods lengthen slightly in the strong motion phase and the damping ratio in the longitudinal direction increases because of the larger amplitude of motion. Based on the strong motion response, the C_t coefficient is 0.029, compared to 0.035 for the code procedure for determining vibration period. The larger amplification of the response between the 2nd floor and roof and the lower vibration mode shapes (Figure 5) obtained from the transmissibility functions indicate that the nonstructural wall in the first level is providing some lateral stiffness for the relatively low amplitude response.

Loma Prieta Earthquake

The unprocessed records from the Loma Prieta earthquake are shown in Figure 2(b) and the peak responses are also listed in Table 1 [2]. The ground motion and building response was significantly greater in Loma Prieta than in Morgan Hill, yet there was no damage to the structural or nonstructural components of the building[1]. The transmissibility functions computed from the processed records for two time windows are shown in Figure 4 for two time windows: (i) zero to nine seconds, and (ii) nine to twenty six seconds. Based

[1] Personal communication with a structural engineer engaged who inspected the building after the Loma Prieta earthquake.

on these functions, the periods are listed in Table 2. The damping was larger than in the Morgan Hill earthquake as can be seen by comparing the peaks of the transmissibility functions between Figures 3 and 4, but the half-power bandwidth method does not give reliable values because of the closely correlated modes. The large amplitude of the response results in significantly longer periods than for the Morgan Hill earthquake, and the C_t coefficient of 0.036 compares favorably with the code value. The fundamental mode shape in each direction (Figure 6) clearly shows the first floor wall does not resist lateral forces because the shape is typical for the racking mode shape of a frame structure.

Mathematical Model and Computed Response

A mathematical model of the linear response of the structural components has been developed based on the plans for the medical center. Although space limitations preclude presentation of the results, close correlation between the measured and analytical response was obtained when mass eccentricity is included. This appears necessary because the symmetrical distribution of stiffness does not explain the coupled modal response and beating apparent in the recorded response.

BUILDING TWO – SIX STORY HOSPITAL

This six story hospital in Sylmar has a rectangular plan in the lower two floors and a cruciform plan in the upper four floors (Figure 7). The floor system is concrete slab on metal decks. The lateral force resisting system consists of concrete shear walls in the lower two stories and steel shear walls in the upper four stories. The structure has both plan and vertical irregularities according to the code definitions.

The building was instrumented with sixteen acceleration transducers in the 1987 Whittier earthquake (although one malfunctioned)[3]. The large stiffness of the lower two floor is clear from the mode shapes obtained from the transmissibility functions (Figure 8), where the relative amplitude of the vibration mode between the third floor and roof is larger than between the base and the third floor.

CONCLUSIONS

The earthquake response records of two hospital buildings with irregular features illustrate the effect of lateral force distribution and the sensitivity to the amplitude of ground motion. More detailed results in the final report will show the correlation with analytical response and compare the lateral force distributions to the provisions of the building codes.

ACKNOWLEDGEMENTS

The CSMIP External Data Utilization Program provided the support for this investigation. Graduate research assistant Pablo Mira offered substantial contributions to the research and this paper.

REFERENCES

1. Cruz, E.F., and Chopra, A.K., "Elastic Earthquake Response of Building Frames," *Journal of Structural Engineering*, ASCE, Vol. 112, No. 3, March, 1986, pp. 443-459.
2. *CSMIP Strong-Motion Records from the Santa Cruz (Loma Prieta) Earthquake of 17 October 1989*, Report OSMS 89-06, California Department of Conservation, November, 1989.
3. *CSMIP Strong-Motion Records from the Whittier Earthquake of 1 October 1987*, Report OSMS 87-05, California Department of Conservation, October, 1987.
4. *CSMIP Processed Data From the Strong-Motion Records of the Morgan Hill Earthquake of 24 April 1984*, Part II, Report OSMS 85-05, California Department of Conservation, December, 1985.
5. International Conference of Building Officials, *Uniform Building Code*, 1988 Edition, May, 1988.
6. National Earthquake Hazards Reduction Program, "Recommended Provisions for the Development of Seismic Regulations for New Buildings," Part 1 and 2, FEMA/95, Federal Emergency Management Agency, February, 1986.
7. Structural Engineers Association of California, *Recommended Lateral Force Requirements and Tentative Commentary*, Fifth Edition, 1988.

Table 1 — Maximum Total Acceleration of Building One - Four Story Hospital in the 1984 Morgan Hill Earthquake and the 1989 Loma Prieta Earthquake

Earthquake	Maximum Response	Transverse Direction	Longitudinal Direction
Morgan Hill	Roof Acceleration (g)	0.17	0.11
	Base Acceleration (g)	0.03	0.02
	Roof/Base Acceleration	5.7	5.5
Loma Prieta	Roof Acceleration (g)	0.61	0.57
	Base Acceleration (g)	0.16	0.14
	Roof/Base Acceleration	3.8	4.1

Table 2 — Lower Vibration Mode Properties of Building One - Four Story Hospital in the 1984 Morgan Hill Earthquake and the 1989 Loma Prieta Earthquake

Earthquake	Time Window	Vibration Property	Transverse Direction	Longitudinal Direction
Morgan Hill	First (0-15 sec)	Period (sec)	0.54	0.54
		Damping Ratio	0.028	0.028
	Second (15-40 sec)	Period (sec)	0.57	0.56
		Damping Ratio	0.029	0.044
Loma Prieta	First (0-9 sec)	Period (sec)	0.65	0.61
		Damping Ratio	(a)	0.055
	Second (9-26 sec)	Period (sec)	0.71	0.71
		Damping Ratio	(a)	(a)

(a) Could not be determined because of closely spaced modes.

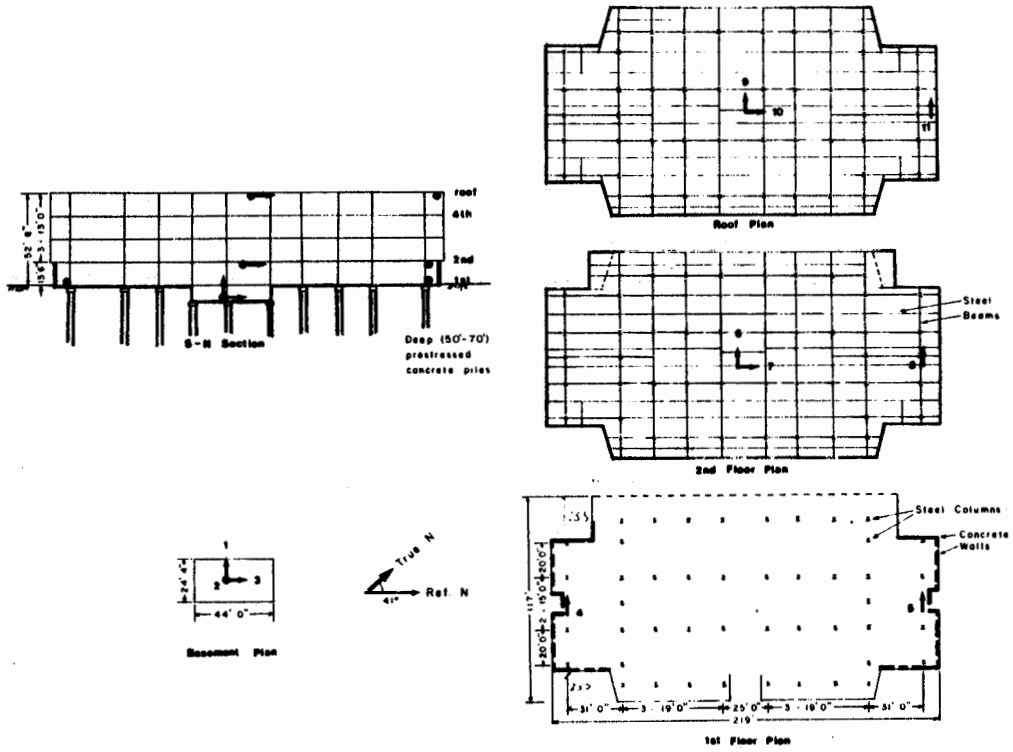

FIGURE 1. Structural Configuration and Instrumentation for Building One - Four Story Hospital [2,4]

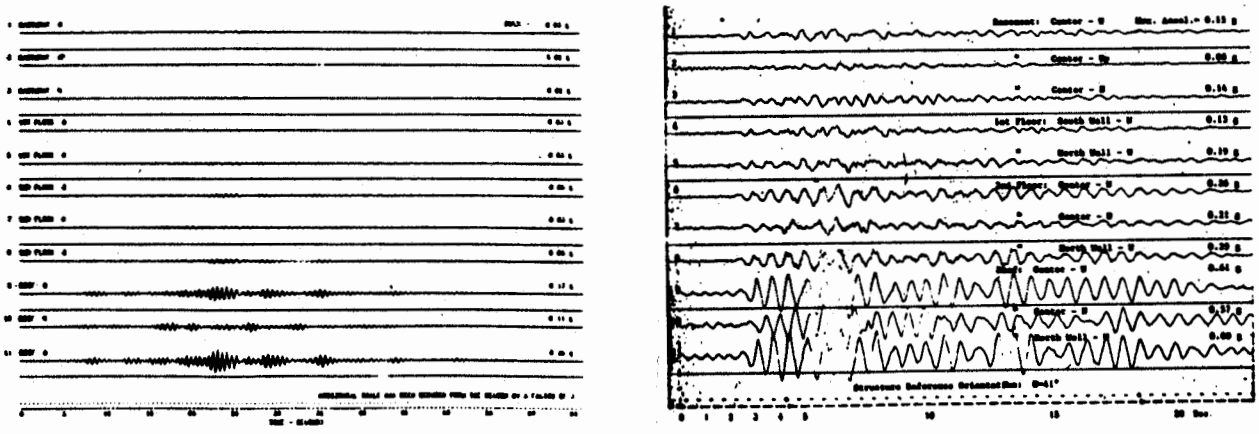

(a) 1984 Morgan Hill Earthquake [4] (b) 1989 Loma Prieta Earthquake [2]

FIGURE 2. Unprocessed Response Records for Building One - Four Story Hospital

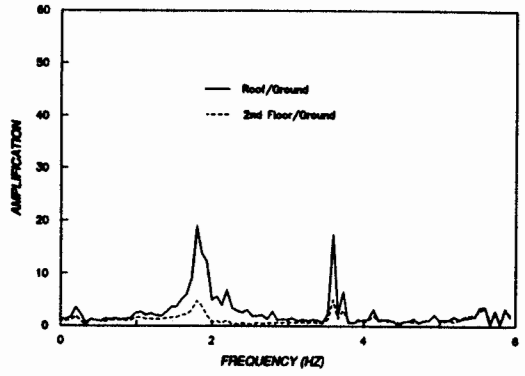

(a) Transverse Direction, 0-15 sec

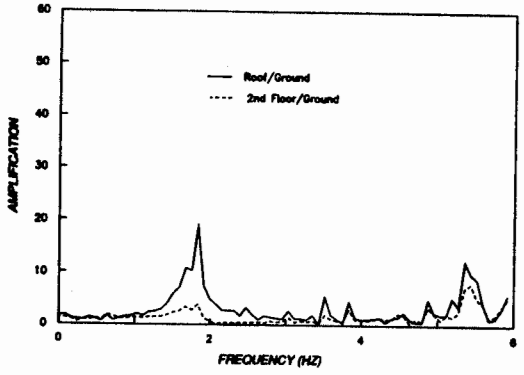

(b) Transverse Direction, 15-40 sec

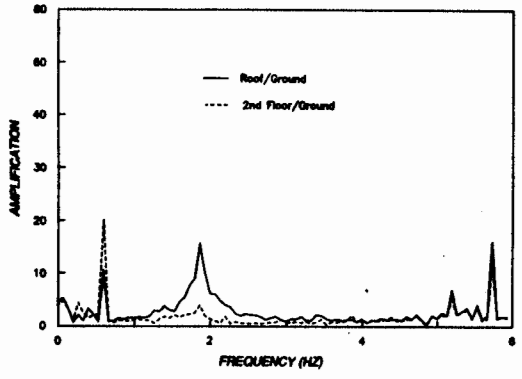

(c) Longitudinal Direction, 0-15 sec

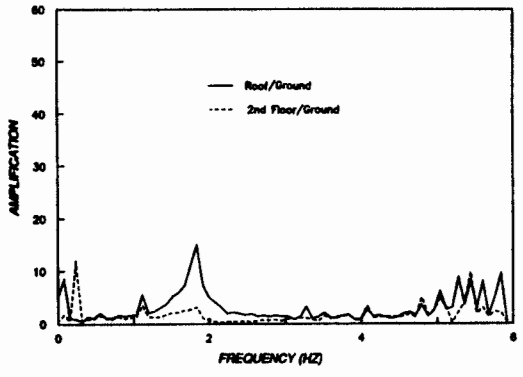

(d) Longitudinal Direction, 15-40 sec

FIGURE 3. Transmissibility Functions for Building One - Four Story Hospital for the 1984 Morgan Hill Earthquake

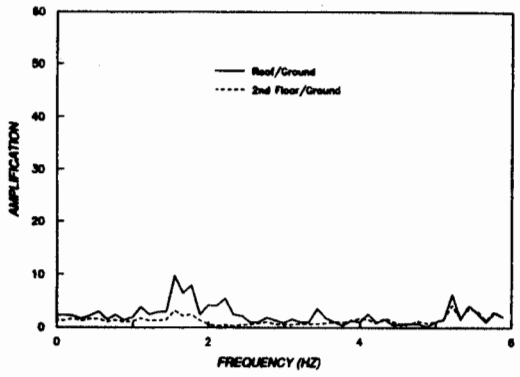

(a) Transverse Direction, 0-9 sec

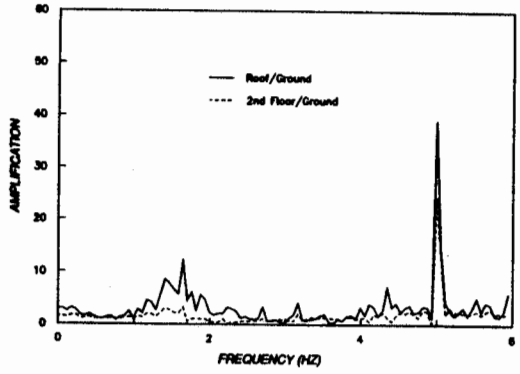

(b) Transverse Direction, 9-26 sec

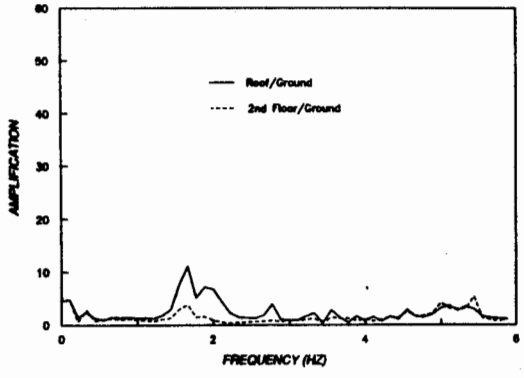

(c) Longitudinal Direction, 0-9 sec

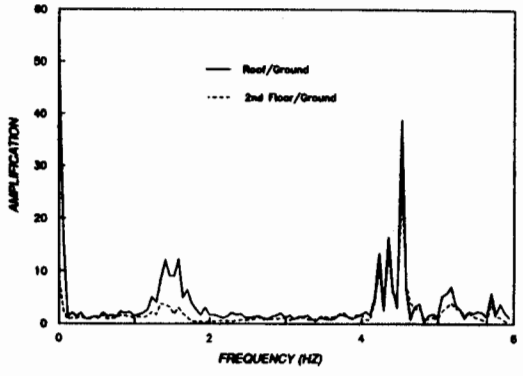

(d) Longitudinal Direction, 9-26 sec

FIGURE 4. Transmissibility Functions for Building One - Four Story Hospital for the 1989 Loma Prieta Earthquake

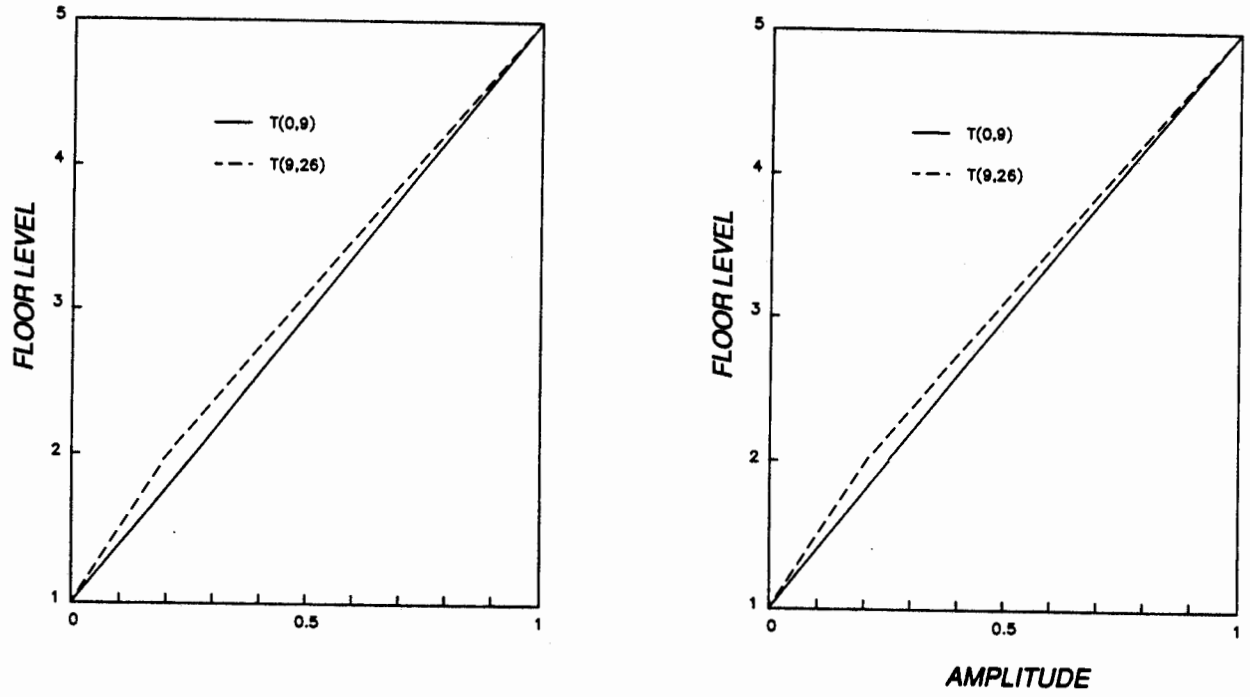

(a) Transverse Direction (b) Longitudinal Direction

FIGURE 5. Lower Vibration Mode Shapes for Building One - Four Story Hospital for the 1984 Morgan Hill Earthquake

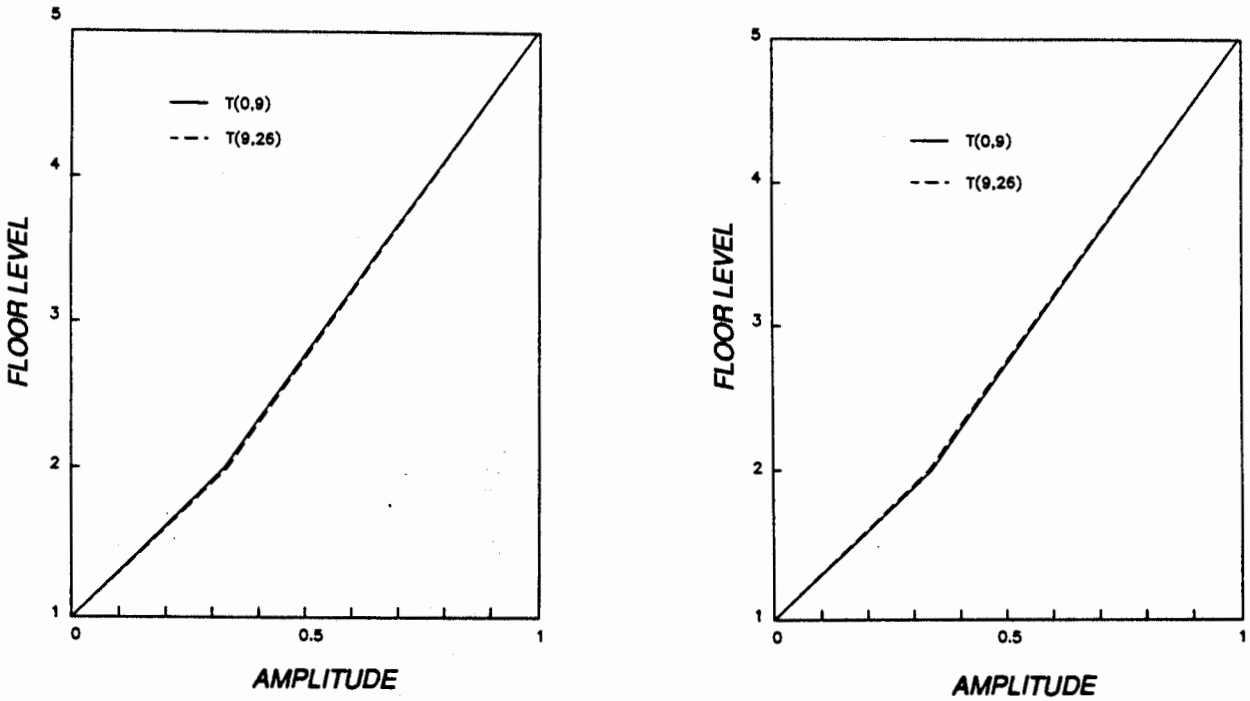

(a) Transverse Direction (b) Longitudinal Direction

FIGURE 6. Lower Vibration Mode Shapes for Building One - Four Story Hospital for the 1989 Loma Prieta Earthquake

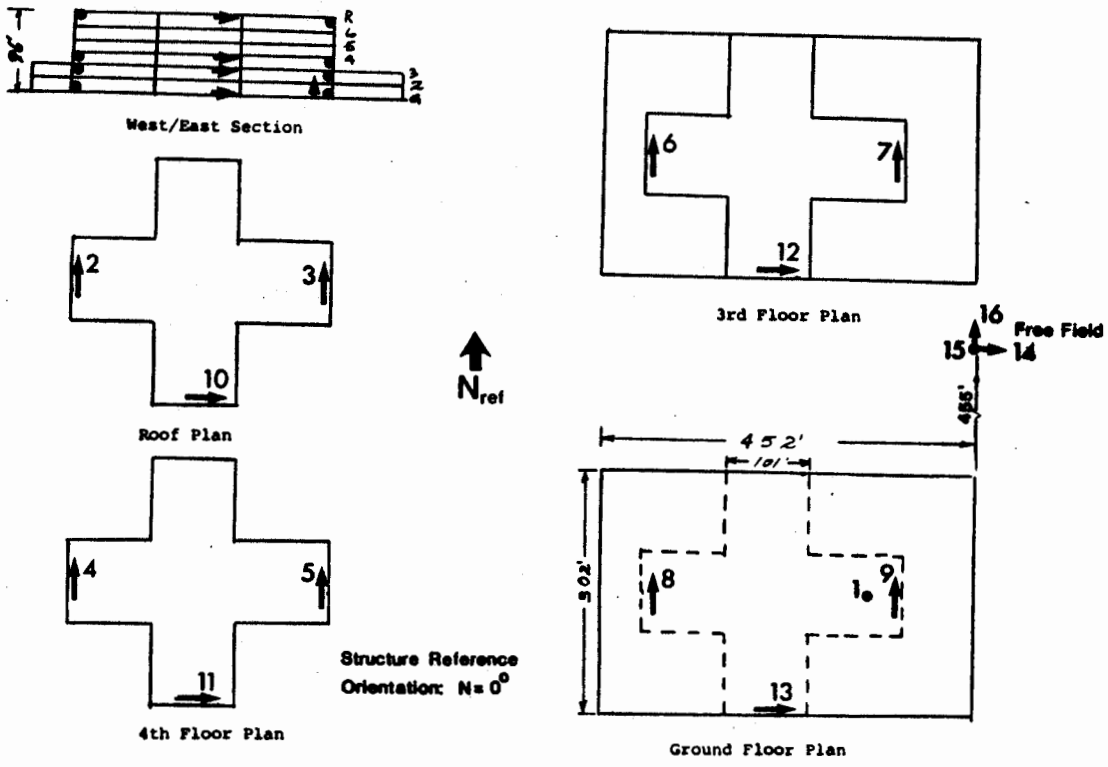

FIGURE 7. Structural Configuration and Instrumentation for Building Two - Six Story Hospital [3]

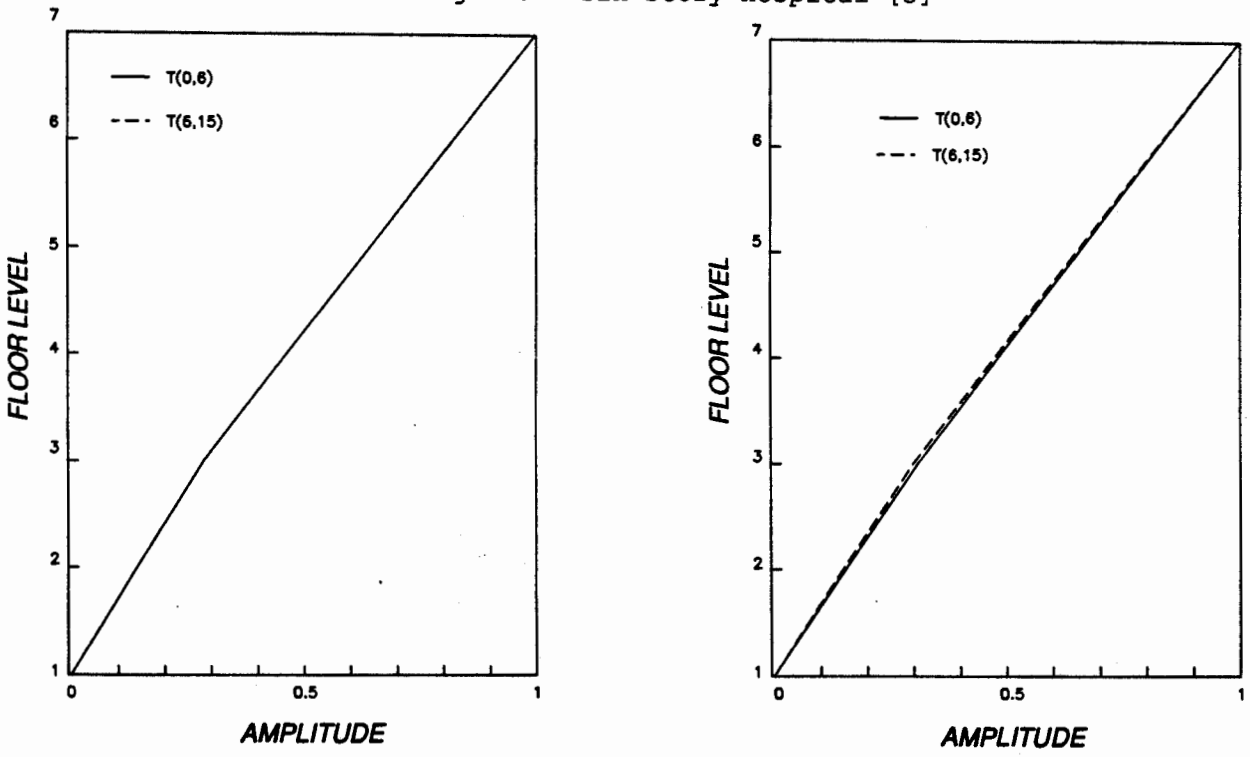

(a) Transverse Direction (b) Longitudinal Direction

FIGURE 8. Lower Vibration Mode Shapes for Building Two - Six Story Hospital for the 1987 Whittier Earthquake

INVESTIGATION OF DESIGN AND ANALYSIS METHODS FOR STEEL FRAMED BUILDINGS

A. Astaneh, S. A. Mahin, J-H. Shen and R. Boroschek

Department of Civil Engineering
University of California at Berkeley

ABSTRACT

The Strong Motion Instrumentation Program (SMIP) of the California Department of Mines and Geology has obtained significant records in a number of steel structures. The objective of this research was to conduct comparative studies of the response of two modern steel structures as predicted by current analytical methods and the response recorded by SMIP.

Realistic models of the structures were developed and were subjected to 3-dimensional dynamic analyses. The analyses indicated that proper modeling of connections, and floor diaphragms can lead to accurate predictions of the response. Also, current code procedures predict a period that usually is significantly smaller than actual period of vibration.

INTRODUCTION

While steel frame buildings have generally performed well during past earthquakes, many questions have been raised regarding the realism and adequacy of methods used in their design and analysis. Modern steel buildings, utilizing perimeter moment frames, are generally much more flexible and irregular than those constructed in earlier eras. Their dynamic response is likely to be lightly damped, more sensitive to nonstructural components, and more susceptible to torsional and higher mode vibrations. Thus, conventional modeling and design assumption may not represent actual dynamic response. The main objective of the study summarized herein was to investigate the adequacy and accuracy of design and analysis methods applied to steel structures by conducting comparative studies of recorded earthquake response and the response predicted using available analytical methods.

DESCRIPTION OF THE BUILDINGS UNDER INVESTIGATION

The Strong Motion Instrumentation Program (SMIP) of the California Department of Mines and Geology has obtained significant records in a number of modern steel frame buildings. Two of these buildings, both constructed in the late 1970's exhibit particularly interesting response: an office building in San Jose identified as CSMIP Station No. 57357 and another office building identified as CSMIP Station No. 24370 located in Burbank.

The San Jose Building is a 13 story frame with a nearly square floor plan (Fig. 1). It was designed in 1972 and construction was completed in 1976. The vertical load carrying system consists of a 3-1/2 inch concrete slab over metal deck supported, on steel beams, girders and columns. The lateral load resisting system consists of a strong perimeter moment resisting frame with tapered

girders, and four interior moment frames in each orthogonal direction. An extra bay is provided along the west and south sides of the building to accommodate stairs, elevators and extra offices. Framing irregularities in this region and differences in architectural treatments on these sides of the building resulted in small torsional eccentricities. Nonetheless, the building would qualify as a torsionally regular building according to the provisions of the 1988 Uniform Building Code [3]. In addition to the recent Loma Prieta earthquake, the building was subjected to the 1984 Morgan Hill earthquake and the 1986 Mt. Lewis earthquake [4]. The building's response is characterized as being both particularly severe and long (Fig. 2) Twenty-two accelerometers were used to record the building motion. Maximum accelerations at the base of the building for both of these latter events was 4%g, while that for the Loma Prieta event was 11%g. Only the response during the 1984 and 1986 events will be examined herein.

The Burbank Building is a six story building with almost symmetric geometry. The building was excited during the 1987 Whittier Narrows earthquake [5]. Details of the steel structure of the building are shown in Figures 3 and 4. The structure of the building consists of hot rolled wide flange columns and beams supporting the floor steel deck and concrete slabs. The structure has a perimeter moment frame to resist the tributary gravity and total lateral load while the internal columns are designed to carry only their tributary gravity load. The beam-to-column connections in the perimeter frame are rigid, and all other connections are designed to act as simple connections and to carry shear only. During the Whittier Narrows earthquake the building was subjected to ground motions with 22% peak acceleration.

SCOPE AND METHODOLOGY

A coordinated investigation of these two buildings was conducted. The focus of study was on the characterization of the basic behavioral parameters as well as on the assessment and improvement of the current design procedures and analysis methods. The project involved the following specific tasks:

1. The engineering design parameters (periods, mode shapes, and damping) and important response characteristics were identified from an interpretation of recorded response.

2. Conventional and "realistic" models of the structures were developed using information obtained from the available structural drawings as well as from the actual survey of the buildings. In the San Jose building, the flexibility of the beam-column joints was modeled as was the architectural exterior finishes. In the Burbank building, the connections of perimeter frame was modeled as rigid whereas the interior connection were modeled as semi-rigid. Also, in this building the interaction of floor diaphragm and steel girders were modeled as partially composite to reflect the actual existing conditions.

3. The structural models were subjected to ground motions recorded at the site of the buildings. Elastic three dimensional analyses were used in the case of the San Jose building whereas inelastic, three dimensional, dynamic analyses were performed on the Burbank building. Using the results of the analyses, comparative studies of the measured and calculated results were conducted.

4. Recommendations are being formulated to improve the accuracy of the calculated response in steel structures.

SUMMARY OF RESULTS

Complete results of the studies are presented in Refs. 1 and 2. A summary of important results is given below:

San Jose Building. -- For the San Jose building, the recorded motions indicate that the building undergoes strongly coupled three-dimensional response. The first two modes are predominantly translational with periods of 2.2 and 2.1 secs. The third mode is predominantly torsional with a period near 1.7 secs. The closeness of these modal periods and the small eccentricities of the building resulted in a strong modal beating phenomenon in the building and coupled lateral- torsional vibrations. The fourth and fifth modes are predominantly translational with periods between 0.7 and 0.6 seconds. The 1985 and 1988 UBC would estimate the predominant translational period of the building to be 1.3 and 1.77 seconds, respectively, indicating the flexibility of the frames.

Drifts computed for the building using a three dimensional elastic analysis and considering 1988 UBC lateral forces are, however, less than 0.0018 times the story height; a value substantially less than permitted by the code. Similarly, the analyses indicated that the building's members would not generally be stressed in excess of code permitted values when subjected to 1988 UBC lateral forces. Thus, current code provisions would indicate that the building was generally quite satisfactory. Nonetheless, during the Mt. Lewis earthquake (with 4%g peak ground acceleration) the base shear actually developed in the building is estimated to be more than 400% greater than the code prescribed value and the drifts are nearly 300% greater than allowed by code.

The records indicate that the building has little damping. However, the closeness of the modal periods made precise interpretation of the records difficult. Damping in the N-S direction ranges between 3-4% and between 2-3% in the E-W direction.

Figures 2 and 5 show some of the response of the building for the two earthquakes considered. The response is notable in its 80 second length, with nearly 30 cycles of intense structural motion. The strong portion of the earthquake was however less than 10 seconds. The intensity of this response is believed to be due to (1) the modal coupling and beating that substantially increased the amplitude and apparent duration of the motion; (2) the apparent resonance of the building with the predominant period of the ground; and (3) the relatively light damping in the system. As a result, the ground accelerations at the site were amplified in the building by 500 to 700 %.

Several analytical models were developed for the building. The standard one was a bare frame model having rigid joints. The period obtained for this model was 1.93 seconds. However, the computed roof displacement was only half of the recorded value for the Morgan Hill earthquake. By modeling the flexibility of the panel zones, the periods and displacements were greatly improved. By further adjusting the mass distribution to reflect actual conditions and by incorporating the additional contributions of the architectural finishes to lateral stiffness, the slight slab contribution to beam stiffness virtually identical results could be obtained (See Fig. 2).

The analyses give some insight into the apparent causes of the severity and duration of the response. In Figure 5 shows response to the Mt. Lewis earthquake. In part 1a of the figure, the

response of the analytical model with 1% viscous damping is compared with the recorded motion. Parts 1b and 1c of the figure show that the first and second modes individually have lightly attenuated response after about 30 seconds of motion. However, the two modes go in and out of phase resulting in constructive and destructive interference which produces a large dip in the combined response at 30 sec. and an increase in response up to time 60 secs. To further confirm that this response is not associated with the input motions, the analysis was run with zero input following time equal 40 secs. Also, an analysis was performed considering 5% viscous damping. In this case (part 2a of Fig. 5), the response of the individual modes attenuate so quickly that virtually no beating under free vibration can occur and little significant motion occurs after about 25 seconds.

Analyses also indicate that many of the members were probably overstressed during the Morgan Hill and Mt. Lewis events. While only a few columns were loaded beyond yield, most of the perimeter beams, especially in the lower levels, exceeded their plastic moment capacity, in several cases by as much as 40%. While these numbers are not by themselves cause for concern, they indicate that the building is particularly susceptible to structural damage and that the potential response of the building to earthquakes larger than the 4%g events considered herein should be examined with care. The motion of the building during the Loma Prieta earthquake, where motions three times larger than the Morgan Hill event were recorded, indicated substantially reduced amplifications and torsional contributions. It may be conjectured that the increased yielding in the structure separated the modes, thereby reducing modal coupling effects, increasing effective damping and moving the apparent periods of the structure away from the predominant period of the ground. Precise determination must await processing of the records and complete inelastic analysis of the building.

Burbank Building. -- In the Burbank building, the recorded period of vibration in seconds for the first five modes were 1.32 (N-S), 1.30 (E-W), 0.83 (torsional), 0.44 (N- S), 0.42 (E-W) and 0.28 (N-S). Using provisions of UBC(1988) the first period of vibration for both N-S and E-W direction would be calculated as 0.95 second. In both directions, the measured as well as calculated periods were much longer than the predictions of the current Uniform Building Code. The longer period of this building is attributed to more flexibility of the perimeter frame steel structure relative to typical moment frames.

Using the Half-Power Method, the modal damping for the Burbank building was calculated to be 4% and 3% of critical damping for the first and second modes respectively.

Figure 6 shows drift response of third floor and roof in N-S and E-W directions. Generally, the response in N-S direction was greater than the response in the E-W direction. Also, the response showed significant higher mode effects in both E-W and N-S directions.

In conducting dynamic analysis of Burbank building, initially a conventional model of the structure was built. In this model mass was established by using weights prescribed by UBC. The connections were modeled as fixed or simple according to the design assumptions. In addition, since floors are non- composite, they were not included in the modeling. This model which represents common modeling procedures used today, was subjected to base accelerations recorded at the foundation level of the building. The response predicted by this model was significantly different from recorded response.

By studying the response of the conventional model and also by surveying the actual building, it was realized that the actual condition of the building differs substantially from code prescribed conditions. The mass in the building was much less than dead load of the code. The floor decks were

connected to the girder by limited number of shear studs resulting in partial composite action. Connections that were assumed to be simple, actually were more or less semi-rigid.

Column base connections are conventionally modeled as fixed or pin, however, the actual base connections were either close to fixed or close to semi-rigid joints. In the refined model of the structure, the realistic conditions were modeled properly.

The three-dimensional realistic model of the steel structure was subjected to base excitations using the Inelastic computer program FACTS. The response of the realistic model was very close to the response recorded by the SMIP. Samples of the predicted and measured drift response are shown in Figure 6 which indicate reasonably close correlation between predicted and recorded responses.

CONCLUSIONS

The results of this study identify the importance of having well instrumented building records. Several interesting phenomena not accounted for in building codes and design practice were identified.

For the San Jose building it was shown that nearly symmetric, lightly damped structures with closely spaced modes can experience severely amplified motion as a result of coupled torsional-translational response. The analysis also confirmed that modeling needed to account for the flexibility of the beam-column panel zones. Current codes were unable to predict the severity of the observed responses of this building. Additional studies of this building in the inelastic range using the Loma Prieta records are needed as are improved instrumentation in the form of free field accelerometers.

The study of Burbank building indicated that in order to obtain realistic response from a dynamic analysis, the major elements of the structure such as floor diaphragms and connections should be modeled properly and more realistically than conventionally done in design offices. Also, realistic value of mass should be used in dynamic analyses and not the nominal values prescribed by building design codes.

ACKNOWLEDGMENTS

The study summarized here was supported by a grant from Office of Strong Motion Studies of Division of Mines and Geology of California Department of Conservation. The financial as well as technical support is sincerely appreciated. The permission by SSD Inc., Berkeley CA for the FACTS program to be used in the analysis of Burbank building is appreciated. The findings of this paper are solely those of the authors.

REFERENCES

1. Shen, J-H. and Astaneh, A. "Seismic Response Evaluation of an Instrumented Six Story Building Subjected to the 1987 Whittier Earthquake", report in preparation, Earthquake Engineering Research Center, University of California at Berkeley.

2. Boroschek, R. and Mahin, S., "Seismic Response Evaluation of an Instrumented Steel Frame Building Subjected to Several Ground Motions," report in preparation, Earthquake Engineering Research Center, University of California, Berkeley, CA.

3. Uniform Building Code., 1988 Edition, International Conference of Building Officials, Whittier, California, May 1988.

4. "Processed Data from the Strong-Motion Records of the Morgan Hill Earthquake of 24 April 1984", Report OSMS 85-05, California Department of Conservation, Division of Mines and Geology, Office of Strong Motion Studies, December 1985.

5. "CSMIP Strong-Motion Records from the Whittier, California Earthquake of 1 October 1987", Report OSMS 87-05, California Department of Conservation, Division of Mines and Geology, Office of Strong Motion Studies, October 1987.

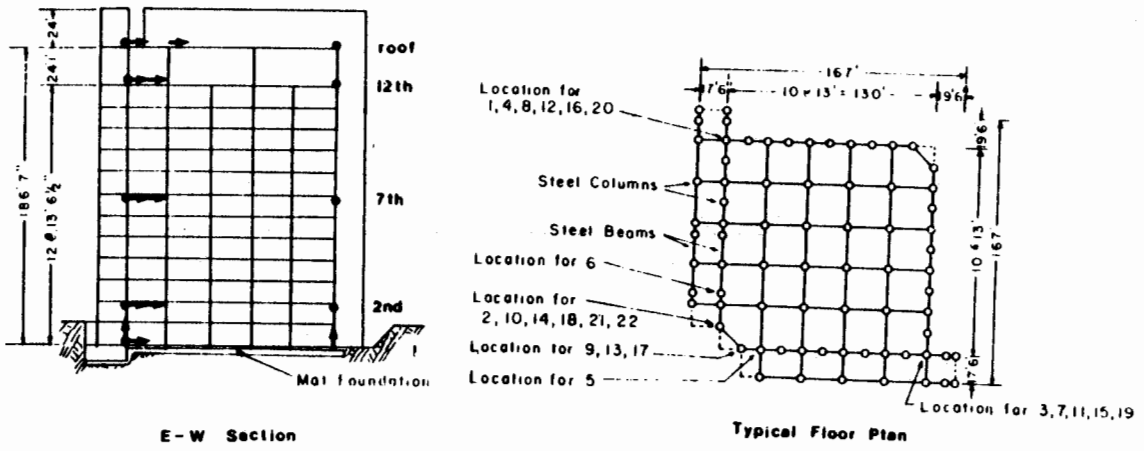

Figure 1 - San Jose Office Building. Plan and sensor layout.

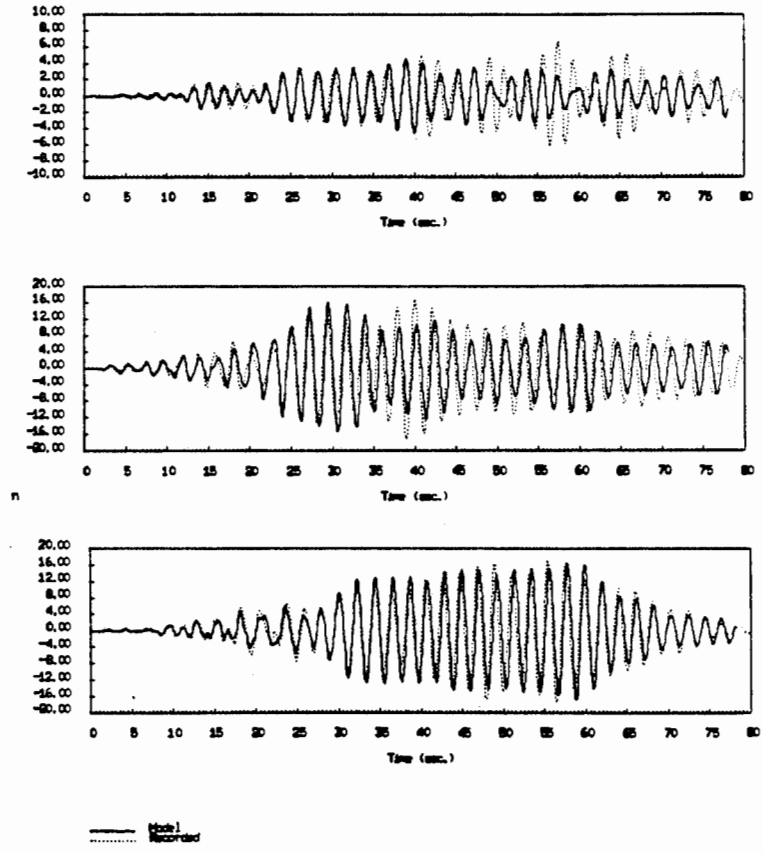

Figure 2 - San Jose Office Building. Best fit Model. Bi-directional input. Morgan Hill Earthquake. Twelfth floor motion. a) Derived torsion (SW-NW corner relative displacement). b) EW relative displacement, SW corner. c) NS relative displacement, SW corner.

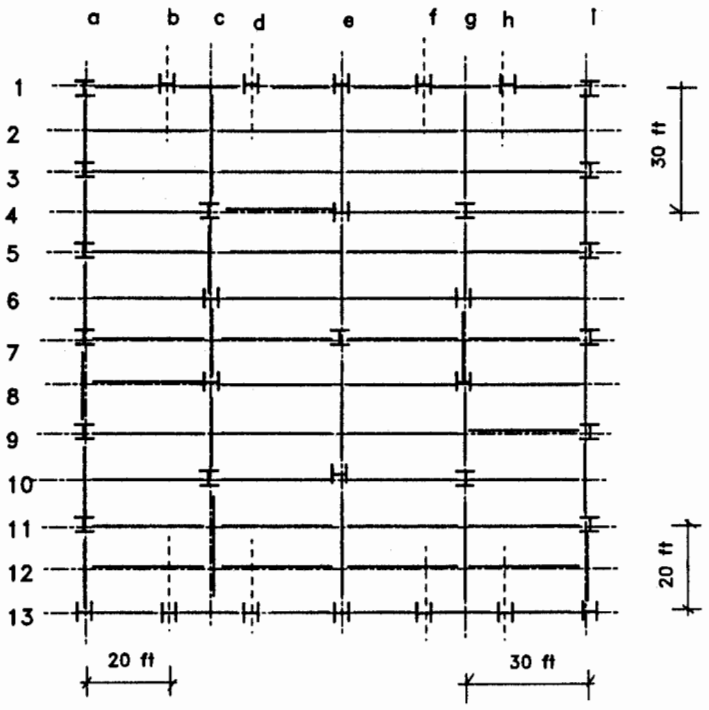

TYPICAL FRAMING PLAN

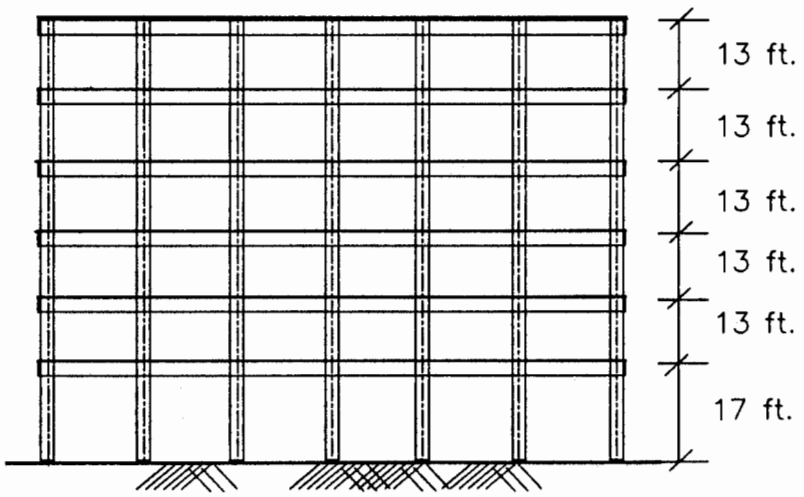

Elevation

Figure 3. Office Building in Burbank

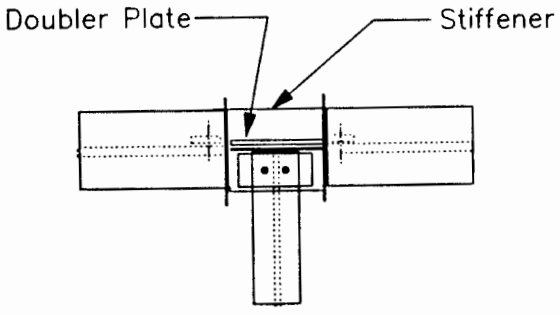

RIGID FRAME MOMENT CONNECTION

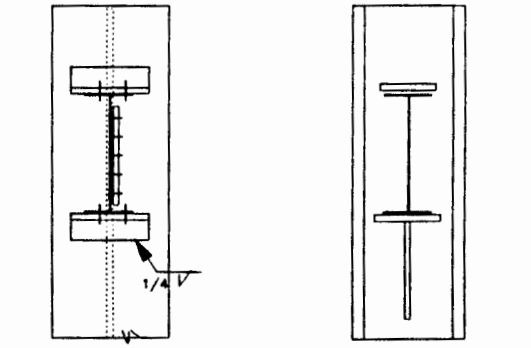

SHEAR CONNECTIONS

Figure 4. Ofice Building in Burbank and its Connection Details

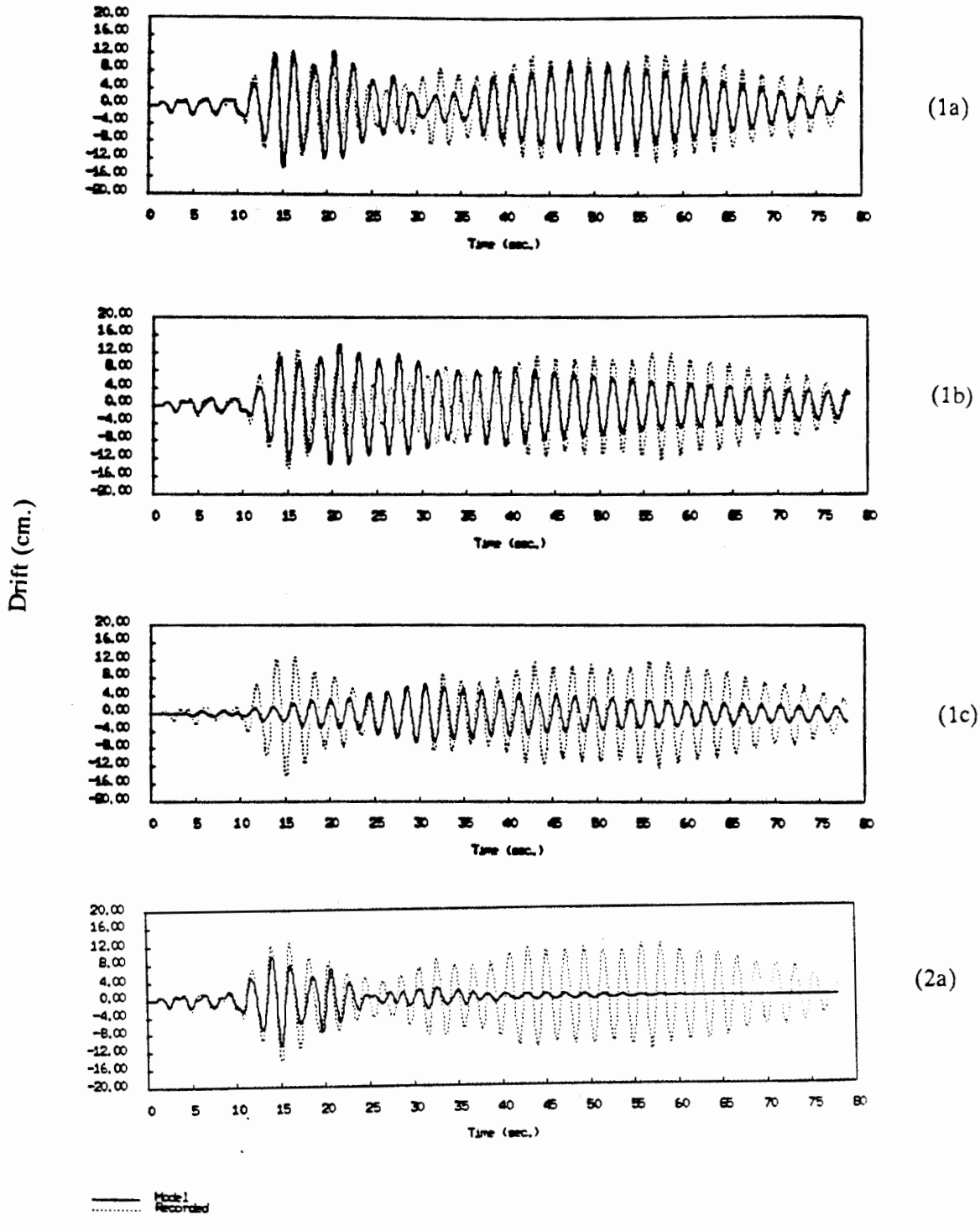

Figure 5. San Jose Office Building. Best fit Model. Bi-directional input. Mt. Lewis Earthquake. Input ground motion 0-40 seconds. Twelfth floor EW relative displacement, SW corner. 1a) First three modes, low damping model (1%) 1b) First mode. 1c) Second mode. 2) First three modes, increased damping model (5%)

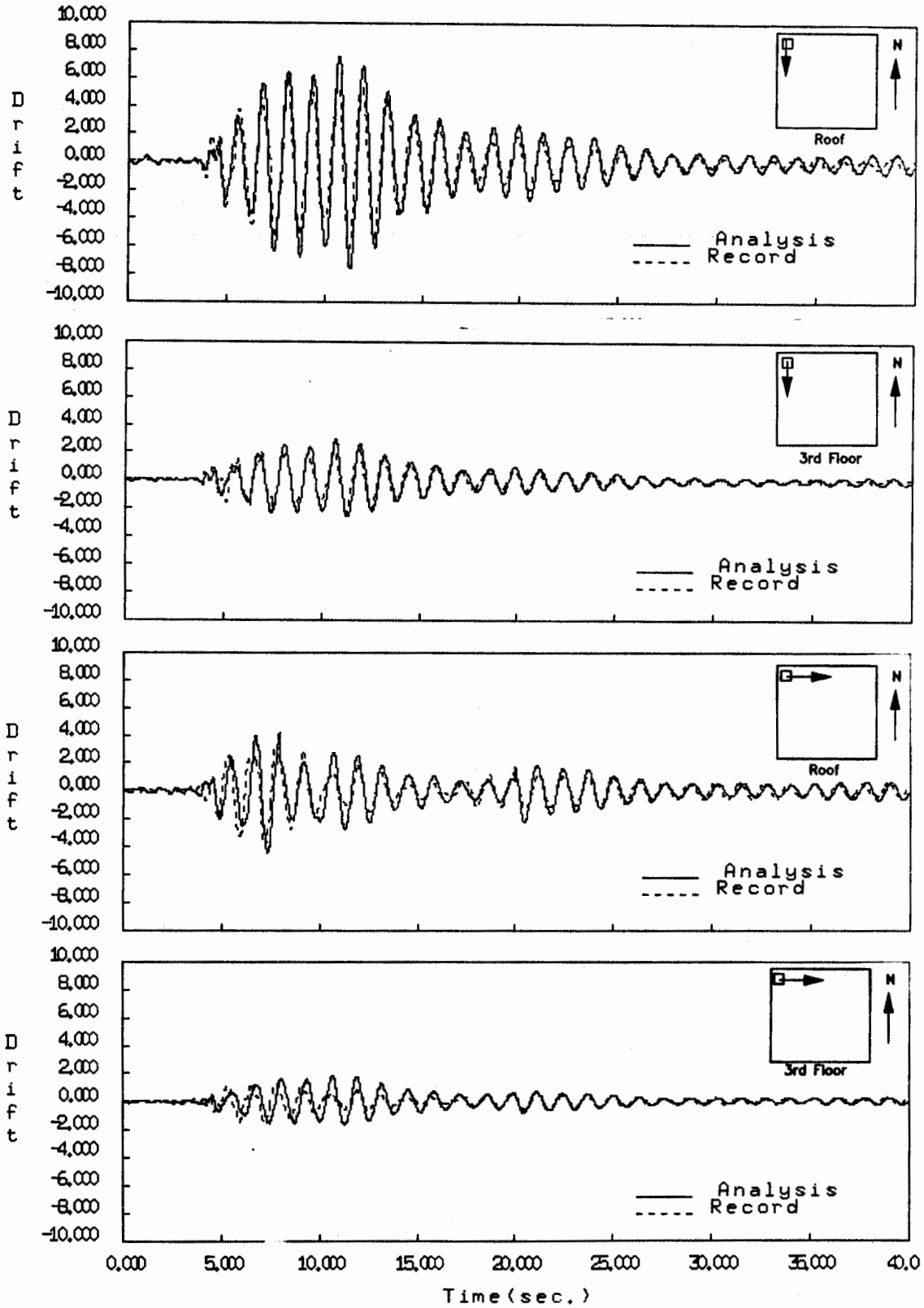

Figure 6. Correlation of Predicted and Recorded Responses for Burbank Building

SEISMIC RESPONSE AND ANALYTICAL MODELING OF THE CSULA ADMINISTRATION BUILDING SUBJECTED TO THE WHITTIER NARROWS EARTHQUAKE

Raymond R. Lui, Graduate Research Assistant
Stephen A. Mahin, Professor
Jack P. Moehle, Associate Professor
Department of Civil Engineering
University of California at Berkeley

Abstract

This study examines the measured seismic response behavior of the CSULA Administration Building during the October 1, 1987 Whittier Narrows Earthquake. The shear forces and interstory drifts calculated from measured seismic responses are compared with UBC design requirements to ascertain the validity of UBC requirements. A three dimensional elastic model was constructed and subjected to the recorded base accelerations to study the correlation of analytical modeling predictions with measured seismic responses.

Introduction

The California State University at Los Angeles (CSULA) Administration Building was subjected to the October 1, 1987 Whittier Narrows Earthquake. The earthquake measured 5.9 on the Richter magnitude scale with an epicentral distance of approximately 9 km. The peak horizontal ground acceleration, as measured at the basement level of the building, was 0.39g.

The eight-story structure, with penthouse and basement levels, is of reinforced concrete construction with composite steel/concrete construction along two transverse frames at the first floor level. The typical floor framing plan, second floor framing plan and the ground floor plan are presented in Figure 1.

The structural system above the second floor level consists of beam and girder floor systems, shear walls and non-ductile moment resisting frames. This system frames into the second floor soffit which transfers loads to the first floor columns. The first floor columns are offset from the perimeter of the building on all sides. The basement level is only partial, so that some columns extend from the first floor to the basement while others stop at the first floor. First floor and basement columns are supported on a foundation of drilled caissons with bell bottoms.

The building was constructed with 4000 psi normal weight concrete at and below the second floor soffit and 4000 psi light weight concrete above the second floor soffit.

Measured Seismic Building Response

The CSULA Administration Building was instrumented with 16 accelerograms to measure seismic building response. Data from these accelerograms is the basis for the discussion herein. The locations of the accelerograms are shown in Figure 2.

The first floor columns are offset from the perimeter of the building on all four sides and the shear walls abruptly stop at the second floor soffit. Large girders in the second floor soffit transfer loads from the shear walls to the first floor columns. In addition, perimeter columns above the second floor soffit, along the north and south perimeters, which help transfer lateral loads in the longitudinal direction, also frame to the columns via transfer girders in the second floor soffit. Hence, the lateral force resisting system is not continuous from the roof to the foundation which leads to the expectation of a soft first story during strong ground shaking.

However, the data obtained during the Whittier Narrows Earthquake indicate that first story did not respond as a typical soft story. The second floor soffit and the first floor columns provided enough stiffness to prevent enormous lateral drifts at the second floor level. The levels of interstory drift are within the limits of the 1988 Uniform Building Code [1].

The absence of a soft first story can be attributed to the flexible frame and shear wall system above the second floor, to the relative stiffness of the second floor soffit and first floor columns, and to the relatively moderate intensity of ground shaking induced by the Whittier Narrows Earthquake. The earthquake was not strong enough to cause inelastic behavior in the structure and consequently unable to produce a soft first story. Despite the lack of soft story behavior during this earthquake, the probability of a soft first story occurring during strong ground shaking is inherently high due to the nature of the building.

The typical shear wall layout tends to promote torsional behavior in the structure. Shear walls are located along the east and west perimeter to resist transverse lateral loads. A shear wall is located in the northwestern quadrant of the building to resist longitudinal lateral loads. The shear wall layout is presented in Figure 1. (Shear walls surrounding stairwells at the east and west perimeter walls are not shown.)

Comparison of recorded displacements at the ground level and at the second floor level indicate that the building experienced torsion during the Whittier Narrows Earthquake. The twisting of the building was limited and the maximum relative displacement between the east and west perimeter walls, at the second floor level, is approximately 0.4 inches. The Whittier Narrows Earthquake was moderately intense and larger magnitude earthquakes may cause larger torsional response which could overstress the first floor columns and induce failure.

In addition, story shear forces were estimated at several time steps from the recorded accelerations. Accelerations at floors 3 to 8 were obtained by linear interpolation of the data from the second floor and the roof. The computed inertia forces were compared with the story shears as calculated per 1988 Uniform Building Code provisions [1] and are presented in Figure 4. It should be noted that the inertia forces only approximate the

total lateral force per floor and is intended as a simplified method for estimating story shears.

Based on the measured data, the maximum base shear encountered by the building is approximately 1570 kips and 1070 kips in the transverse and longitudinal directions, respectively. The base shear, as calculated by the UBC seismic provisions, is approximately 1130 kips at working stress levels. The longitudinal base shear calculated from measured data is within the limits of the UBC working stress base shear. On the other hand, the transverse base shear calulated from measured data exceeds the working stress level provided by the UBC seismic design requirements. However, the inclusion of load factors by the UBC to calculate base shears at yield stress levels increases the base shear to approximately 1760 kips. The measured base shears for both directions are within this limit and no inelastic behavior is expected. It should be noted that in its determination of design lateral forces, the UBC assumes inherent inelastic behavior and general overdesign of the structure by the designer. Hence, shear forces calculated from recorded data may be larger than those computed per UBC seismic provisions.

Finally, displacement time-histories were evaluated to further understand the behavior of the CSULA Administration Building during the Whittier Narrows Earthquake. The motion encountered by the building is typical of many structures. At the start of the earthquake, ground accelerations and displacements are small and the building moves in the same direction as the ground without exhibiting considerable deformations. As the earthquake progresses, the ground accelerations and the ground displacements increase. With the increased lateral displacement, the structure is dragged along in the same direction as it tries to keep up with the ground motion. However, when the displacements suddenly change direction, the building is whipped beyond the maximum ground displacement. This behavior is characteristic of higher mode effects and is presented in Figure 5.

Analytical Seismic Building Response

In order to adequately predict the three-dimensional response of the structure, including torsional behavior, a three-dimensional analytical model was constructed and analyzed using SAP90 [2].

The following considerations were made in the development of the three-dimensional analytical model:

1. Fixed support conditions were assumed at the base of the first story columns and/or top of the basement walls. Because no acceleration records are available at this level, accelerations recorded at the basement level are assumed to propogate unaltered to the base of the first story columns. In addition, soil conditions were not available; hence, soil-structure interaction was not considered. The analytical studies support the validity of this assumption.

2. All floor slabs were assumed to be rigid diaphragms. The slabs have a minimum thickness of 6 inches and the floor joists are closely spaced. Again, the validity of this assumption is supported by the analytical studies.

3. Transverse shear walls along the east and west perimeter are modeled as two shear walls, one on each side of the building. Only the shear wall in the northwest quadrant is modelled for the longitudinal direction. Shear walls around stairwells were not considered.

4. A time-history analysis was performed using the recorded ground accelerations as measured at the basement level. Based on the recorded response data, a viscous damping value of 5 percent is used.

5. Uncracked gross cross-sectional properties were used for all structural members.

Computed and measured relative roof displacements for the transverse and longitudinal directions are compared in Figure 3. The seismic building responses calculated from the three-dimensional analytical model agree well with the responses from the recorded data. The calculated fundamental period of vibration is 1.63 and 1.58 seconds in the transverse and longitudinal directions, respectively. This compares well with the measured fundamental period of vibration of approximately 1.6 seconds. In the range of strong ground motion, i.e., the range from approximately 3 to 12 seconds, the calculated displacement response is slightly less than that obtained from measured data. Furthermore, the calculated response from the analytical model exhibits more higher mode effects than the measured response.

In the range of free vibration, i.e., the range from approximately 12 seconds and beyond, the seismic building responses calculated from the analytical model are virtually identical to the responses from the measured data. The similarity in the period of vibration and the amplitude of displacement suggests that the modeling assumptions made above are adequate to simulate actual building behavior.

In addition, base shears were also calculated for the three-dimensional analytical model subjected to the ground motions recorded for the Whittier Narrows Earthquake as measured at the basement of the CSULA Administration Building. The maximum base shears, calculated with the SAP90 computer program, are approximately 970 kips and 2900 kips in the longitudinal and transverse directions, respectively. The base shear computed in the longitudinal direction is similar to that computed from the measured response. However, the base shear calculated in the transverse direction is approximately twice as large as that computed from the measured response. This is not necessarily a modeling error since the calculation of base shear is time dependent and the maximum accelerations per floor may occur at the same moment creating a relatively large base shear. This response requires further investigation.

Conclusions

Based on the study of the CSULA Administration Building, the following conclusions can be made:

1. The structure performed well during the Whittier Narrows Earthquake as evidenced by the minimal damage observed. Since cracking was minimal, it is apparent that the interstory drift requirements per 1988 UBC are adequate. The anticipated soft first story did not occur during the

Whittier Narrows Earthquake, but is likely to occur during larger magnitude earthquakes.

2. Measured story shears were similar to those stipulated by the 1988 UBC design provisions for working stress. All shear forces were within the limitations for yield stress as provided by the UBC. The code assumptions of inherent inelastic behavior and general overdesign appear to be adequate.

3. The seismic building responses predicted by the three-dimensional analytical model, especially the free vibration responses, were in adequate agreement with the recorded seismic responses. The modeling assumptions of fixed base, 5 percent viscous damping, and uncracked sections were adequate in representing the actual structure.

4. Based on analysis of the recorded data and the three-dimensional analytical model, higher mode affects dominate the response of the CSULA Administration Building. Omission of higher modes in the analysis of the structure may be critical.

Further analysis of the three-dimensional model is presently in progress and will be reported on in a future paper.

Acknowledgements

This study is supported by a grant from the Strong Motion Instrumentation Program of the California Department of Conservation. Their support and continued efforts are greatly appreciated. The efforts of Ruben Boroschek for his assistance in analyzing the recorded displacements are also greatly appreciated. The opinions expressed in this report are solely those of the authors and do not represent those of the sponsoring agency.

References

1. Uniform Building Code, 1988

2. E. L. Wilson and A. Habibullah, "SAP90, A Series of Computer Programs for the Static and Dynamic Finite Element Analysis of Structures," 1989.

3. "Addition to Administration Building, California State University at Los Angeles," drawings prepared by John Sheffet, structural engineer, and Maynard Lyndon, architect, June 23, 1967.

4. SMIP, "Strong-Motion Data (Vol.2), Los Angeles - CSULA Admin. Building, Channels 1, 3 - 16, Whittier Earthquake of 1 October 1987," CSMIP Serial No. 762.

5. Albert C. Martin and Associates, "Preliminary Dynamic Analysis Survey, California State University, Los Angeles, California, Administration Building, Volume 1, Summary Report," August 1988.

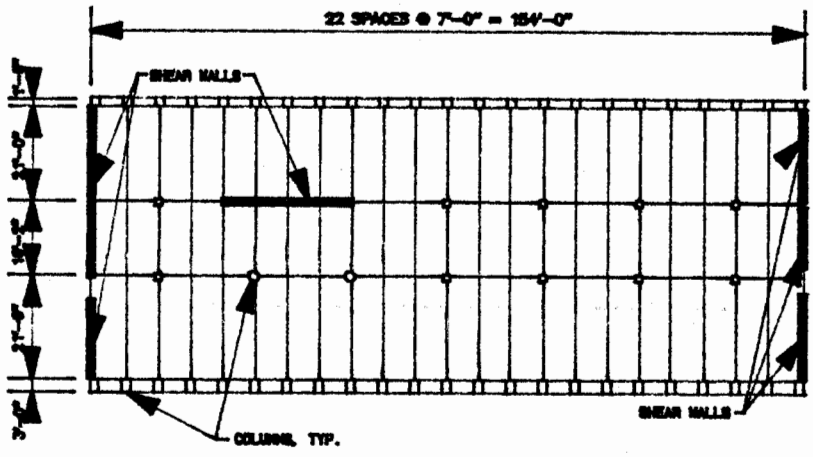

Typical Floor Framing Plan (Floors 3 to 8)

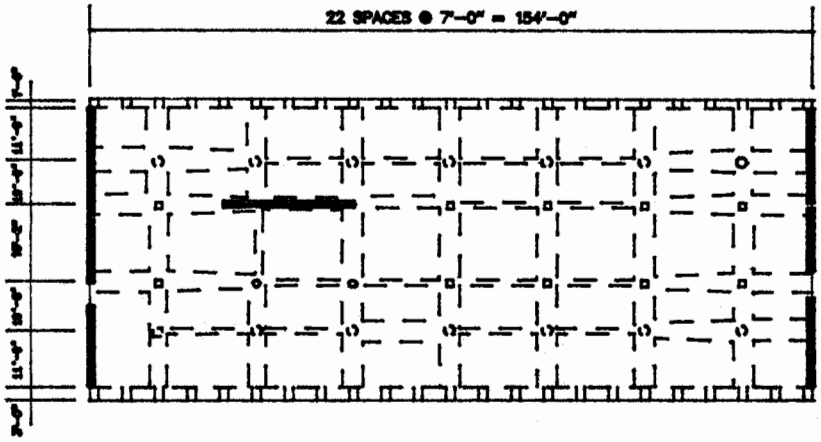

Second Floor Framing Plan

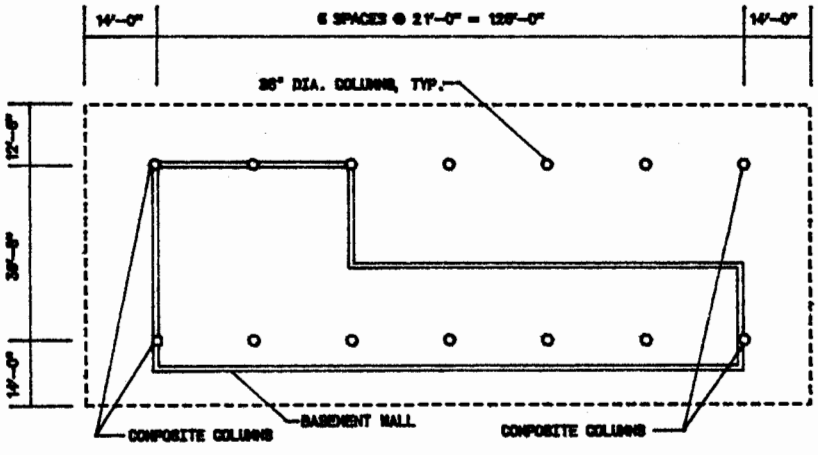

Ground Floor Plan

Figure 1

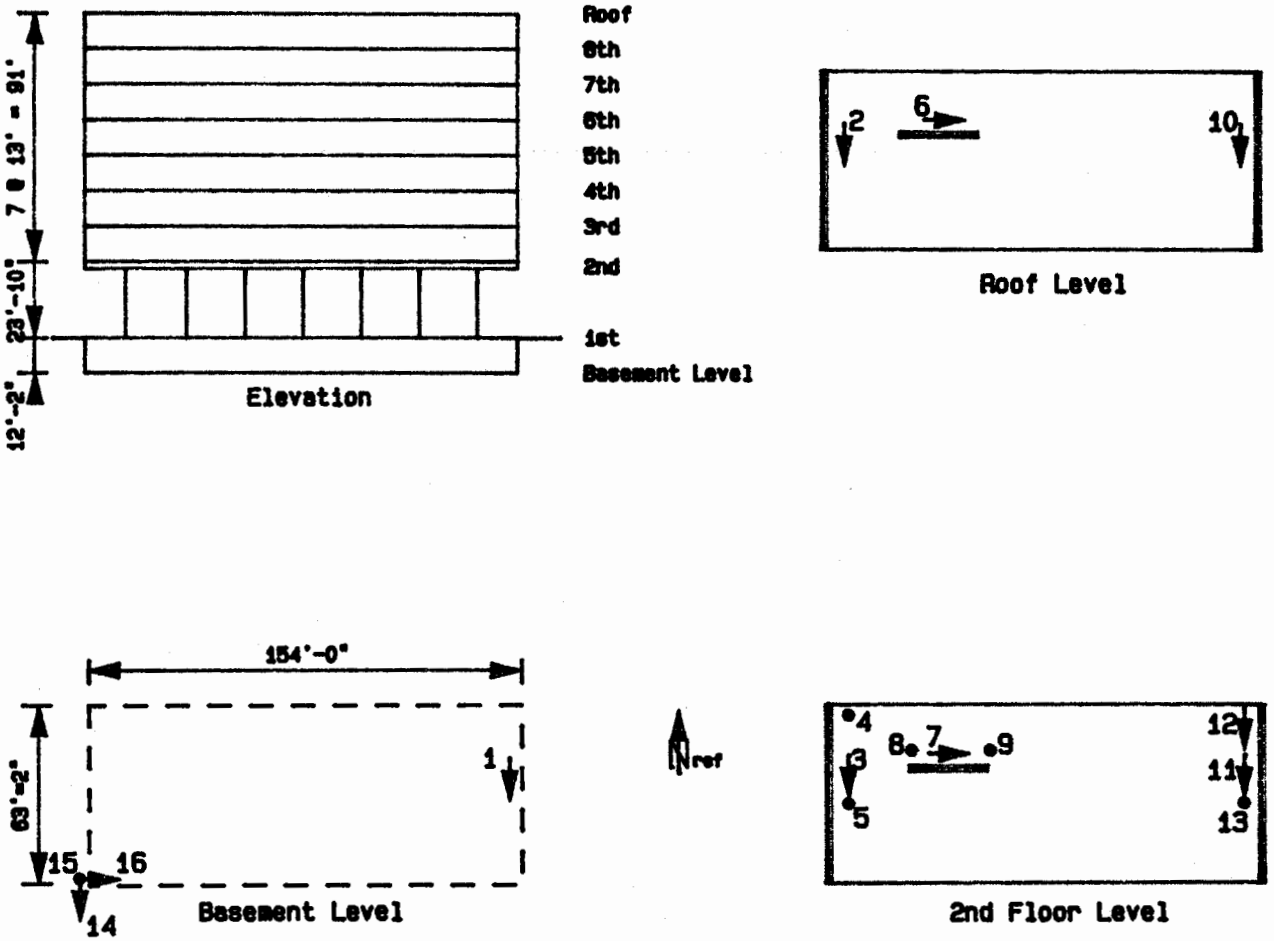

Figure 2 Sensor Layout for CSULA Administration Building
(CSMIP Station No. 24468)

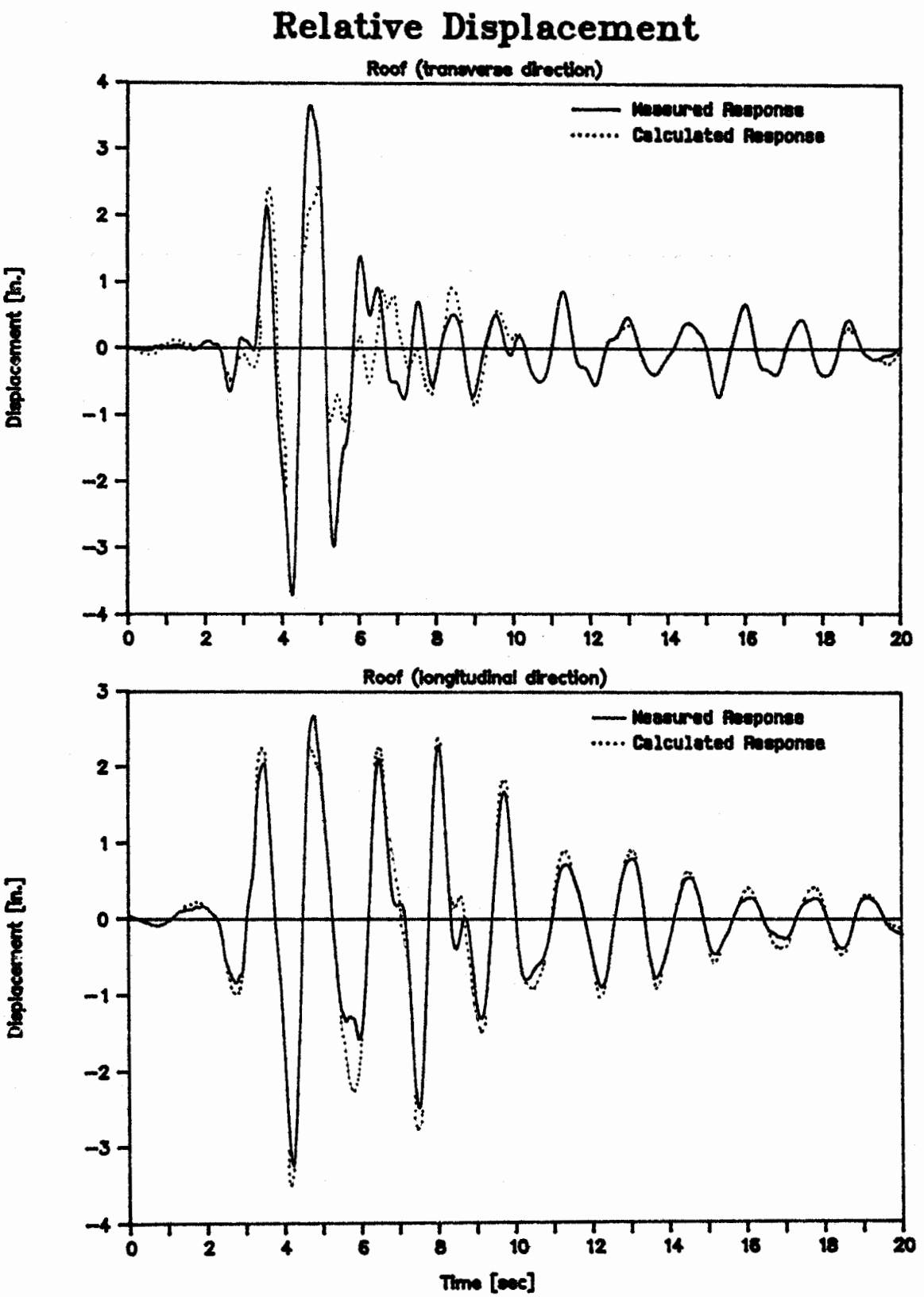

Figure 3 Calculated and Measured Response

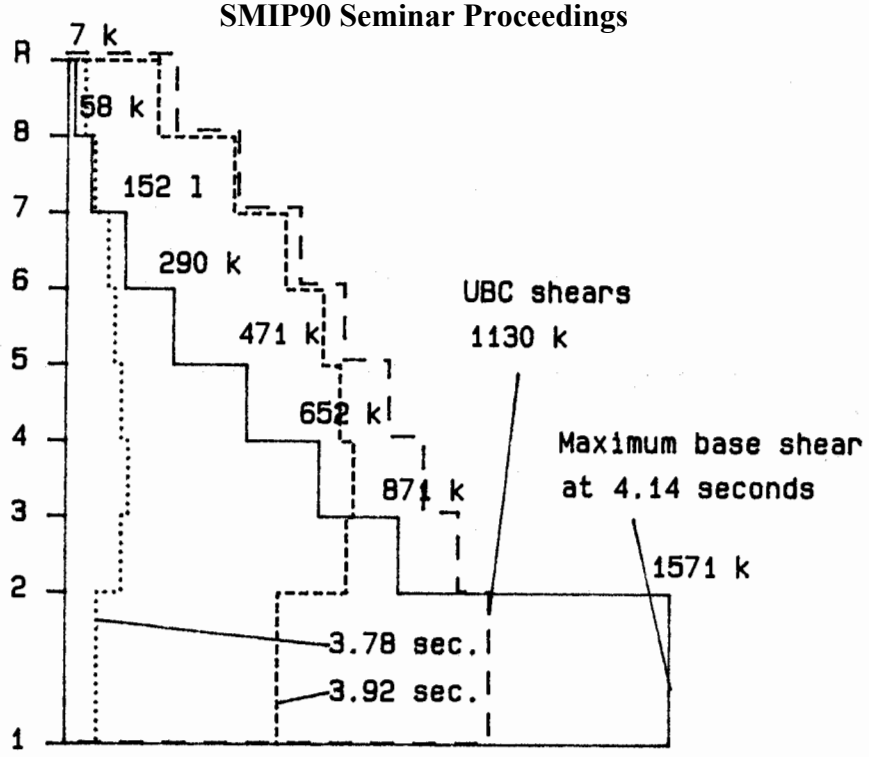

Base Shear in the Transverse Direction

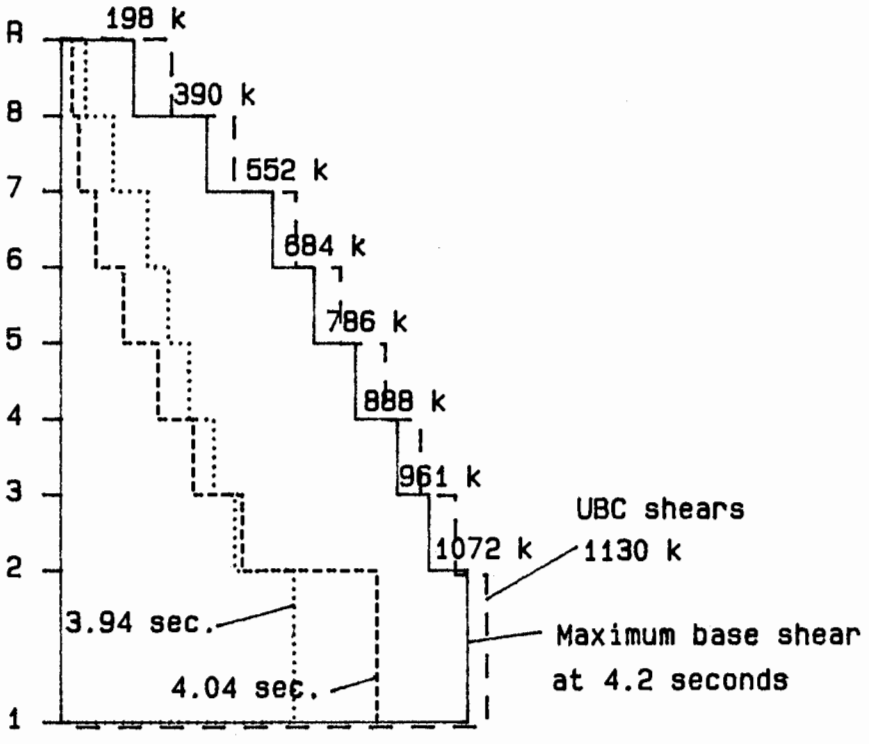

Base Shear in the Longitudinal Direction

Figure 4 Story Shears

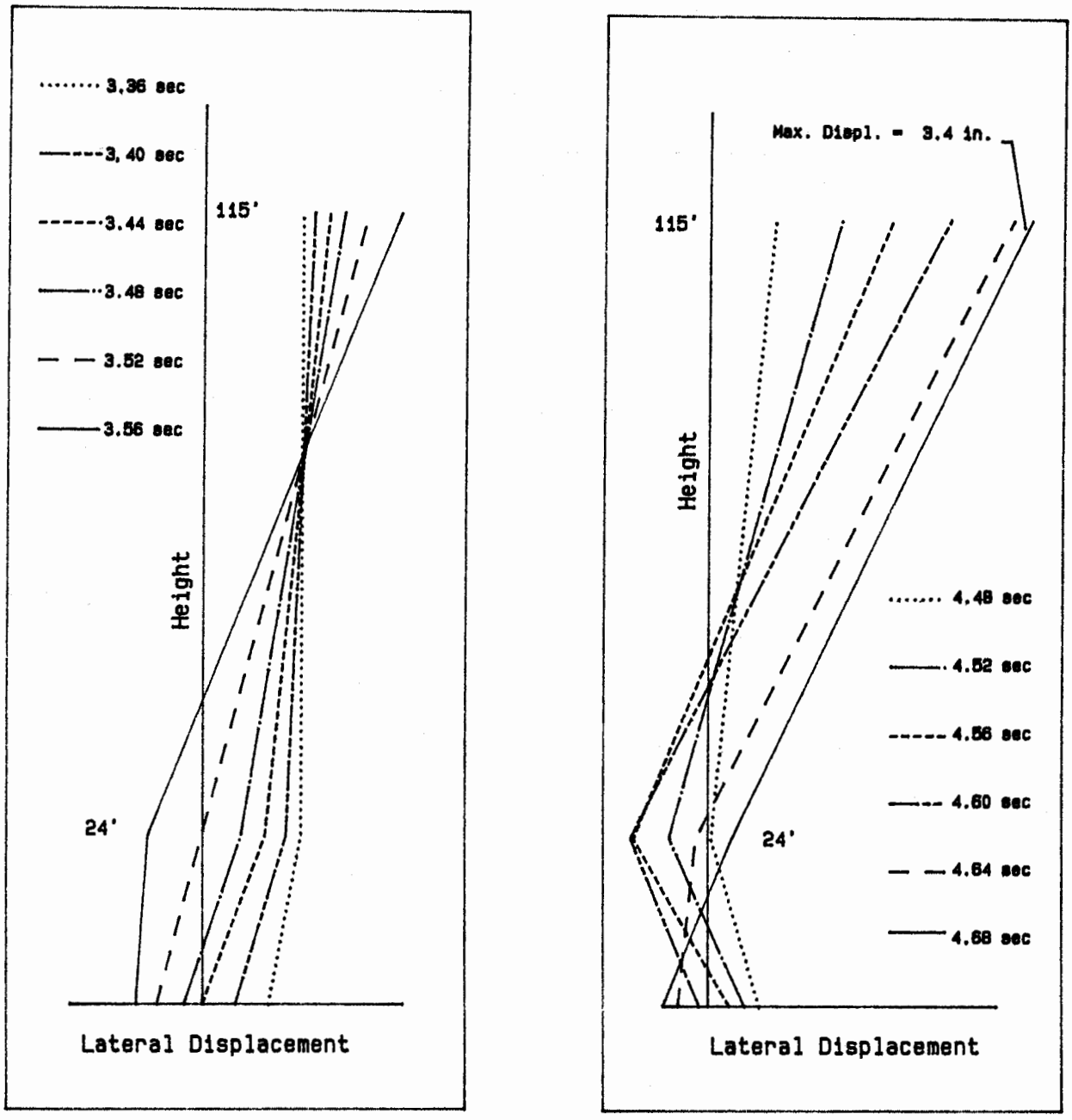

Figure 5 Absolute Displacement Time-Histories